The Genetic and Molecular Etiologies of Two Spontaneous Mouse Models of Skeletal Dysplasia and Infertility

by

Krista Anne Geister

A dissertation submitted in partial fulfillment
of the requirements for the degree of
Doctor of Philosophy
(Cellular and Molecular Biology)
in the University of Michigan
2013

Doctoral Committee:

      Professor Sally Ann Camper, Chair
      Professor Gregory R. Dressler
      Professor Renny T. Franceschi
      Associate Professor Catherine Elizabeth H. Keegan
      Professor Miriam H. Meisler

TABLE OF CONTENTS

LIST OF TABLES

LIST OF FIGURES

ABSTRACT

High-throughput genotyping and sequencing technologies have stimulated an accelerated pace of Mendelian gene discovery. Forty-one novel genetic causes of skeletal dysplasia have been uncovered in the last two years. The genetic heterogeneity of the skeletal dysplasias is extremely high, with 450 forms described. Multiple organ systems can be affected, including the reproductive system. I present the discovery of two different genes that are mutated in spontaneously occurring mouse mutants that cause skeletal dysplasia and infertility. These discoveries demonstrate the value of mouse mutations for understanding the pathophysiology of disease and testing treatments.

The *peewee* mouse exhibits female infertility and skeletal dysplasia associated with reduced progression of cells through the zones of the growth plate. The phenotype is caused by a loss-of-function mutation in the gene that encodes natriuretic peptide receptor 2, *Npr2*. Human *NPR2* mutations cause a form of extreme short stature known as acromesomelic dysplasia, Maroteaux type (AMDM). Nothing is known about the fertility of these patients. We demonstrate that *Npr2* loss-of-function affects growth by increased activation of the ERK MAPK pathway. We can correct the $Npr2^{pwe/pwe}$ growth defect in explant cultures of embryonic bones with drugs that inhibit MEK1/2 action. We also show that female infertility is rooted in the requirement for *Npr2* activation to generate the cGMP necessary to maintain meiotic arrest of oocytes.

The *chagun* mouse exhibits severe short stature and male infertility. The phenotype is caused by a hypomorphic mutation in a gene also mutated in human patients with a form of primordial dwarfism. The fertility of these patients is unknown. I demonstrate that *chagun* serves as a model for this human disorder. I show that the growth insufficiency is caused by disorganization of the cells at the growth plate, and that male infertility is due to progressive germ cell loss.

Both of these mouse mutations model human skeletal dysplasia disorders, predict infertility, illuminate the pathophysiology of the disorders and pave the way for the development of therapeutic interventions to improve growth.

CHAPTER 1

Skeletal Dysplasias in the Genome Era: Molecular Diagnostics, Outcomes Prediction and Improved Therapeutic Potential

Outline:

Overview of Early Skeletal Development and Endochondral Ossification

The Skeletal Dysplasias

>　Genetic Heterogeneity of Skeletal Dysplasia

>　Skeletal Dysplasia Genetics: A Historical Perspective

A Geneticist's Best Friends: High-Throughput Technologies and Mutation Discovery

How Mouse Models Impact Skeletal Dysplasia Research

Signaling Pathways Implicated In Skeletal Dysplasias

>　IMAGe Syndrome: The Importance of Imprinting

>　Proteus Syndrome: A Disorder of Mosaicism

>　*INPPL1* Mutations in Opsismodysplasia

>　cAMP signaling and Acrodysostosis

>　*FGFR2* and Bent Bone Dysplasia

>　*SMAD4* and Myhre Syndrome

Epigenetics: Histone Acetyltransferase *KAT6B/MYST4* Mutations Cause a Variety of Disorders

Could Mutations in miRNAs Cause Severe Short Stature?

Abstract:

Skeletal dysplasias result from disruptions in normal skeletal growth and development, and are a major contributor to severe short stature in humans. They occur in approximately 1/5000 births, and some of them result in lethality. The Nosology and Classification of Genetic Skeletal Disorders is published once every five years. In the two years since the most recent publication, 39 new genetic causes of skeletal disorders have been uncovered, and 11 novel skeletal syndromes have been described. This remarkable rate of discovery is largely due to the expanded use of high-throughput genomic technologies. This review is intended to supplement the most recent edition of the Nosology and Classification, and provide the reader with a historical appreciation of the field of skeletal dysplasia genetics. We discuss the major contributions of mouse models to understanding the molecular mechanisms behind skeletal dysplasia phenotypes, and their utility in the development of therapies. The rate of discoveries in genetics and molecular mechanisms is truly spectacular. These advances hold great promise for diagnostics, risk prediction and therapeutic design.

Overview of Early Skeletal Development and Endochondral Ossification

The bones of the skeleton are formed through two processes: intramembranous ossification and endochondral ossification. Both of these developmental programs begin with the condensation of mesenchymal cells in areas of the body where a skeletal element will eventually form (1-3). The condensations that will form the cranium, and parts of the clavicle and pubic bone, undergo intramembranous ossification, where the mesenchymal cells differentiate directly into osteoblasts that will transform the condensation into true bone tissue. This review will concentrate on genetic disorders of endochondral ossification.

The bones of the body that form through endochondral ossification are mainly responsible for determining an individual's final stature (2). Early in endochondral ossification, the mesenchymal cells of the condensation differentiate into chondrocytes instead of osteoblasts. These intermediary chondrocytes will proliferate and undergo terminal hypertrophic differentiation, which directs the invasion of the vasculature into the nascent element, leading to the recruitment of osteoblasts (1-3). The infiltrating osteoblasts replace the dead or dying hypertrophic chondrocytes with mature bone matrix. The progressive mineralization and maturation of the cartilage template occurs along its length (out from the primary ossification center), as well as at either end (secondary ossification centers). As this new element begins to take on more characteristics of a true bone, a population of undifferentiated chondrocytes becomes sealed within either end of the forming element. These pools of reserved chondrocytes are known as the epiphyseal growth plates, and they regulate the growth of the skeletal elements and the individual over time.

The growth plate is a highly organized tissue. It is composed of three distinct zones: the resting zone, the proliferative zone, and the hypertrophic zone, which culminates in chondrocyte

cell death (1-4) (Figure 1.1). Lesser-differentiated cells in the resting zone are recruited to the enter the proliferative zone where they divide perpendicular to the plane of the growth plate, intercalate over each other, and adopt a flattened shape to form pillars of discoid chondrocytes (3-6). Eventually, the cells in the proliferative zone receive signals that promote their further differentiation into hypertrophic chondrocytes. Once in the hypertrophic zone, the cells express a new combination of transcription factors, signaling molecules, and matrix proteins. Chondrocyte hypertrophy also leads to a tremendous increase in cell volume and apoptosis. Osteoblasts will then replace the chondrocytic remnants with bone matrix at the ossification front, where the newest bone tissue is formed in the growing element.

The Skeletal Dysplasias

Numerous genetic mutations have the ability to disrupt the organization and function of the growth plate (1, 2, 7-9). Studies in humans and mice have discovered many genes that regulate growth plate architecture and the rates of chondrocyte proliferation and/or differentiation (Figure 1.2). In humans, mutations in these genes profoundly impact the growth of the individual such that he or she is unable achieve a normal adult height for his or her age, ethnicity, and sex. These disorders of skeletal growth are known as the skeletal dysplasias. There are over 400 skeletal dysplasias documented in the medical literature (8). They are predicted to occur in approximately 1/5000 children (2), and they can have a wide range of effects on the individual from relatively mild effects to lethality. Most lethal forms of skeletal dysplasia result from thoracic hypoplasia, where the thoracic cage is not large enough to allow for proper lung development (10). In such cases, the infant dies of respiratory distress soon after birth.
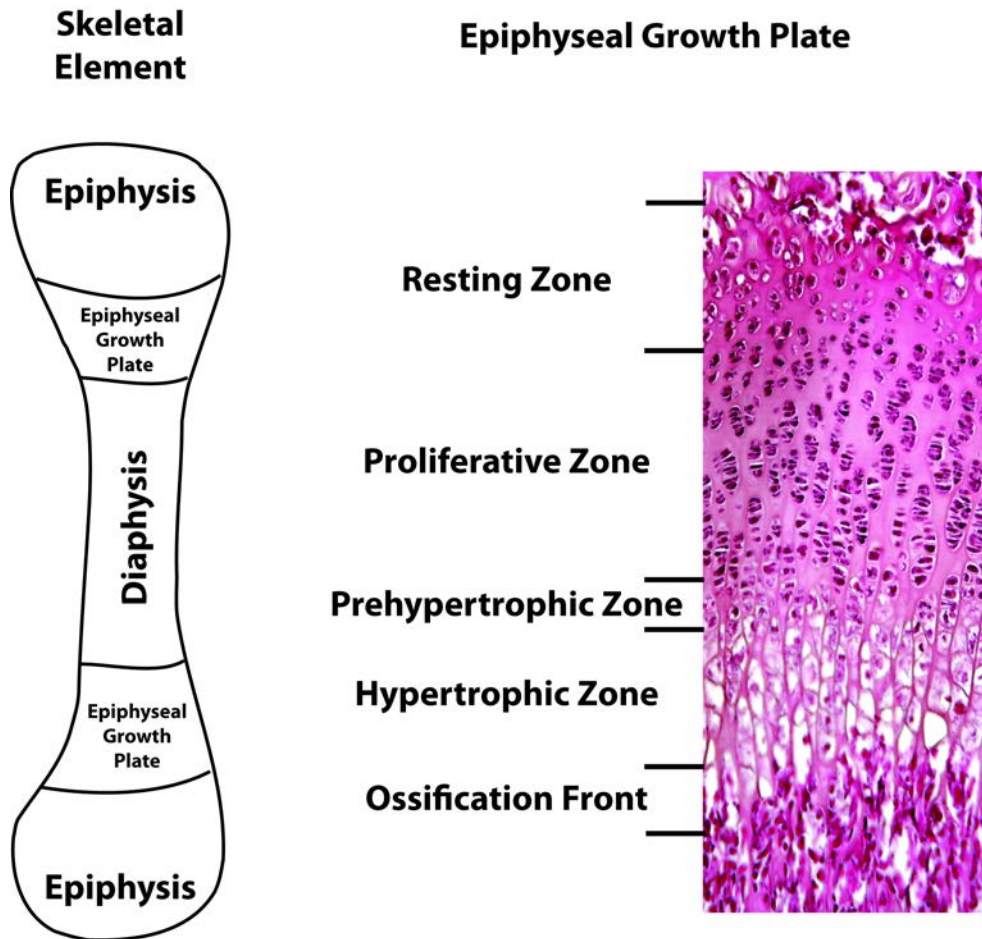
Figure 1.1. Formation of the growth plate and growth plate architecture. On the left is a diagram of a typical long bone, which forms early in embryonic development through the condensation of mesenchymal cells that then differentiate into chondrocytes. The hypertrophy of these chondrocytes promotes the vascularization of the element, which brings osteoblasts to the element to facilitate the addition of true bone matrix. The diaphysis, or shaft of the bone, bridges the ends, or epiphyses of the bone. The epiphyseal growth plates lie between these two structures, retain their chondrocytic identity, and serve as a pool of reserved chondrocytes to regulate growth of the long bone throughout one's growth period. On the right is a section through a 3-week old mouse tibial growth plate stained with hematoxylin and eosin. The zones of the growth plate are clearly recognizable. As the lesser-differentiated cells in the resting zone begin to divide, they enter the proliferative zone. This zone is characterized by chondrocytes that form columns of flattened chondrocytes that resemble stacks of coins. These dividing cells terminally differentiate in the hypertrophic zone, where they greatly increase their cell volume and alter their gene expression profile to express different transcription factors, enzymes, and extracellular matrix proteins. At the edge of the hypertrophic zone, known as the ossification front, osteoblasts will begin to lay down mature bone tissue in the place of the dying hypertrophic chondrocytes. This process is spatially and temporally regulated to allow for coordination of the growth of the long bones throughout an individual's growth period, ensuring that they grow to a normal adult height.

Many forms of skeletal dysplasia result in severe short stature, but are compatible with life. In some cases, other organ systems are affected. Disorders that affect the skeleton and the reproductive organs have been documented (11-18) (Table 1.1). Also, a significant number of skeletal dysplasia patients have been reported to have hearing loss (2, 16, 19, 20). In patients with achondroplasia, the most common non-lethal form of skeletal dysplasia (2), hearing loss could be due to chronic otitis media (19), but the involvement of otitis media in hearing impairment in other forms is not well documented. Individuals may also have neurological involvement and vision problems (2). It is recommended that patients are carefully monitored for all of these potential complications, as they may require immediate intervention (2, 21).

Studies focused on individuals affected with achondroplasia, the most common form of skeletal dysplasia, reveal the impact on quality of life that are likely to apply to other skeletal dysplasias (22). Achondroplasia patients report effects on overall health, employment opportunities, income, and intimate relationships. Adolescence can be a difficult time, with the effects of normal adolescence being exacerbated and extended into adulthood. Support groups for individuals with severe short stature can be helpful. Perhaps the most well known organization is Little People of America, which holds annual meetings and gatherings and provides skeletal dysplasia patients a venue through which they can share their experiences and network (2).

Currently, there are no pharmacological therapies available for individuals affected with any of the various forms of skeletal dysplasia, although there are some promising candidates. Growth hormone therapy can accelerate the growth rate, but in cases of idiopathic short stature, GH therapy does not substantially improve target height (23). Controversial surgical procedures have been performed that successfully lengthened the limbs of a child, but the

Table 1.1 Skeletal Disorders that Affect Reproductive Organs

Disorder	Skeletal Features	Reproductive Features	Gene(s) Involved
Turner's Syndrome(12)	Short stature	Gonadal dysgenesis	XO Karyotype *SHOX2*
Campomelic Dysplasia (11)	Bent bones Short stature	XY Sex reversal Ambiguous genitalia	*SOX9*
IMAGe Syndrome (13, 24)	Intrauterine growth restriction	Cryptorchidism Genital hypoplasia Hypogonadotropic hypogonadism	*CDKN1C*
Acrodysostosis (14, 17, 25, 26)	Brachydactyly Facial dysostosis Nasal hypoplasia	Hypogonadism Hormonal resistance	*PRKAR1A* *PDE4D*
Genitopatellar Syndrome (15)	Absence of patellae Joint contractures	Cryptorchidism Clitoral/labial anomalies	*KAT6B*
Myhre Syndrome (16)	Short stature Brachydactyly Reduced joint mobility	Cryptorchidism	*SMAD4*
Short-Rib Polydactyly Syndromes (9, 18)	Extreme short stature, ribs, and polydactyly Lethality	Genitourinary atresia Occasional sex reversal	Many primary cilium associated genes (*DYNCH1*, etc.)

surgeries are numerous, expensive, fraught with potential complications, and require dedication of much of one's childhood years to medical care (2, 21). Molecular diagnosis of skeletal dysplasias is highly desired, and treatment options are sought after by many patients and their families.

The Genetics of Skeletal Dysplasia

Skeletal dysplasias have historically been characterized by the inheritance pattern, associated symptoms, and radiological features. These classifications are confounded by the

fact that mutations in the same gene can cause many different forms of skeletal dysplasia (8).

The best examples of this phenomenon are the forms that result from mutations in *FGFR3*, the gene that encodes fibroblast growth factor receptor 3. Remutation of the same codon in *FGFR3* creates an activating mutation that causes semi-dominant achondroplasia, but patients with alternative mutations have thanatophoric dysplasia (type I or II) and die *in utero* or very shortly after birth of respiratory failure. Another obstacle in classifications is that mutations in different genes can cause the same form of skeletal dysplasia. Osteogenesis Imperfecta (OI) is a premier example of this phenomenon. Genes that encode collagens are a major cause of the various forms of OI (*COL1A1* and *COL1A2*), but so are genes that encode molecular chaperones (*SERPINH1*, *FKBP10*). There are also cases in which the affected individual has many hallmarks of a particular form, but additional clinical features that have not been previously associated with that form of skeletal dysplasia (27). These cases may involve modifying loci of the various forms of skeletal dysplasia.

Genes implicated in skeletal dysplasias encode products that are involved in a diverse array of cellular processes. The major processes include signal transduction, extracellular matrix components, control of protein trafficking and glycosylation, and control of gene expression at the levels of transcription, RNA processing and translation (Table 1.2). Among the newest discoveries are genes that influence ciliogenesis and cilia maintenance.

Skeletal Dysplasia Genetics: A Historical Perspective

Throughout the 1980s, defects in collagen genes reigned as the major genetic cause for such conditions as Osteogenesis Imperfecta (*COL1A1*) (28, 29), Stickler syndrome (*COL2A1*) (30), and spondyloepiphyseal dysplasia (*COL2A1*) (31). These studies made use of genetic material collected from nuclear families with multiple affected individuals, and utilized such

techniques as linkage analysis, positional cloning (30-32) and traditional Sanger sequencing to uncover the causative mutations. The discovery of collagen mutations in skeletal disorders heralded a shift in the field from cataloguing the clinical manifestations of the disorder to understanding genetic causes that could be used for molecular diagnostics and risk prediction.

These successes were quickly followed by discovering the common genetic etiologies of achondroplasia and thanatophoric dysplasia. Achondroplasia does not co-segregate with *COL2A1*, meaning that the disorder was not due to mutations in this gene (33). In 1994 three groups mapped achondroplasia to the distal region on the small arm of human chromosome 4 (34-36). All three studies had several (6-18) unrelated, nuclear families with multiple affected individuals to analyze for linkage analysis. A locus on chromosome 4p16.3 co-segregated with achondroplasia in all of the families, indicating no evidence for genetic heterogeneity. The analysis was performed in roughly the same way in all studies. First, sets of polymorphic microsatellite markers were tested across the genome to narrow the locus to a large region of a chromosome. This was followed by finer mapping with additional polymorphic markers flanking the original marker. Munnich and colleagues included patients with hypochondroplasia, which was thought to be allelic to achondroplasia at that time. Their results supported this hypothesis, as both conditions mapped to the same region on chromosome 4 (34). This region included several candidate genes, one of which was *FGFR3*.

Only a few months after achondroplasia and hypochondroplasia were mapped, the achondroplasia mutation in *FGFR3* was discovered (37, 38). Astonishingly, all of the patients screened had the same nucleotide disrupted—the guanosine at position 1138 of the *FGFR3* transcript was substituted with an adenosine or a cytosine resulting in a missense mutation that substituted an arginine for a glycine at codon 380 (G380R). The glycine residue lies within the

transmembrane domain of the receptor. At the time, the detrimental effects of the mutation were speculated to cause a dominant-negative effect, but it was not clear how this would occur. Soon after the publication of these findings, a large-scale screen of an additional 154 achondroplasia patient samples was published and confirmed the importance of residue 380—all of these patients had the same missense mutation, G380R. The guanosine's location in a CpG island is speculated to make this region a hot spot for mutagenesis (37), but there is no clear molecular explanation as to what makes this nucleotide so vulnerable. Subsequently, normal FGF signaling was shown to have an inhibitory affect on the regulation of skeletal growth (39), and the molecular mechanism underlying achondroplasia was realized to be constitutive activation of FGFR3 by the G380R substitution (40, 41).

Both types of thanatophoric dysplasia and hypochondroplasia are caused by mutations in *FGFR3*. Missense mutations in the extracellular portion (R248C) and the second kinase domain (K650Q) of FGFR3, cause thanatophoric dysplasia types I and II, respectively (42). Thanatophoric dysplasia is also caused by point mutations that disrupt the normal termination codon, resulting in read-through translation into the 3' untranslated region of the *FGFR3* transcript (43). Patients with hypochondroplasia are negative for the *FGFR3* G380R mutation (44), but have a missense mutation (N540K) in the first kinase domain of the receptor (45).

The time elapsed from the initial mapping of the achondroplasia mutant locus to the discovery of all of these *FGFR3* mutations was only about 1 year. This timeline is impressive given the technology of the time. Importantly, all of these studies took place before the release of the sequence of the human genome. *FGFR3* mutations cause additional types of skeletal dysplasias and the related family members *FGFR2* and *FGFR1* are also involved (7, 8). The rate of mutation discovery has accelearated, given the availability of the reference genome sequence

and high-throughput genomic mapping and sequencing technologies, which have revolutionized how these types of studies are conducted today.

A Geneticist's Best Friends: High-Throughput Technologies and Mutation Discovery

Table 1.2 outlines the genetic causes of disorders that affect skeletal growth and/or development that have been discovered since the last edition of the Nosology of Skeletal Disorders. Of the 43 studies included, 36 of them (84%) make use of some type of high-throughput technology, including whole genome SNP mapping, comparative genomic hybridization arrays, whole exome or genome sequencing, and targeted enrichment of a locus followed by next-generation sequencing (Table 1.2). More than half of the mutations listed (65%) were discovered through the use of some form of next-generation sequencing of patient genomic DNA samples. Clearly, the strategy has changed.

Approximately half the mutations in Table 1.2 were discovered by exome sequencing. As more efficient and cost-effective sequencing technologies are developed (46, 47), whole genome sequencing will ultimately become the preferred strategy, likely eliminating genetic mapping and exome sequencing. Most patients will have their genomes sequenced, and the unique variants that are predicted to affect function will be confirmed by Sanger sequencing technology (47). We are truly in an age of revolutionary genomic analysis, which will substantially aid in the diagnosis, understanding, and treatment of many genetic disorders (46), including those that affect the skeleton.

How Mouse Models Impact Skeletal Dysplasia Research

Studies conducted in mice have contributed to understanding the genetic basis of skeletal dysplasias, the pathophysiology of disease and therapeutic testing (48-57). In many of these studies, the description of the mouse model was soon followed by publications of mutations in

Table 1.2 Causative Mutations of Skeletal Disorders Discovered After the Publication of the 2011 Nosology

Primary Cilium

Gene Name	Skeletal Dysplasia	Chr.	Mutations	Inheritance	Gene Function
NIN (58)	Novel Microcephalic Primordial Dwarfism	14q22.1	p.Q1222R p.N1709S	AR	Centrosome-mediated asymmetric cell division
POC1A (59)	SOFT Syndrome	3p21.1-3p21.31	p.L171P	AR	Centrosome maintenance, Golgi assembly and retrograde trafficking
POC1A (60)	SOFT Syndrome	3p21.2	p.R81X	AR	Proper mitotic spindle orientation, cilogenesis,
TCTN3 (61)	Mohr-Majewski Syndrome	10q24.1	p.E408X p.Y217SfsX6 p.Q443X p.E189VfsX52 p.L450SfsX14 p.G314R	AR	Cilogenesis, Hedgehog signaling
IFT140 (62)	Mainzer-Saldino Syndrome	16p13.3	c.2399+1G>T p.G163G p.E164fsX10 p.G212R p.I233M p.Y311C p.E664K	AR	Ciliogenesis, part of IFT-A complex (retrograde ciliary transport)
KIF2 (63)	Spondyloepimetaphyseal dysplasia with joint laxity, Type II	16p11.2	p.P148L p.R149Q p.R149L	AD	Not known. Speculated role in intracellular trafficking or cilia transport
KIF22 (64)	Spondyloepimetaphyseal dysplasia with joint laxity, Type II	16p11.2	p.P148S p.P148L p.R149Q	AD	Not known. Speculated role in primary cilium and hedgehog signaling
WDR19 (65)	Sensenbrenner Syndrome	4p14	p.L710S p.A1103X	AR	IFT-A complex, retrograde ciliary trafficking, ciliogenesis
WDR19 (65)	Jeune Syndrome	4p14	p.L7P	AR	IFT-A complex, retrograde ciliary trafficking, ciliogenesis
B9D2 (56)	Meckel Syndrome	19q13.2	p.S101R	AR	Ciliogenesis, ciliary protein localization, Hh signaling
WDR35 (66)	Short-Rib Polydactyly Syndrome Type V	2p24	Deletion of Exon 5 p.R545X p.W261R	AR	Ciliogenesis and cilium maintenance

Gene Name	Skeletal Dysplasia	Chr.	Mutations	Inheritance	Gene Function
NEK1 (67)	Short-Rib Polydactyly Syndrome Type II	4q32.1-34.3	p.R127X c.869-2A>G p.N547KfsX2	AR	Serine/Threonine Kinase, DNA repair, cell cycle progression, ciliogenesis, cilium maintenance, retrograde ciliary trafficking
TMEM216 (68)	Meckel Syndrome	11p12-q13.3	p.L114R p.T78KfsX30 p.R85X	AR	Ciliogenesis, cilium maintenance, planar cell polarity signaling
Signaling Pathways					
Gene Name	**Skeletal Dysplasia**	**Chr.**	**Mutations**	**Inheritance**	**Gene Function**
INPPL1 (69)	Opsismodysplasia	11q13.4	p.P659L p.E258AfsX45 p.A13RfsX62 p.T563GfsX3 p.S182X p.G9WfsX13 p.Q251H p.R691W	AR	AKT-PI3K Signaling modulation
INPPL1 (70)	Opsismodysplasia	11q13.4	p.R949X p.Q93PfsX3 p.P659S p.R401W p.F722I p.R907X p.I616YfsX14 p.T443IfsX23 p.W688K p.E32MfsX77	AR	AKT-PI3K Signaling modulation
CDKN1C (13)	IMAGe Syndrome	11p15	p.F276V p.F276S p.R279P p.D274N p.K278E	AD Maternally imprinted	Inhibition of cell cycle progression
PDE4D (14)	Acrodysostosis 2	5q12.1	p.Q228E p.E590A p.G673D	AD	Degradation of cAMP/inhibiting signaling pathway
PDE4D (71)	Acrodysostosis 2	5q12.1	p.S190A p.P225T pF226S p.T587P	AD	Degradation of cAMP/inhibiting signaling pathway
FGFR2 (72)	Bent Bone Dysplasia-FGFR2 Type	10q26.13	p.M391R p.Y381D	AD	Proper regulation of chondrocyte proliferation and differentiation
SMAD4 (16)	Myhre Syndrome	18q21.2	p.I500T p.I500V p.I500M	AD	TGF-β and BMP signaling modulation
AKT1 (73)	Proteus Syndrome	14q32.33	p.E17K	AD Somatic	PI3K-AKT signaling, cell

Gene Name	Skeletal Dysplasia	Chr.	Mutations	Inheritance	Gene Function
				Mosaicism	proliferation, and cell growth
FBN1 (74)	Acromicric Dysplasia	15q21.1	p.A1728T p.S1722C p.S1750R p.G1726V p.Y1699C p.Q1735dup p.D1758V p.Y1700C p.M1714R	AD	Integrin and TGF-β signaling
FBN1 (74)	Geleophysic Dysplasia	15q21.1	p.Y1696C p.Y1699C p.G1762S p.C1706Y p.C1719W p.A1728T p.Y1699D p.C1733Y	AR	Integrin and TGF-β signaling
PRKAR1A (17)	Acrodysostosis 1	17q24.2	p.R368X	AD	PKA/cAMP mediated signaling
SERPINF1 (75)	Osteogenesis Imperfecta Type IV	17p13.3	p.Y109SfsX5 p.Y232X p.Q378X	AR	Secreted inhibitor of angiogenesis
IHH (76)	Syndactyly Type I	2q35	Microduplication of long-acting enhancer		Regulation of chondrocyte proliferation and hypertrophy

Intracellular Protein Trafficking (Golgi, Endoplasmic Reticulum)

Gene Name	Skeletal Dysplasia	Chr.	Mutations	Inheritance	Gene Function
TMEM165 (77)	Congenital Disorder of Glycosylation Type II	4q12	c.792+182G>A p.R126C c.910G>A	AR	Glycosylation in the Golgi
IMPAD1 (78)	Chondrodysplasia with Joint Dislocations	8q12.1	p.D177N p.T183P	AR	AMP Formation

Transcription Factors

Gene Name	Skeletal Dysplasia	Chr.	Mutations	Inheritance	Gene Function
MAFB (79)	Multicentric Carpotarsal Osteolysis	20q12	p.P54L p.P59L p.T62P p.P63R p.S66C p.S69L p.S70A p.S70L p.P71S	AD	Negative regulation of osteoclasts

Epigenetic Regulation

Gene Name	Skeletal Dysplasia	Chr.	Mutations	Inheritance	Gene Function
KAT6B (15)	Genitopatellar Syndrome	10q22.2	p.K1263RfsX7 p.K1258GfsX13	AD	Histone acetyltransferase
KAT6B (80)	Say-Barber-Biesecker Variant of Ohdo Syndrome (SBBYSS Syndrome)	10q22.2	p.S1469FfsX18 p.I1792QfsX12 p.Q1007RfxX5 p.Q1357X	AD	Histone acetyltransferase

			p.S1402CfsX5 p.R1912X p.T1677MfsX38 p.Q1737HfsX41 p.Y176X p.V1638AfsX27 p.R1797X p.Q360K		

Translation/Post-Translational Gene Regulation

Gene Name	Skeletal Dysplasia	Chr.	Mutations	Inheritance	Gene Function
miR-17~92 (81)	Feingold Syndrome	13q31.3	Microdeletions	AD	Unknown
CCDC8 (82)	3-M Syndrome	19q13.2-q13.32	p.K29X p.K205EfsX58	AR	Ubiquitin mediated protein degradation and IGF-1 levels

Matrix Components

Gene Name	Skeletal Dysplasia	Chr.	Mutations	Inheritance	Gene Function
COL9A2 (20)	Stickler Syndrome	1p34.2	p.N281QfsX70	AR	Extracellular matrix

Miscellaneous

Gene Name	Skeletal Dysplasia	Chr.	Mutations	Inheritance	Gene Function
ATRIP (83)	Seckel Syndrome	3p21.31	p.R760X	AR	DNA Repair
PAPSS2 (84)	Brachyolmia	10q23.2	p.A113GfsX18	AR	Catalyzes formation of sulfate donor PAPS
ABCC9 (85)	Cantu Syndrome	12p12.1	p.A478V p.C1043W p.R1154W p.R1154Q	AD	ATP-sensitive potassium channel
RBBP8 (86)	Seckel Syndrome	18q11.31-11.2	p.T763SfsX20	AR	DNA Repair
ORC4 (87)	Meier-Gorlin Syndrome	2q22.3-23.1	p.Y174C c.874_875insAACA	AR	Subunit of the origin recognition complex, DNA replication
ORC1 (88)	Microcephalic Primordial Dwarfism	1p32.3	p.F89S p.R105Q p.E127G p.R720Q	AR	Member of origin replication complex, DNA replication
ORC1 (89)	Meier-Gorlin Syndrome	1p32.3	p.R105Q p.V667QfsX24 c.874_875insAACA	AR	Subunit of the origin replication complex, DNA replication
ORC4 (89)	Meier-Gorlin Syndrome	2q22.3-23.1	p.Y174C p.A292fsX19	AR	Subunit of the origin replication complex, DNA replication
ORC6 (89)	Meier-Gorlin Syndrome	16q11.2	p.F86X p.Y232S	AR	Subunit of the origin replication complex, DNA replication
CDT1	Meier-Gorlin Syndrome	16q24.3	p.A66T	AR	Recruited to fully

			p.Q117H p.Q361X p.R453W p.R462Q p.Y520X		assembled pre-replication complex
CDC6 (89)	Meier-Gorlin Syndrome	17q21.2	p.T323R	AR	Recruited to fully assembled pre-replication complex
BANF1 (90)	Nestor-Guillermo Progeria Syndrome	11q13.1	p.A12T	AR	Nuclear lamina
RNU4ATAC (91)	Microcephalic Osteodysplastic Primordial Dwarfism Type I (MOPD I)	2q14.2	g.30G>A g.51G>A g.55G>A g.111G>A	AR	RNA splicing
RNU4ATAC (92)	TALS Developmental Disorder (MOPD I)	2q14.2	g.51G>A g.50G>A g.50G>C g.53C>G	AR	RNA splicing
POP1 (93)	Novel Skeletal Dysplasia	8q22.2	p.G583E p.R513X	AR	RNA processing

human patients that cause a similar skeletal phenotype. Recently, an ENU-induced mutation in

mice was found to be a model of achondrogenesis type 1A in humans (57). This autosomal

recessive mutation caused perinatal lethality, severely disrupted endochondral ossification,

greatly reduced the mineralization of skeletal elements, and disturbed the trafficking of

extracellular matrix proteins, resulting in acute intracellular stress in affected chondrocytes.

Mapping of the mutant locus to mouse chromosome 12 was conducted using a SNP array, and

was subsequently winnowed down to a 3.7 Mb interval. Screening of candidate genes in the

interval led to the discovery of a nonsense mutation (c.5003T→A, p.L1668X) in *Trip11*, which

encodes GMAP-210, or Golgi microtubule-associated protein 210. Due to the overlapping

phenotypic characteristics between the *Trip11*^{-/-} mice and achondrogenesis type 1A in humans,

the authors considered *Trip11* as a candidate gene for this form of skeletal dysplasia. They

screened 10 patients diagnosed with achondrogenesis type 1A for mutations in *Trip11*, and all 10

of them harbored mutations in this gene. Clearly, the mouse can contribute to the genetic

diagnosis of patients with skeletal dysplasias because of the phenotypic similarities.

The true power of mouse models of the skeletal dysplasias is in unraveling the molecular mechanisms that lead to the pathology and for testing potential therapies. The data collected from skeletal dysplasia patients are usually limited to measurements or samples that can be gathered with minimal invasiveness: radiographs, photographs, height, weight, hormone measurements, and isolation of skin fibroblasts, blood leukocytes and genomic DNA. If the patient is affected with a lethal form of skeletal dysplasia, and the investigators have consent to collect tissue, there may be additional analyses performed on the tissues collected, including histological analysis of the growth plate. The mouse models provide researchers with accessible tissue throughout development and the potential for assessing genetic interactions with genetic complementation studies (94, 95). Thus, mouse studies have contributed greatly to our understanding of how gene mutations result in the growth defects and skeletal anomalies.

Recent development of pharmacologic therapies to treat skeletal dysplasias has relied heavily on mouse models for testing efficacy and efficiency (96-102). Developing a therapy for achondroplasia is a top priority, given that it is the most common form (2). Two main approaches are being taken: thwarting the over-activity of the mutant receptor directly by inhibiting FGFR3 (96, 100), or treating with C-type natriuretic peptide (CNP), the ligand for an opposing pathway. Supplementation with C-type natriuretic peptide (CNP), the ligand for natriuretic peptide receptor 2 (NPR2), inhibits the activation of the MEK/ERK MAPK pathway, which lies downstream of FGFR3 activation (103). The inhibition of MEK/ERK occurs through the generation of cyclic GMP, which inhibits RAF-1 and leads to inhibition of the downstream components of the pathway. These mechanistic insights are supported by experiments conducted on chondrocyte cell lines (103), and our recent demonstration of ERK pathway overactivation in mice with a loss-of-function mutation in *Npr2* (102).

CNP treatment improves growth in a mouse model of achondroplasia (96, 104-106).

Patients with loss-of-function mutations in the CNP receptor, *NPR2,* have acromesomelic

dysplasia, Maroteaux type (AMDM) (107), and would obviously not benefit from this mode of

therapy. We took advantage of a mouse model of AMDM, known as the *peewee* mouse

($Npr2^{pwe/pwe}$) to test the efficacy of drugs that act downstream of *Npr2.*   Inhibition of the

MEK/ERK MAPK pathway improved fetal tibia growth in cultures (102). This type of

intervention may be adapted as a therapy for AMDM patients. This illustrates the power of

mouse models to understand of the pathophysiology of skeletal dysplasias and to assess

treatments.

Signaling Pathways Implicated In Skeletal Dysplasias

Several signaling pathways are known to regulate a chondrocyte's transition through all

three zones of the growth plate (Figure 1.2). Indian hedgehog (IHH), Parathyroid hormone-

related peptide (PTHrP), Fibroblast growth factor (FGF), C-type natriuretic peptide (CNP), TGF-

beta, Bone Morphogenetic Protein (BMP), Notch, and Wnt (canonical and non-canonical)

signaling pathways all aide and guide chondrocytes properly through the growth plate (1, 3, 7)

(Figure 1.2). The function of these signaling pathways in growth, patterning, and mineralization

are illustrated in Figure 1.2 and have been reviewed extensively (1, 3, 7).   We will discuss

selected recent genetic discoveries in the arena of signal tranduction and skeletal dysplasia.

Mutations in signaling-associated genes continue to be discovered in many forms of

skeletal dysplasia. Opsismodysplasia patients have been found to have loss-of-function

mutations in *INPPL1*, which encodes SHIP2 and is a mediator of signaling through the

phosphotide-inositol phosphate pathway (69, 70, 108). Mutations have been uncovered in the
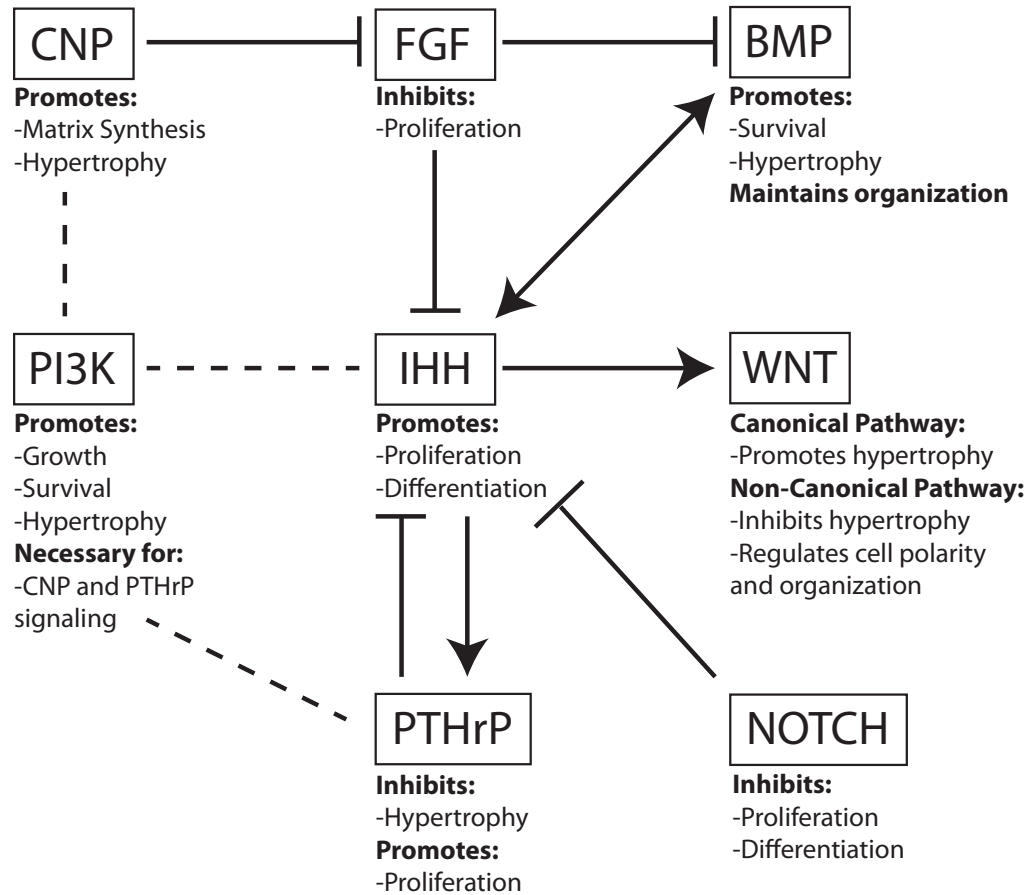
Figure 1.2. Interaction of signaling pathways in the growth plate. A number of signaling pathways are active in the various zones of the growth plate, and many of them exhibit cross-talk with one another. The combination of these signals allows the cells within the growth plate to respond accordingly depending on where and when they encounter activation of the pathway. Arrows indicate an activation of one pathway by another. A line with a bar-shaped arrowhead indicates inhibition of that pathway. Finally, dashed lines indicate that there is evidence that there is cross talk between the pathways, but the nature is not clear. For example, PI3K is thought to affect CNP, IHH, and PTHrP signaling pathways. Many of these pathways also have been implicated in many different forms of skeletal dysplasia. (CNP: C-type natriuretic peptide, FGF: Fibroblast growth factor, BMP: Bone morphogenetic protein, PI3K: Phosphoinositide-3 Kinase, IHH: Indian hedgehog, PTHrP: Parathyroid hormone related peptide)

PTHRP-mediated cyclic AMP (CAMP) signaling pathway that cause acrodysostosis (14, 17, 25,

26, 71). Novel mutations in *FGFR2* cause bent-bone dysplasia (72), and the mutations in the

TGFβ-BMP signaling effector *SMAD4* that have been shown to cause Myhre syndrome (16, 109).

Two skeletal disorders, IMAGe and Proteus syndrome, are caused by mutations in genes involved in critical signaling pathways (13, 73). These examples underscore the importance of the mode of inheritance of the causative mutation in the development of a patient phenotype.

IMAGe Syndrome: The Importance of Imprinting

IMAGe Syndrome is characterized by Intraunterine growth restriction, Metaphyseal dysplasia, Adrenal hypoplasia congenita, and Genital abnormalities (IMAGe) (24). The IMAGe phenotype encompasses many different organ systems and leads to hypoplasia in the affected tissues. The skeletal abnormalities present in these patients are variable, and include defects at the level of the growth plate (metaphyseal dysplasia, epiphyseal dysplasia, short arms and legs) and the bone tissue itself (osteopenia, delayed bone age) (13, 24). This disorder is caused by mutations in *CDKN1C*, which encodes cyclin dependent kinase inhibitor 1 C, also known as $p57^{Kip2}$. *CDKN1C* is imprinted, and the maternal copy is expressed. Thus, the lack of expression of the paternal allele contributes to the apparent autosomal dominant inheritance from the mother. This phenomenon was observed in all the patients screened in a large five-generation Argentinian family.

The IMAGe mutations (Table 1.2) occur specifically in the proliferating cell nuclear antigen (PCNA)-binding domain of CDKN1C. This domain confers ubiquitin-targeted protein degradation of CDKN1C after PCNA-binding (13). The mutant form of CDKN1C does not bind PCNA, resulting in abnormal stabilization of the cell-cycle inhibitor and the hypoplasia phenotypes. CDKN1C blocks entry into S-phase, and expression of the mutant form in the proliferative zone could profoundly inhibit the rate of chondrocyte proliferation. Transcriptional

activation of *CDKN1C* by C/EPBβ is thought to regulate the transition from proliferation to hypertrophic differentiation in the growth plate (110). Inhibition of IMAGe growth plate chondrocyte division could cause cell cycle exit and premature differentiation into hypertrophic chondrocytes, resulting in dwarfism. Targeted inhibition of CDKN1C in IMAGe patients could be therapeutic, if the problems of specificity and delivery could be overcome. Parathyroid hormone-related hormone (PTHRP), is another therapeutic candidate because it promotes chondrocyte proliferation, and is thought to downregulate p57 (111).

Proteus Syndrome: A Disorder of Mosaicism

The genetic etiology of Proteus Syndrome is a recent, highly celebrated discovery because of the role of somatic mosaicism. Proteus Syndrome is a debilitating disorder characterized by patchy, asymmetrical hyperplasia that affects a variety of tissues, including bone and connective tissue (73, 112). The disorder is incredibly rare, occurring in <1:1 million individuals. The asymmetric nature of the disorder led to the hypothesis that it results from a *de novo* mutation occurring early in development, and only affecting a portion of cells in the embryo. The mutation would cause abnormal cell division and growth. This phenomenon is known as somatic mosaicism, where patients are composed of two populations of cells: normal cells, and cells that harbor the causative mutation. Furthermore, cases are typically sporadic, lending more support to the somatic mosaicism hypothesis.

The highly progressive rate of asymmetrical hyperplasia in Proteus Syndrome patients begins approximately a year after birth (112). The bones of the limbs are particularly affected, with the hyperplasia altering normal bone patterning and potentially leading to immobility of joints, and/or bowing and rotation of the long bones. There is also a high rate of premature death

21

(20%), which is typically due to venous thrombosis and pulmonary embolism. Vascular abnormalities and tumors also occur (73, 112).

Inactivating mutations in *PTEN*, a tumor suppressor gene involved in the PI3K-AKT pathway, had been suspected to cause Proteus Syndrome, and were recently shown to cause a similar condition known as SOLAMEN (Segmental Overgrowth, Lipomatosis, Arteriovenous Malformation, and Epidermal Nevus) syndrome (73, 113). The affected areas in SOLAMEN patients are nullizygous for *PTEN*, the result of inheriting a germline mutation in *PTEN*, and a *de novo* somatic mutation in the affected area. Because *PTEN* inhibits activation of the AKT kinase, *PTEN* deficiency leads to over-activation of the PI3K-AKT signaling pathway in the affected areas, results in increased cell proliferation and reduced apoptosis (73, 113).

Proteus and SOLAMEN Syndrome are caused by disruptions in the same signaling pathway. Tissues affected by Proteus Syndrome harbor a missense mutation (c.49G$\rightarrow$A, p.Glu17Lys) in *AKT1* (73). Western blots demonstrated an increase in phophorylated AKT1 in affected areas, which is indicative of over-activation of the PI3K-AKT pathway. Thus, Proteus Syndrome patients are somatic mosaics with a gain-of-function mutation in *AKT1* in their affected tissues and SOLAMEN Syndrome patients are somatic mosaics with loss of function in PTEN, leading to AKT activation (113).

How does overactive AKT1 cause the skeletal phenotype? The role of PI3K-AKT signaling in bone is controversial (114). Most of the data are consistent with the pathway acting to promote hypertrophic differentiation of growth plate chondrocytes. Over-activation of this pathway in mice through the conditional loss of *PTEN* activity leads to an overgrowth of the skeletal elements, caused by an accelerated rate of hypertrophic differentiation (114-117). Possible downstream effectors of the PI3K-AKT pathway in the growth plate include mTOR,

SOX9, IHH, RUNX2, as well as COL2A1 and proteoglycans. While more work is necessary to define PI3K-AKT pathway function(s) in bone, it is clear that the role of AKT is primarily to promote endochondral ossification in both humans and mice (73, 114). In Proteus Syndrome patients, the mutant protein has the ability to cause accelerated, disorganized bone growth in asymmetric patches, leading to the debilitating phenotype (112). Inhibitors of AKT1 or some of the downstream effectors may offer potential therapeutic avenues.

INPPL1 Mutations in Opsismodysplasia

Opsismodypslasia is an autosomal recessive skeletal disorder that results in delayed bone age, extreme shortening of the bones in the hands and the feet, and short long bones. Other features include craniofacial anomalies and macrocephaly, with variable viability. The growth plates are typically highly disorganized, and the number of hypertrophic chondrocytes is reduced. Mutations in the inositol polyphosphate phosphatase-like 1 gene (*INPPL1*) cause opsismodysplasia (69, 70). *INPPL1* encodes SHIP2, which acts in the phophostidyl inositol signaling pathway (108). SHIP2 catalyzes the reaction to form PI(3, 4)P2 from PI(3, 4, 5)P3. This reduces the amount of PI(3, 4, 5)P3 available as a secondary messenger, causing accumulation of PI(3, 4)P2. PI(3, 4)P2 can act as a context-dependent secondary messenger affecting signaling by insulin, EGF and FGF (108).

Mice with *Inppl1* loss-of-function are resistant to obesity, smaller than their littermates, and have distinctive craniofacial abnormalities (118). The skeletal phenotypes in these mutant mice are similar to those reported in opsismodysplasia patients. Thus, these mice could be used to uncover the mechanistic details downstream of *Inppl1* loss-of-function. SHIP2 is thought to interact with the EGF and FGF signaling pathways (108, 119). Loss of *inppl1* in zebrafish leads to an over-activation and broader expression patterns of downstream effectors of the FGF

pathway (108, 120). These observations support a role for *INPPL1* in the inhibition of FGF

signaling, which may explain the skeletal phenotype to some extent, should it mediate signaling

downstream of *FGFR3*. This also means that opsismodysplasia patients might benefit from the

therapies being developed for achondroplasia patients, which are based on limiting the effects of

overactive FGFR3.

cAMP signaling and Acrodysostosis

Mutations in effectors of cAMP-dependent signaling processes have been discovered in

cases of acrodysostosis (14, 17, 71). This disorder exhibits autosomal dominant inheritance, and

has variable presentation that can affect the skeleton, nervous system, and/or endocrine systems

(25, 26). Patients typically present with midface hypoplasia, brachydactyly, spinal stenosis, and

short stature. Resistance to parathyroid hormone, thyrotropin, and occasionally the

gonadotropins has been observed in acrodysostosis patients. Males exhibit hypogonadism, and

females can experience menstrual cycle disruption.

The PTHRP receptor and many other hormone receptors critical for growth are coupled

to G-proteins that activate adenylate cyclases, and generate the secondary messanger cyclic AMP

(cAMP). Thus, the strategy of sequencing genes that regulate signaling events downstream of G-

protein coupled receptors led to the discovery of mutations in the cyclic AMP-dependent

regulatory subunit of protein kinase A (*PRKAR1A*) in acrodysostosis patients (17). Mutations in

PRKAR1A cause reduced PKA activity, and reduced phosphorylated CREB, a downstream

effector of PKA signaling. This is most likely due to defective binding of cAMP by the

regulatory subunit, which renders it incapable of dissociating from the catalytic subunit, resulting

in loss of function (25).

Mutations in cyclic AMP-specific phosphodiesterase 4D (PDE4D) also cause

acrodysostosis (14, 71). Mutations in *PDE4D* are thought to reduce the activity of the enzyme

by acting as a dominant negative, interfering with PDE4D dimer function. The loss of

phosphodiesterase activity leads to an increase in cAMP levels and desensitization of the cAMP

pathway in the affected tissues.

After the genetic etiologies of acrodysostosis were uncovered, some potential genotype-

phenotype correlations have emerged (25, 26). Hormone resistance is reported more often in

patients with mutations in *PRKAR1A* than in individuals with *PDE4D* mutations. Mutations in

PDE4D appear to cause varied degrees of intellectual disability. Mutations in *PRKAR1A* tend to

have a more pronounced effect on adult stature. All the patients with mutations in this gene have

been reported to be <-2.5 SD below the mean height, while less severe growth insufficiency is

associated with mutations in *PDE4D*.   The sample size is small, and there are exceptions in each

group, but the emerging correlations may help predict the course of disease.

FGFR2 and Bent Bone Dysplasia

The function of *FGFR2* in skeletal development has emerged from studies of human

patients. Gain-of-function mutations in *FGFR2* cause a number of craniosynostosis syndromes

(7), while loss-of-function mutations are reported in patients with Lacrimoauriculodentodigital

syndrome (LADD). LADD patients are heterozygous for the mutation, indicating a

haploinsufficiency disorder, and the skeletal defects mainly affect the digits. Based on these

studies, the skull and the digits appear to be the two components of the skeleton most sensitive to

changes in signaling through *FGFR2*.

FGFR2 mutations can also cause a perinatal lethal form of skeletal dysplasia, known as

Bent Bone Dysplasia-*FGFR2* type (72). Aspects of the phenotype include bent long bones,

osteopenia, craniosynostosis, dysmorphic facies, poorly mineralized calvaria, hypoplasia of the clavicle and pubic bone, and prenatal teeth. Hypertrophic chondrocytes in the growth plates of these patients were smaller than control hypertrophic chondrocytes. Two different *FGFR2* missense mutations each substitute a charged amino acid for a hydrophobic amino acid within the transmembrane domain of the receptor. Both of these substitutions are predicted to cause loss of a transmembrane domain. Experiments support the conclusion that this mutation impairs receptor trafficking to the plasma membrane, leading to a reduction in activated ERK1/2. Thus, loss of function of *FGFR2* causes Bent Bone Dyplasia. These cases demonstrate the requirement for *FGFR2* signaling in the long bones of the more proximal elements of the appendicular skeleton and the skull.

SMAD4 and Myhre Syndrome

Mutations in a number of components of the TGFβ-BMP signaling pathway are associated with forms of skeletal dysplasia (7, 121). Mutations in SMAD4, a co-mediator SMAD for the downstream effectors (R-SMADS) of TGFβ and BMP signaling, have been discovered in patients with Myhre syndrome. First described in 1980, this dominant syndrome results in short stature, brachydactyly, muscular build, distinctive facies, thickened skin, and limited mobility of the joints (16, 122, 123). Additional features are frequently reported, including deafness, cryptorchidism, intellectual disability, hypertension, heart defects and eye defects.

Interestingly, all known mutations discovered in Myhre syndrome patients to date alter the same residue in *SMAD4*: Isoleucine 500 (16, 109, 124) (Table 1.2). There is much speculation as to how mutations in this residue are affecting the function of this critical mediator of TGFβ-BMP signaling. The mutations increase the level of phosphorylated SMAD2/3 and

SMAD1/5/8 in the nucleus, meaning that the mutant *SMAD4* is likely capable of allowing nuclear entry of the SMAD complex (16). *SMAD4* is ubiquitinated on a nearby residue (16, 109), and the mutations lead to a decrease in ubiquitinated *SMAD4* (16). Furthermore, the mutation affected the transcript levels of TGFβ and BMP target genes, lending support to the hypothesis that mutant *SMAD4* is most likely capable of entering the nucleus, but is defective in modulating transcription of its target genes. This could be due to the fact that the domain of *SMAD4* that harbors the mutation, the MAD homology domain, contains two sites that associate with known receptor SMADS, SMAD2 and SMAD3 (109). It is surmised that introduction of the various substitutions for the isoleucine residue would render one of these sites defective, hampering the ability of SMAD4 to bind to R-SMADS, which would affect the complex's ability to act as a transcriptional mediator (109). This could have profound, wide spread effects throughout the body, and further experiments are required to determine the molecular pathogenesis and specificity of SMAD4 mutations that cause this genetic disorder.

Some aspects of TGFβ and BMP signaling in the growth plate remain enigmatic. More is known about BMP signaling than TGFβ signaling in this context. Loss of BMP signaling affects hypertrophic differentiation, as growth plates from BMP-deficient animals exhibit reduced hypertrophic zones. These pathways may also play a role in organizing the growth plate, which has been shown to be critical for proper skeletal growth (125). In the context of Myhre syndrome, it is possible that the disruption of the R-SMAD-SMAD4 association affects the rates of proliferation and differentiation of chondrocytes in the growth plate, and/or the organization of the growth plate (125), leading to the short stature noted in Myhre syndrome patients. Further molecular inquiries are necessary to determine if this is true.

Epigenetics: Mutations in Histone Acetyltransferase *KAT6B/MYST4* Cause a Variety of Disorders

The modification of histones by chromatin modifying enzymes maintains cellular identity and regulates cell fate transitions during differentiation (126, 127). These processes are important to ensure proper organogenesis and growth. Chromatin modifying enzymes include histone methyltransferases, histone demethylases, histone acetyltransferases (HATs), histone deacetylases (HDACs), and enzymes that facilitate the phorphorylation and ubiquitination of histones (126-128). *HDAC4* has been shown to affect the skeleton (129, 130).

Mutations in *KAT6B*, a member of the MYST family of histone acetyltransferases, cause two distinct disorders that affect skeletal growth (15, 80). Mutations in the 3' end of *KAT6B* have been reported in patients with Say-Barber-Biesecker-Young-Simpson (SBBYS) Sydrome, or Ohdo Syndrome. This disorder causes intellectual disability and facial abnormalities, and distinct skeletal characteristics including hypoplastic or absent patellae, joint laxity, and abnormally long first digits. These patients are heterozygous for *de novo* mutations near the end of the last exon of the gene, which encodes a RUNX2-binding domain (80). RUNX2 is a homeodomain transcription factor that can regulate chondrocyte hypertrophy, and it is well known as the master regulator of osteoblast differentiation (1, 131). Thus, the skeletal phenotype in these patients could be due to defects in either or both cell types present in the skeletal elements.

Distinct loss of function mutations in *KAT6B* cause a related disorder known as genitopatellar syndrome (15). This form of skeletal dysplasia is relatively rare. The disorder encompasses intellectual disability, absence or hypoplasticity of the patellae, craniofacial abnormalities, and genital malformations. The causative mutations are *de novo* indels that cause

frameshifts or nonsense mutations at the start of the last exon of *KAT6B* (15). These mutant

forms of KAT6B lack the transcriptional activation domain and the RUNX2 binding domain.

The mutant transcript does not undergo nonsense-mediated decay, and it is possible that the

mutations of this exon in SBBYS and Genitopatellar syndrome patients cause KAT6B to act as a

dominant negative (15, 80). If this hypothesis is correct, it may explain the more severe

phenotypes seen in these latter two syndromes in comparison to a Noonan-like patient and a

hypomorphic allele of *Kat6b* in the mouse (80, 132). If mutant KAT6B is unable to acetylate

histones, a logical potential therapy would be histone deacetylase (HDAC) inhibitors to

counteract the loss of this function, provided the appropriate specificity could be achieved.

Clearly, *KAT6B* is another example of a gene that can cause multiple skeletal disorders when

mutated, and future studies will clarify this at the mechanistic level.

Could Mutations in miRNAs Cause Severe Short Stature?

Recently, the deletion of a miRNA cluster was associated with Feingold syndrome, a

disorder that can involve multiple organ systems, but the skeleton is consistently affected (133).

Short stature, microcephaly, and brachydactyly of the second and fifth digits of the hands, and

brachysyndactyly of the toes are the hallmark skeletal anomalies associated with this syndrome.

Previous work on human patients had mapped the interval to human chromosome 2p23-p24

(134). Subsequent analysis of human patients uncovered heterozygous mutations in *MYCN*, or

N-myc, which encodes the helix-loop-helix transcription factor v-myc myelocytomatosis viral

related oncogene (135). Prior to these discoveries, a locus distal to human chromosome 13q14

was hypothesized to be associated with Feingold syndrome (133), but evidence confirming a

second locus was lacking (134, 136). Five years later, a mouse lacking the miR-17~92 miRNA

locus had a homozygous phenotype that resembled Feingold Syndrome, and the human ortholog maps distal to 13q14 implicating it as a second locus (55).

Genomic DNA from Feingold patients negative for mutations in *MYCN* were analyzed by comparative genomic hybridzation (CGH) arrays to screen for disease causing copy number variations. These patients were heterozygous for microdeletions on human chromosome 13q31.3, a region that segregated with the phenotype in two families, and encompassed the miR-17~92 microRNA cluster (81). There is mounting evidence that *MYCN* directly activates transcription of this microRNA cluster (81, 137-141). The hemizygous loss of function of either *MYCN* or this miR cluster lead to very similar skeletal phenotypes in mouse and human (81, 142-144). An in depth molecular understanding of the mechanism underlying the roles of *MYCN* and this microRNA cluster in the pathophysiology of Feingold Syndrome will include defining the targets of these microRNAs. Discovering the essential role of miR-17~92 in skeletal development begs the question of whether other noncoding RNA mutations may cause skeletal dysplasia or other types of severe short stature.

The Primordial Dwarfisms

Many of the skeletal dysplasias are characterized by disproportionate bone growth, with long bones being the most affected (2, 145). Skeletal dysplasia patients also tend to have relatively normal-sized heads. Primordial dwarfism, on the other hand, causes a proportionate reduction in growth, similar to that caused by deficiencies in insulin-like growth factor 1 (IGF-1) or growth hormone (GH), both of which lead to proportionate short stature (145). Patients with IGF-1 deficiency and primordial dwarfism are smaller at birth, and are sometimes ascertained *in utero*, while GH deficiency is not manifested until later in life. Primordial dwarfism patients differ from most skeletal dysplasia patients in that they have a proportionate reduction in skull

size or microcephaly. Primordial dwarfism patients have severe short stature, with some

reaching only 1 meter as adults.

The primordial dwarfisms' phenotypic resemblance to GH/IGF-1 deficiency challenges

the current classification of disorders of skeletal growth. GH/IGF-1-deficient patients do not

have skeletal dysplasia. Their defects are systemic in nature, rather than local, as is the case with

achondroplasia patients (7). In addition, many growth defects attributable to GH/IGF-1

deficiency are treatable with supplementation, resulting a normal adult target height (146). This

is not the case for traditional skeletal dysplasia patients (2). Therefore, the primordial dwarfisms

represent an interesting genetic and physiological state. Causative mutations uncovered to date

regulate overall cell number, but do not affect endocrine processes (145). It is not clear whether

the differences in cell number are due to augmentation of cell death, a delay or reduction in cell

proliferation, or both. Mouse models and cell culture studies should clarify these genes' roles in

cases of primordial dwarfism.

There are several disorders that fall into the primordial dwarfism category: Seckel

syndrome, Meier-Gorlin Syndrome, and microcephalic osteodysplastic primordial dwarfism I-III

(MOPD I-III). A review of these disorders was recently published (145). We provide an

abbreviated description of each disorder below.

There are differences in the severity of various aspects of the phenotype in each of these

conditions (145). Seckel syndrome patients tend to have moderate to mild intellectual disability,

microcephaly, and distinctive facies. MOPD I/III causes curvature of the long bones, drastic

growth insufficiency, and early death by three years of age. This disorder also leads to skin

abnormalities and sparseness of hair. MOPD II is compatible with life, and patients have normal

intellect. They have a predisposition to developing vascular abnormalities and insulin resistance,

Table 1.3 Genetic Causes of the Primordial Dwarfisms			
Gene Category	**Genes Involved**	**Form of Primordial Dwarfism**	**Features**
DNA Repair	*ATR* (149) *ATRIP* (83) *RBBP8* (86) *CEP152* (150)	Seckel Syndrome	Moderate learning disability Marked Microcephaly>Height Reduction
DNA Replication	*ORC1* (88, 89, 148) *ORC4* (87, 89, 148) *ORC6* (89, 148) *CDT1* (89, 148) *CDC6* (89, 148)	Meier-Gorlin Syndrome	Normal Intellect Microcephaly Growth Variably Affected
Centrosome	*CENPJ* (151) *CEP152* (150) *PCNT* (152, 153) *NIN* (58) *POC1A* (59, 60) *ORC1* (88, 89, 148)	Seckel Syndrome Seckel Syndrome MOPD II Novel MOPD SOFT Syndrome Meier-Gorlin Syndrome	Mild Learning Disability-Normal Intellect Proportionate Microcephaly/height reduction
Splicing	*RNU4ATAC* (91, 92)	MOPD I	Severe Pleiotropic Phenotypes Neonatal Lethality

which can lead to type II diabetes. Meier-Gorlin syndrome causes hypoplasia or complete absence of the patellae, microtia, microcephaly, and can result in short stature, but the effect on growth is highly variable from patient to patient (147, 148). These characteristics are listed in Table 1.3.

Sequencing genomic DNA samples from patients with primordial dwarfism have yielded genetic aberrations in genes with diverse functions that are expected to affect all of the cells in the body (145) (Table 1.3). Seckel syndrome is associated with mutations in the DNA-damage response genes *ATR* (149), *ATRIP* (83), and *RBBP8* (86), as well as the centriole-associated genes *CPAP* (*CENPJ*) (151) and *CEP152* (150). MOPD II is caused by mutations in *PCNT*, a gene that encodes a pericentriolar protein involved in the generation of the mitotic spindle and centrosome maturation. Recently, a novel form of microcephalic primordial dwarfism has been associated with mutations in *NIN*, the gene that encodes another centrosomal protein ninein (58). Little is known about the function of ninein, although it is thought to be important in the

regulation of asymmetric cell division (154-156). Additionally, mutations in genes that encode

components of the origin recognition complex (ORC), which regulates the licensing of DNA

replication origins, are the cause of Meier-Gorlin Syndrome (87-89, 148) (Table 1.2 and 1.3).

Finally, MOPD I has been shown to be caused by mutations in *U4ATAC*, which is involved in

the splicing of U12 introns, a minor subset of introns present in a distinct grouping of genes in

the human genome (91, 92). Many of the genes that contain this type of intron are involved in

the processes highlighted above, and it is thought that the primordial dwarfism phenotype in

MOPD II is due to alterations in the splicing of specific transcripts that are required for proper

modulation of cellular growth and cell number (145).

Clearly, genes that encode DNA repair components, centrosomal proteins, and genes

involved in DNA replication have profound impacts on human growth when they are disrupted.

Genes within these categories should be considered as likely candidates in patients with novel

forms of primordial dwarfism or without mutations in the genes that have been previously

mentioned. Also, while a number of cellular processes are represented in these primordial

dwarfism-associated genes, one common theme is clear—these are all genes that feed into the

regulation of the cell cycle (Figure 1.3).

The phenotypes of individuals with primordial dwarfisms generally fall into two classes

that correspond with the two major types of genes involved: DNA repair and replication or

centrosome associated proteins. MOPD I is an exception, as the mutation in *U4ATAC* likely

disrupts a number of cellular functions, causing pleiotropic effects and early lethality. Mutations

in *ATR* and *CEP152* in Seckel syndrome patients cause similar phenotypes—moderate learning

disability and a more marked reduction in the size of the skull as opposed to an overall decrease

in height. In contrast, patients with mutations in *CENPJ* (*CPAP*) have clinical features similar to
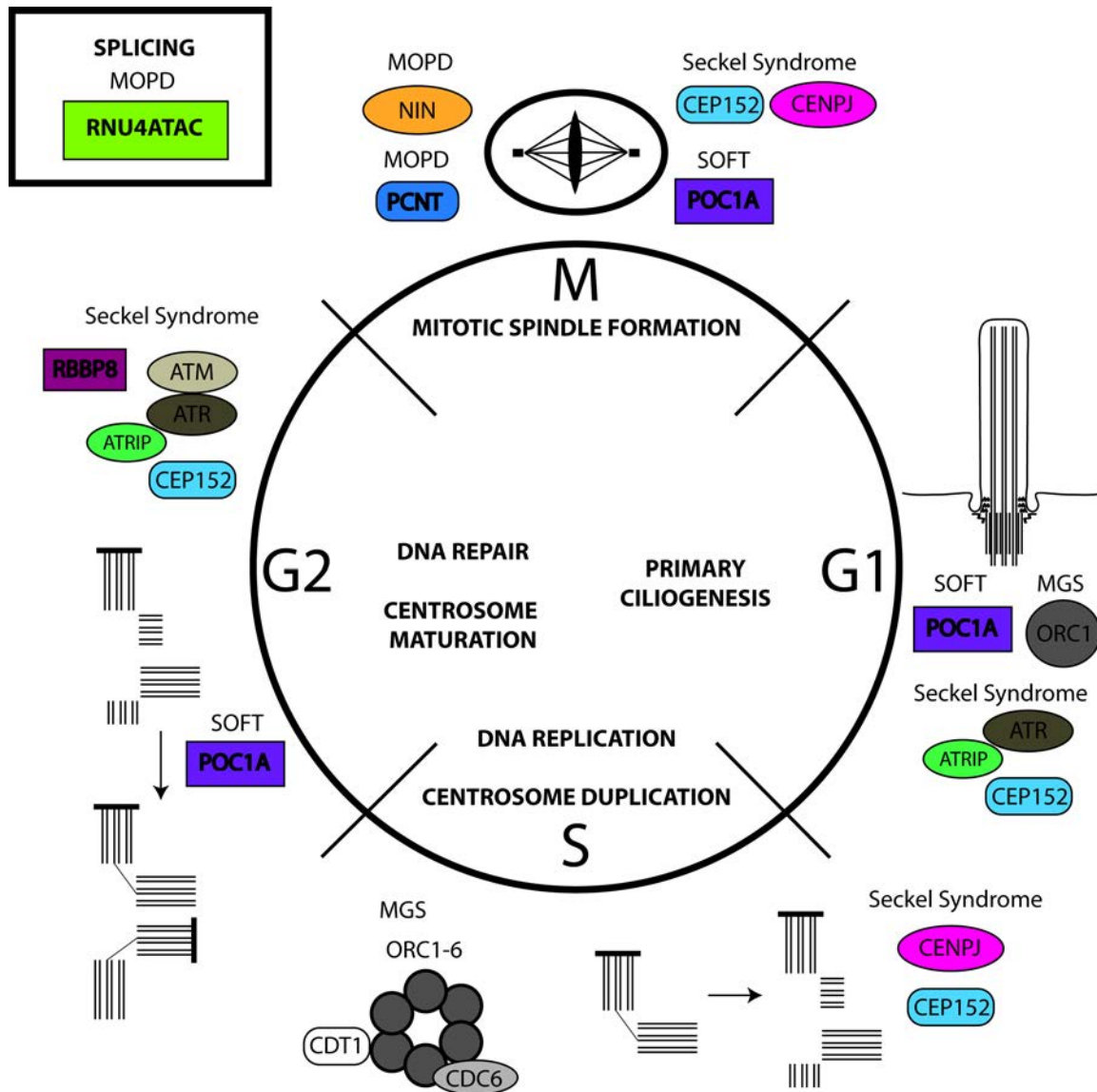
Figure 1.3. Cellular pathways disrupted in primordial dwarfism. Most genes implicated in primordial dwarfism [microcephalic osteodysplastic primordial dwarfism (MOPD) I/II, Seckel Syndrome, Meier-Gorlin Syndrome (MGS), Short stature, Onychodysplasia, Facial dysmorphism, and Hypotrichosis (SOFT) Syndrome] are involved in cell cycle regulation and cell division. These processes include: primary ciliogenesis (G1 phase), DNA replication and centrosome duplication (S phase), DNA Repair and centrosome maturation (G2 phase) and mitotic spindle formation (M phase). Many of the genes function in more than one phase of the cell cycle. Some genes affect the rate of progression through the cell cycle, and some lead to aneuploidy, probably because of defects in DNA repair or mitotic spindle formation. In some cases the cell cycle becomes disrupted after several rounds of cell division, due to disturbances in centriole duplication and/or maturation. All the processes listed involve replication and repair or maturation of the genome and the centrosome, except *RNU4ATAC*, but its critical role in splicing could disrupt one or more genes involved in cell cycle regulation or division.

MOPD II patients with mutations in *PCNT*, in that both groups of patients have a proportionate reduction in head size and body size. Intellectual disability in the Seckel *CENPJ* patients is mild, while MOPD II/PCNT patients have a normal intellect. ORC-associated proteins such as *ORC1* associate with the centrosome (157, 158), and mutations in *ORC1* cause more severe reductions in height and head circumference than any other cause of Meier-Gorlin syndrome (148, 158). All but one of these *ORC1* patients had normal intellect, and the one exception had mild intellectual disability.

Mutations in genes affecting centrosome biology apparently cause more severe dwarfism than genes involved in DNA repair and replication. Conversely, genes involved in DNA repair and replication tend to have a greater impact on intellectual development and size of the brain and skull. The effect of the centrosomal-associated genes on stature may be due to the requirement of the centrosome to form the primary cilium, a structure required to maintain the organization of the growth plate (4, 5, 9). There are exceptions to these general correlations between clinical features and the type of gene mutated. For example, mutations in the centrosomal protein encoded by *NIN* cause both severe short stature and profound intellecutal disability (58). Morpholino-induced knock down of NIN in zebrafish or loss of ninein in mice reduces the number of cells in a distinct part of the developing nervous system (154). While NIN deficiency does not appear to impact overall cell division, it could affect asymmetric divisions required for specific populations of cells, and it could have important undiscovered functions distinct from its role in centrosome biology

The mechanistic underpinnings of Meier-Gorlin syndrome have begun to emerge from studies on *ORC1*. ORC1 binds dimethylated lysine 20 of histone H4 (H4K20me2), a chromatin modification commonly present at replication origins, and mutations in the binding domain cause

Meier-Gorlin syndrome (159).   Loss of the H4K20me2 binding domain is associated with reduced ORC1 at replication origins, presumably leading to disrupted cell cycle progression.   In contrast, *in vitro* studies suggest that slow progression through S-phase is not a determinant of the MGS phenotype (160). The generation and analysis of mouse models could clarify the role of cell cycle and cell number on the MGS phenotype.

ORC1 is linked to the regulation of centrosome duplication, an event that is triggered by cyclin E-CDK2 activity (158, 161).   ORC1 mediated inhibition of cyclin E-CDK2 is defective in specific *ORC1* mutants (R105Q and E127G). These mutated residues are located on the surface of the H4K20me2 binding domain, which is hypothesized to confer differential binding to cyclins A and E. These mutations cause centrosome reduplication/amplification in transfected cells, likely though a failure to inhibit cyclin E/CDK activity.

MGS-associated mutations in *ORC1* profoundly reduce the rate of primary cilium formation and alter the collection of signaling components present within the cilium (160). Cilia that do form have a normal appearance. Meier-Gorlin Syndrome and related forms of primordial dwarfism could be considered as ciliopathies.

The multiple functions of *ORC1* explain the pleiotropic features of Meier-Gorlin syndrome patients. Future work will clarify the complex functions of this gene and may identify mutations in other members of the Origin Recognition Complex that cause primordial dwarfism.

The Skeletal Ciliopathies

Mutations in components of the centrosome in primordial dwarfisms could influence the formation and maintenance of the primary cilium (160). The primary cilium is involved in maintaining the ornate architecture of the growth plate (5), and disruptions in ciliogenesis can

lead to the development of many severe forms of skeletal dysplasia (9). These conditions are known as the skeletal ciliopathies, which may include primordial dwarfisms (160).

The term skeletal ciliopathy refers to skeletal dysplasias that are caused by mutations in genes that encode components of the primary cilium or its regulation (9). Some of these skeletal ciliopathies spare the tissues typically damaged in ciliopathies such as kidney, retina, brain, and liver. Many skeletal ciliopathies are embryonic or perinatal lethal, and many of them result in short ribs and polydactyly, presumably due to altered IHH signaling. The short ribs may impair lung development and function, causing lethality at birth (10, 57).

The primary cilium is a microtubule-based structure present on the majority of non-cycling cell types, including chondrocytes. The axoneme of this non-motile cilium extends outward from the basal body, the foundation of the cilium generated by the mother centriole of the centrosome (162) (Figure 1.4). Sheathed in plasma membrane and decorated with numerous receptors and channels, the primary cilium serves as a major signaling center, particularly for the Hedgehog and Wnt signaling pathways (163). Due to the importance of IHH signaling in the growth plate, it is clear that perturbation of the primary cilium or the trafficking of necessary signaling components have the potential to disrupt skeletal growth.

The primary cilium maintains growth plate architecture and organization and is thought to regulate cellular positioning in the growth plate (5). Chondrocytes typically divide perpendicular to the plane of the growth plate, and slide back over one another to form the highly ordered columns in the proliferative zone. This process, known as chondrocyte rotation (5), is regulated by Wnt signaling and the planar-cell polarity pathway (4, 6). Mouse models of skeletal ciliopathies have disorganized growth plates that underlie the growth insufficiency. The disorganized growth plate may arise from perturbation of cell polarity (Wnt), and the rate of
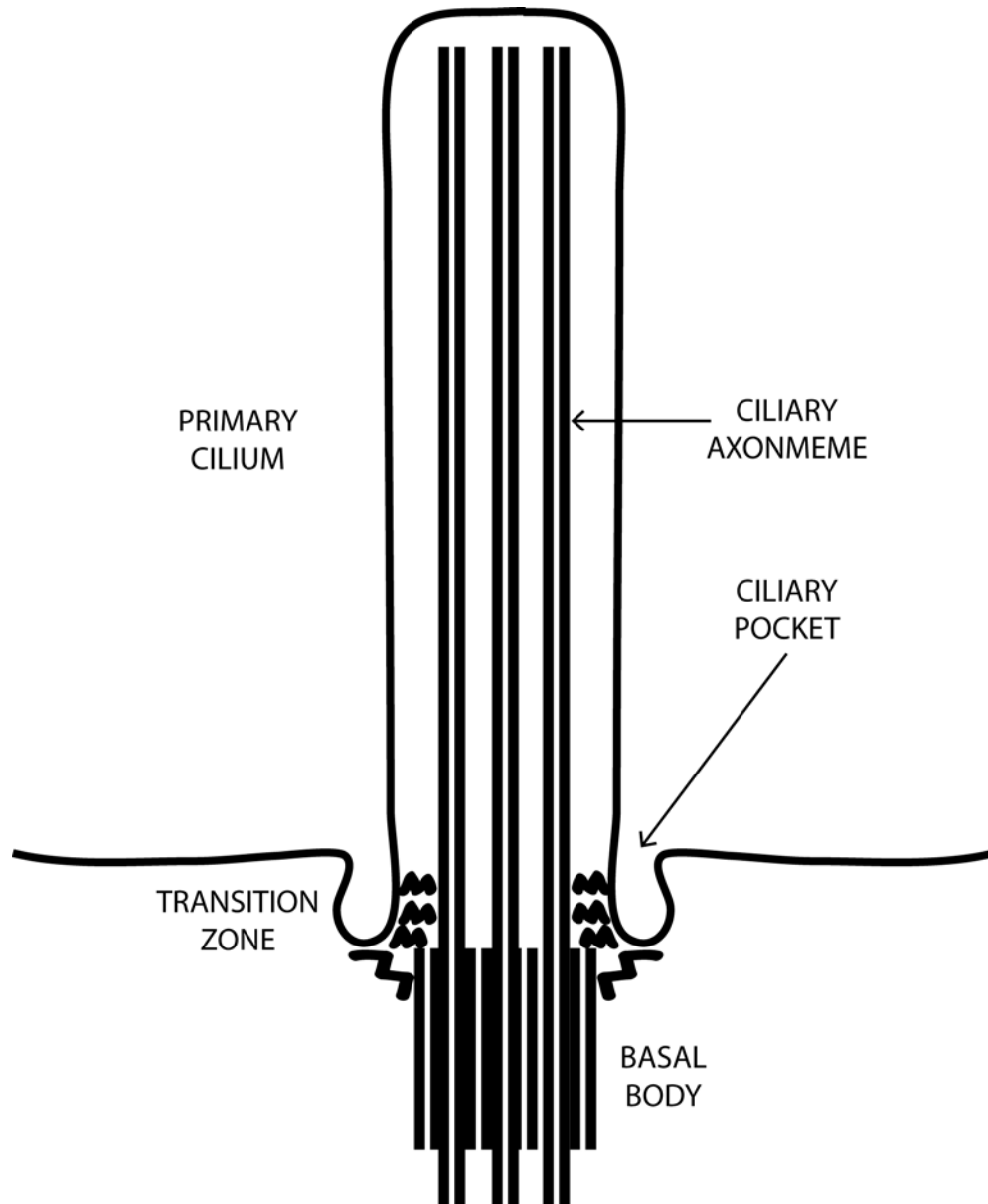
PRIMARY
CILIUM

CILIARY
AXONMEME

CILIARY
POCKET

TRANSITION
ZONE

BASAL
BODY

Figure 1.4. The primary cilium. The primary cilium is a structure present on most cell types, including chondrocytes. In the growth plate, the primary cilium serves to maintain growth plate organization, presumably as a center for signaling pathways such as the WNT/Planar Cell Polarity pathway and IHH. The primary cilium is a microtubule-based structure that extends out from the mother centriole of the centrosome. The mother centriole forms the basal body, the foundation of the ciliary axoneme. The cell membrane wraps around the cilium, and numerous motor proteins and cargo-binding proteins allow for proper transport of components into and out of the cilium by intraflagellar transport (IFT). The ciliary pocket is a depression in the cell membrane near the basal body, and the transition zone is the area between the basal body and the primary cilium, which is thought to play a role in regulating intraflagellar traffic into and out of the cilium.

growth plate chondrocyte proliferation and hypertrophic differentiation (IHH). Loss of these critical mechanisms could lead to short stature in affected animals and human skeletal ciliopathy patients. Ciliary genes comprise a large and growing family (9). Many regulate intraflagellar transport (IFT), the mechanism responsible for trafficking components into the cilium (IFT complex B, anterograde trafficking) or out of the cilium (IFT complex A, retrograde trafficking) (Figure 1.5). Kinesin motors carry IFT-B components, while dynein motors carry IFT-A components. This trafficking system ensures that the cilium is maintained, lengthened, and that receptors and downstream effectors of signaling pathways are targeted properly to the cilium. A number of mutations in the genes that encode these proteins cause skeletal ciliopathies (Figure 1.5). Mutations in genes affiliated with the basal body (Figure 1.5) could cause disruptions in primary cilium formation and maintenance, or affect mitotic spindle formation and orientation. Mutations in these genes may interfere with completion of cell division, and/or impact the plane of division affecting chondrocyte rotation and stacking.

Mutations in *NEK1*, a basal body-associated component of the cilium, cause Short-Rib Polydactyly Syndrome Type Majewski (67). The NEK kinases (never-in-mitosis gene a-related kinases) constitute a large gene family composed of eleven members (*NEK1-NEK11*) (164). NEKs regulate microtubule dynamics, cell cycle progression and ciliogenesis. Mutations in other NEK genes may cause skeletal dysplasia (including, but not limited to, primordial dwarfisms), classical ciliopathies, or cancer. Moreover, all gene families encoding cilia-associated proteins, including *NEK, CEP*, *WDR* and *TMEM,* are excellent candidates for human disease genes and worthy of functional analysis in model organisms.
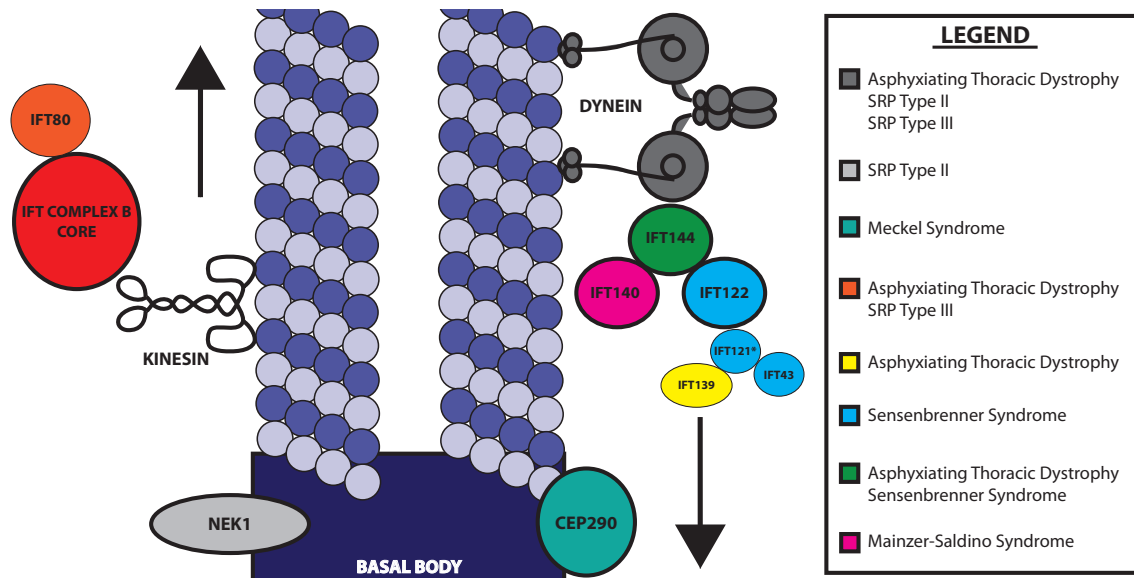
Figure 1.5. Primary cilia proteins implicated in skeletal dysplasias. Components of the primary cilium are disrupted in many different forms of skeletal dysplasia. These include genes that encode parts of motor proteins (dynein), and parts of both the IFT-A complex and IFT-B complex, which regulate retrograde and anterograde ciliary trafficking, respectively. The colors of the cilium components signify the forms of skeletal dysplasia with which they are associated. *IFT121 has been shown to cause SRP type V in addition to Sensenbrenner syndrome (9)

A Missing Link: Mutations in *POC1A* Cause a Novel Form of Primordial Dwarfism That Exhibits Defects in the Primary Cilium

The newest member of the skeletal ciliopathy group is a novel form of primordial dwarfism caused by mutations in the gene *POC1A,* which encodes protein of centriole 1A. Patients are smaller than average size *in utero*, and remain so throughout their lives (59, 60). Two homozygous mutations were found in highly consanguineous families: a premature stop codon (R81X) (60), and a missense mutation (L171P) (59). Surprisingly, the premature stop codon undergoes efficient read-through in patient fibroblast cultures, and POC1A protein levels are only reduced 15-50% (60). The fibroblasts have abnormal mitotic spindle orientation, form multipolar spindles, and have multiple centrosomes in non-cycling cells. The frequency of primary cilia is only about half of the control, and the cilia that do form are 2/3 normal size. The

missense mutation is a non-conservative change, but the protein may retain some functions. Fibroblasts from these patients have more centrosomes and exhibit alterations in cholera toxin trafficking (59). POC1A protein misfolding could create ER and/or Golgi stress that contributes to the phenotype, although the clinical features appear similar in both families.

The effects both mutations have on cilia and centrosomes may be sufficient to produce the growth insufficiency. Two lines of evidence support this idea. First, knock down of both *POC1A* and the related *POC1B* gene in HeLa cells alters the orientation of the mitotic spindle, causing unequal bipolar, monopolar, or even multipolar spindles (165). These knockdowns cause failure of daughter centrioles to mature into new mother centrioles, which may lead to the disruption in mitotic spindle formation. The lack of mother centrioles could affect the cells' abilities to form primary cilia, as the mother centriole is responsible for the formation of the basal body and the extension of the ciliary axoneme (162). This could lead to profound effects on growth plate organization and signaling (5, 163), leading to severe short stature. Secondly, mutations in *POC1A*, *ORC1*, *CENPJ*, and *PCNT* cause very similar growth deficiencies and microcephaly, and all of these genes encode proteins associated with the centrosome (151-153, 158, 160, 165).

It will be interesting to determine whether defects in the other primordial dwarfism genes cause the cilia defects similar to those observed in cells from *POC1A* patients, or whether, like *ORC1* mutations, the cells form relatively normal cilia, but at a slower rate (160). Genetically engineered mice that model these diseases could be a source of primary fibroblasts or bone cells for functional studies. In addition, they could be used to determine which of these genes cause disorganization of the growth plate. This type of study would clarify the roles of these genes in

the cause of postnatal growth retardation in this subset of primordial dwarfism patients, which may be considered as skeletal ciliopathy patients.

Novel Skeletal Disorders of Unknown Etiology

While the genetic causes of the over 450 forms of skeletal disorders (8) are being uncovered at a rapidly expanding rate, there are still distinct skeletal disorders being discovered that have no known genetic etiology. Eleven novel skeletal disorders have been reported since 2010 (Table 1.4). While many are not named, some of their features resemble previously described forms of skeletal dysplasia, suggesting that mutations in known genes could be responsible. It is likely that some are caused by mutations in novel genes important for normal skeletal growth and development.

Given the high degree of genetic heterogeneity already evident for this group of growth disorders, the best strategy for identifying the genetic etiology in a new patient may be to conduct exome sequencing or genome sequencing. In some cases the utilization of high-throughput genotyping strategies could map the loci, facilitating the analysis of variants. The temporal gap between the description of a particular patient phenotype and uncovering the genetic etiology is becoming narrower and narrower.

Future Directions: How Mutation Discovery Advances Skeletal Dysplasia Research

Geneticist's contributions to understanding skeletal dysplasia begin by assigning a gene to a disorder and extend to understanding the pathophysiology of the disease and development of treatments. Receiving a molecular diagnosis often gives patients and their families relief because they can understand the cause, the progression of disease over a lifetime, and the risk for future pregnancies. Human disease gene discovery is a starting point for understanding the normal regulation of skeletal growth and for studying development in model systems. Mouse models for

Table 1.4 Novel Skeletal Disorders							
Name	# Pts	Inheritance	Onset of Growth Delay	Skeletal Features	Other Features	Similarity to Other SD	Gene/Locus
Syndrome of Facial Dysmorphism, Intellectual Disability, and Primordial Dwarfism (166)	10	AR	Birth	-Scoliosis -Abnormal phalangeal epiphyses	-Malar hypoplasia -Deep-seated eyes -Broad nose -Short philtrum -Macrostomia -Intellectual disability	Primordial dwarfism	*LARP7*
Severe Lateral Tibial Bowing and Short Stature (167)	2	AR or AD	N/A	-Severe distal lateral tibial bowing -Moderate fibular curving -Abnormal distal tibial epiphyses -Differential cortical thickness -Winged scapulae -Mild genu valgum	-Synophrys -Low-set right ear with absence of helical folding	Weismann-Netter Syndrome Rickets	1q21.3 (gain) 3q26.1 (loss) 22q13.33 (loss)
Novel Pleiotropic Sclerosing Bone Dysplasia Syndrome (168)	2	AD	N/A	-Cranial, rib, and long bone sclerosis -Increased bone density	-Dysmorphic facies -Macrocephaly -Hearing loss -Palatal clefting -Developmental delay -Hypotonia	-Mixed Sclerosing Bone Dysplasia -Osteopathia Striata with Cranial Sclerosis	N/A
Novel Microcephalic Primordial Dwarfism with Developmental Brain Malformations (169)	2	AR	In Utero	-Microcephaly -Intrauterine and postnatal growth retardation -Minimal skeletal dysplasia -Broad metaphyses	-Absent cranial vault -Sloping forehead -Large beaked nose -Large ears -Mandibular micrognathia -Brain malformations -Early Lethality	N/A	N/A
Novel Skeletal Dysplasia With Characteristic Facial Features and Developmental Delay (170)	7 Males	AR or X-linked	In Utero	-Patellar dislocation -Short tubular bones -Mild metaphyseal changes -Brachymetacarpalia -Stub thumbs -Short femoral necks -Shallow acetabular roofs -Platyspondyly	-Flattened midface -Broad nasal bridge -Cleft palate -Bifid uvula -Synophrys -Cognitive developmental delay -Shortened attention span	Desbuquois Dysplasia	N/A
Severe Disproportionate Short Stature With Short Long Bones, Brachydactyly, and Hypotrichosis (171)	8	AR	In Utero	-Severe disproportionate short stature -Short long bones -Brachydactyly -Clinodactyly -Small hands -Mild metaphyseal changes -Short femoral necks	-Large head -Long triangular face -Prominent nose -High-pitched voice -Small ears -Hypoplastic fingernails Waddling gait Sparse hair	Silver-Russell Syndrome, Hypochondroplasia, 3-M Syndrome, Floating-Harbor Syndrome, Acrocapitofemoral Dysplasia SOFT Syndrome	Ruled out *CUL7, OBSTL1, ADAMTSL2, SRCAP, IHH*
A New Lysosomal Storage Disorder Resembling Morquio Syndrome (172)	2	AR	Neonatal	-Short stature -Short trunk -Barrel chest -Micromelia with rhizomelic shortening -Severe kyphoscoliosis -Pectus carinatum -Short hands -Short feet -Metatarsus adductus Excessive joint laxity -Platyspondyly Hypolasia of odontoid process -Epiphyseal	-Learning difficulties -Coarse inclusions in eosinophils -Mild Alder anomaly in polymorphonuclears	Morquio Syndrome	N/A

				-dysplasia -Abnormal metaphyses -Trident acetabular roofs			
Lethal Skeletal Dysplasia Type al Gazali (173)	2	AR	In Utero	-Brachycephaly -Flat face -Hypertelorism -Sclerotic skull -Prominent parietal bones -Large anterior fontanel -Hypoplastic thorax -Short extremities -Brachydactyly -Increased bone density -Short, poorly modeled tubular bones -Wide diaphyses -Smooth, rounded metaphyses -Thick cortical bones -Vertebral endplates -Normal growth plate structure	Low-set ears, hypertrichosis, fetal hydrops	Achondrogenesis Hypochondrogenesis	Ruled out *COL2A1*, no abnormalities in gene dosage
Ectodermal, Skeletal, and Gentiourinary Abnormalities with Neonatal Hyperekplexia (174)	1	N/A	N/A	-Kyphoscoliosis -Short stature -Barrel chest -Brachydactyly -Clinodactyly -Acetabular hypoplasia -Flat acetabular roofs -Sclerotic metaphyses	-Hyperekplexia -Distichiasis -Lymphedema -Wiry hair -Dermatitis -Keratosis pilaris -Congenital nevus -Penile chordae -Hypospadias -Hydrocoele -Inguinal hernia	NA	Ruled out *FOXC2* and *GLRA1*
Short Stature, Microcephaly, Mental Retardation, and Retinoschisis (175)	2	AR or X-linked	N/A	-Short stature -Microcephaly	-Intellectual disability -Retinoschisis	X-linked mental retardation, X-linked retinoschisis	Xp22.33-p22.2 Xp11.3-q21.31 Xq23-q25 Xq27.1-q28 13q21.33 4q28.3 14q13.3-q21.1 16p12.3
Mandibular Hypoplasia, Deafness, and Progeroid Features Associated with Lipodystrophy, Undescended Testes, and Male Hypogonadism (176)	7	AD or AR	N/A	-Mandibular hypoplasia -Short stature -Joint contractures	-Sclerodermatous skin -Subcutaneous fat loss -Male hypogonadism -Undescended testes -Sensorineural hearing loss Corneal opacities -Dry eyes -Beaked nose	Mandibuloacral Dysplasia (MAD)	Ruled out *LMNA* and *ZMPSTE24* (MAD)

human skeletal dysplasias and chondrocyte cell lines have been invaluable for mechanistic

insight that explains the clinical features of many skeletal dysplasia phenotypes at the molecular

level. This insight is a foundation for developing and testing therapeutic interventions,

completing the circle of bedside to bench and back to the bedside.

Achondroplasia remains one of the best examples of how the discovery of a mutation can lead to the discovery of potential therapies in less than 20 years. Interestingly, the discovery of mutations in NPR2 in AMDM patients (107) has helped shape the trajectory of this area of research. Work in cell culture and mouse models has revealed that the genetic and molecular etiologies of both disorders are intertwined with one another. Activation of NPR2 inhibits FGFR3-mediated activation of the MEK/ERK MAPK pathway (103), which allows the growth plate to promote chondrocyte differentiation. Loss of CNP-NPR2 mediated inhibition of FGF signaling in a mouse model of AMDM leads to over activation of the MEK/ERK MAPK pathway (102), and treatment of chondrocytes with CNP leads to reduced ERK activation (103). Treating achondroplasia patients with CNP, the ligand for NPR2, was a rational therapy based on knowledge of the effect of the FGF mutation on MEK/ERK and the oppositional effects of CNP signaling. This therapy is somewhat successful in mouse models with various methods of continuous administration (96, 104, 106). Parathyroid hormone (PTH) (97), FGFR3 inhibitors (98, 99), and CNP analogs (100) are all being explored as potential treatments for achondroplasia. Finally, the administration of MEK/ERK inhibitors has been postulated to be a method of intervention in mouse models of Apert syndrome (gain-of-function mutation in *FGFR2*) (101), and AMDM (102). While these modes of therapy are still under development, it is promising that targeting these pathways has improved growth *in vitro* and *in vivo*. Future research will involve identifying additional compounds that modulate this interconnected signaling network, potentially with greater specificity, and improved delivery of therapeutics to the growth plate. Lastly, the progression from mutation discovery to the development of therapies in this case should serve as a model for researchers to follow when considering the testing and development of treatments for the other forms of skeletal dysplasia.

Skeletal Dysplasia Mutations Further Our Understanding of Height Variation

Do mutations uncovered in skeletal dysplasia patients provide any information about height variation in the human population? The answer to that question is probably "yes" because some skeletal dysplasia-associated genes have been implicated in human height. A genome-wide association study (GWAS) conducted on human height variation (177) reported 21 of 241 genes (8.7%) known to cause a human growth disorder in their height-associated genomic loci, including genes influencing the endocrine system and skeleton. An important next step is to identify functional variants in the candidate genes. In any case, the GWAS studies explain only a small portion of the known heritability of height variation in humans. It is likely that genetic interactions contribute a great deal to the missing heritability.   The known skeletal dysplasia genes implicate several pathways, and it is likely that multiple hits in a pathway could have synergistic effects.

Concluding Remarks

In the past two years remarkable progress has been made in understanding skeletal dysplasia. Forty-one new genetic causes have been uncovered (Table 1.2), and eleven novel skeletal growth disorders have been reported (Table 1.4). The speed and volume in which these discoveries are being made leads us to propose the generation of a Nosology and Classification of Skeletal Disorders Database, where researchers could ask for information to be uploaded as it is discovered.   Such a database could be expanded to include all types of growth disorders, providing a valuable resource for clinical, basic and translational research.

References

1   Karsenty, G., Kronenberg, H.M. and Settembre, C. (2009) Genetic control of bone formation. *Annu Rev Cell Dev Biol*, **25**, 629-648.
2   Krakow, D. and Rimoin, D.L. (2010) The skeletal dysplasias. *Genet Med*, **12**, 327-341.
3   Kronenberg, H.M. (2003) Developmental regulation of the growth plate. *Nature*, **423**, 332-336.
4   Romereim, S.M. and Dudley, A.T. (2011) Cell polarity: The missing link in skeletal morphogenesis? *Organogenesis*, **7**, 217-228.
5   Song, B., Haycraft, C.J., Seo, H.S., Yoder, B.K. and Serra, R. (2007) Development of the post-natal growth plate requires intraflagellar transport proteins. *Dev Biol*, **305**, 202-216.
6   Li, Y. and Dudley, A.T. (2009) Noncanonical frizzled signaling regulates cell polarity of growth plate chondrocytes. *Development*, **136**, 1083-1092.
7   Baldridge, D., Shchelochkov, O., Kelley, B. and Lee, B. (2010) Signaling pathways in human skeletal dysplasias. *Annu Rev Genomics Hum Genet*, **11**, 189-217.
8   Warman, M.L., Cormier-Daire, V., Hall, C., Krakow, D., Lachman, R., LeMerrer, M., Mortier, G., Mundlos, S., Nishimura, G., Rimoin, D.L. *et al.* (2011) Nosology and classification of genetic skeletal disorders: 2010 revision. *Am J Med Genet A*, **155A**, 943-968.
9   Huber, C. and Cormier-Daire, V. (2012) Ciliary disorder of the skeleton. *Am J Med Genet C Semin Med Genet*, **160C**, 165-174.
10   Dighe, M., Fligner, C., Cheng, E., Warren, B. and Dubinsky, T. (2008) Fetal skeletal dysplasia: an approach to diagnosis with illustrative cases. *Radiographics*, **28**, 1061-1077.
11   Kwok, C., Weller, P.A., Guioli, S., Foster, J.W., Mansour, S., Zuffardi, O., Punnett, H.H., Dominguez-Steglich, M.A., Brook, J.D., Young, I.D. *et al.* (1995) Mutations in SOX9, the gene responsible for Campomelic dysplasia and autosomal sex reversal. *Am J Hum Genet*, **57**, 1028-1036.
12   Sybert, V.P. and McCauley, E. (2004) Turner's syndrome. *N Engl J Med*, **351**, 1227-1238.
13   Arboleda, V.A., Lee, H., Parnaik, R., Fleming, A., Banerjee, A., Ferraz-de-Souza, B., Delot, E.C., Rodriguez-Fernandez, I.A., Braslavsky, D., Bergada, I. *et al.* (2012) Mutations in the PCNA-binding domain of CDKN1C cause IMAGe syndrome. *Nat Genet*, **44**, 788-792.
14   Lee, H., Graham, J.M., Jr., Rimoin, D.L., Lachman, R.S., Krejci, P., Tompson, S.W., Nelson, S.F., Krakow, D. and Cohn, D.H. (2012) Exome sequencing identifies PDE4D mutations in acrodysostosis. *Am J Hum Genet*, **90**, 746-751.

15   Campeau, P.M., Kim, J.C., Lu, J.T., Schwartzentruber, J.A., Abdul-Rahman, O.A., Schlaubitz, S., Murdock, D.M., Jiang, M.M., Lammer, E.J., Enns, G.M. *et al.* (2012) Mutations in KAT6B, encoding a histone acetyltransferase, cause Genitopatellar syndrome. *Am J Hum Genet*, **90**, 282-289.

16   Le Goff, C., Mahaut, C., Abhyankar, A., Le Goff, W., Serre, V., Afenjar, A., Destree, A., di Rocco, M., Heron, D., Jacquemont, S. *et al.* (2012) Mutations at a single codon in Mad homology 2 domain of SMAD4 cause Myhre syndrome. *Nat Genet*, **44**, 85-88.

17   Linglart, A., Menguy, C., Couvineau, A., Auzan, C., Gunes, Y., Cancel, M., Motte, E., Pinto, G., Chanson, P., Bougneres, P. *et al.* (2011) Recurrent PRKAR1A mutation in acrodysostosis with hormone resistance. *N Engl J Med*, **364**, 2218-2226.

18   Merrill, A.E., Merriman, B., Farrington-Rock, C., Camacho, N., Sebald, E.T., Funari, V.A., Schibler, M.J., Firestein, M.H., Cohn, Z.A., Priore, M.A. *et al.* (2009) Ciliary abnormalities due to defects in the retrograde transport protein DYNC2H1 in short-rib polydactyly syndrome. *Am J Hum Genet*, **84**, 542-549.

19   Tunkel, D., Alade, Y., Kerbavaz, R., Smith, B., Rose-Hardison, D. and Hoover-Fong, J. (2012) Hearing loss in skeletal dysplasia patients. *Am J Med Genet A*, **158A**, 1551-1555.

20   Baker, S., Booth, C., Fillman, C., Shapiro, M., Blair, M.P., Hyland, J.C. and Ala-Kokko, L. (2011) A loss of function mutation in the COL9A2 gene causes autosomal recessive Stickler syndrome. *Am J Med Genet A*, **155A**, 1668-1672.

21   Savarirayan, R. and Rimoin, D.L. (2002) The skeletal dysplasias. *Best Pract Res Clin Endocrinol Metab*, **16**, 547-560.

22   Thompson, S., Shakespeare, T. and Wright, M.J. (2008) Medical and social aspects of the life course for adults with a skeletal dysplasia: a review of current knowledge. *Disabil Rehabil*, **30**, 1-12.

23   Allen, D.B. and Cuttler, L. (2013) Clinical practice. Short stature in childhood--challenges and choices. *N Engl J Med*, **368**, 1220-1228.

24   Vilain, E., Le Merrer, M., Lecointre, C., Desangles, F., Kay, M.A., Maroteaux, P. and McCabe, E.R. (1999) IMAGe, a new clinical association of intrauterine growth retardation, metaphyseal dysplasia, adrenal hypoplasia congenita, and genital anomalies. *J Clin Endocrinol Metab*, **84**, 4335-4340.

25   Silve, C., Clauser, E. and Linglart, A. (2012) Acrodysostosis. *Horm Metab Res*, **44**, 749-758.

26   Linglart, A., Fryssira, H., Hiort, O., Holterhus, P.M., Perez de Nanclares, G., Argente, J., Heinrichs, C., Kuechler, A., Mantovani, G., Leheup, B. *et al.* (2012) PRKAR1A and PDE4D mutations cause acrodysostosis but two distinct syndromes with or without GPCR-signaling hormone resistance. *J Clin Endocrinol Metab*, **97**, E2328-2338.

27   Ott, C.E., Hein, H., Lohan, S., Hoogeboom, J., Foulds, N., Grunhagen, J., Stricker, S., Villavicencio-Lorini, P., Klopocki, E. and Mundlos, S. (2012) Microduplications upstream of MSX2 are associated with a phenocopy of cleidocranial dysplasia. *J Med Genet*, **49**, 437-441.

28   Dickson, L.A., Pihlajaniemi, T., Deak, S., Pope, F.M., Nicholls, A., Prockop, D.J. and Myers, J.C. (1984) Nuclease S1 mapping of a homozygous mutation in the carboxyl-propeptide-coding region of the pro alpha 2(I) collagen gene in a patient with osteogenesis imperfecta. *Proc Natl Acad Sci U S A*, **81**, 4524-4528.

29   Pihlajaniemi, T., Dickson, L.A., Pope, F.M., Korhonen, V.R., Nicholls, A., Prockop, D.J. and Myers, J.C. (1984) Osteogenesis imperfecta: cloning of a pro-alpha 2(I) collagen gene with a frameshift mutation. *J Biol Chem*, **259**, 12941-12944.

30   Francomano, C.A., Liberfarb, R.M., Hirose, T., Maumenee, I.H., Streeten, E.A., Meyers, D.A. and Pyeritz, R.E. (1987) The Stickler syndrome: evidence for close linkage to the structural gene for type II collagen. *Genomics*, **1**, 293-296.

31   Lee, B., Vissing, H., Ramirez, F., Rogers, D. and Rimoin, D. (1989) Identification of the molecular defect in a family with spondyloepiphyseal dysplasia. *Science*, **244**, 978-980.

32   Tsipouras, P., Myers, J.C., Ramirez, F. and Prockop, D.J. (1983) Restriction fragment length polymorphism associated with the pro alpha 2(I) gene of human type I procollagen. Application to a family with an autosomal dominant form of osteogenesis imperfecta. *J Clin Invest*, **72**, 1262-1267.

33   Francomano, C.A. and Pyeritz, R.E. (1988) Achondroplasia is not caused by mutation in the gene for type II collagen. *Am J Med Genet*, **29**, 955-961.

34   Le Merrer, M., Rousseau, F., Legeai-Mallet, L., Landais, J.C., Pelet, A., Bonaventure, J., Sanak, M., Weissenbach, J., Stoll, C., Munnich, A. *et al.* (1994) A gene for achondroplasia-hypochondroplasia maps to chromosome 4p. *Nat Genet*, **6**, 318-321.

35   Velinov, M., Slaugenhaupt, S.A., Stoilov, I., Scott, C.I., Jr., Gusella, J.F. and Tsipouras, P. (1994) The gene for achondroplasia maps to the telomeric region of chromosome 4p. *Nat Genet*, **6**, 314-317.

36   Francomano, C.A., Ortiz de Luna, R.I., Hefferon, T.W., Bellus, G.A., Turner, C.E., Taylor, E., Meyers, D.A., Blanton, S.H., Murray, J.C., McIntosh, I. *et al.* (1994) Localization of the achondroplasia gene to the distal 2.5 Mb of human chromosome 4p. *Hum Mol Genet*, **3**, 787-792.

37   Shiang, R., Thompson, L.M., Zhu, Y.Z., Church, D.M., Fielder, T.J., Bocian, M., Winokur, S.T. and Wasmuth, J.J. (1994) Mutations in the transmembrane domain of FGFR3 cause the most common genetic form of dwarfism, achondroplasia. *Cell*, **78**, 335-342.

38   Rousseau, F., Bonaventure, J., Legeai-Mallet, L., Pelet, A., Rozet, J.M., Maroteaux, P., Le Merrer, M. and Munnich, A. (1994) Mutations in the gene encoding fibroblast growth factor receptor-3 in achondroplasia. *Nature*, **371**, 252-254.

39   Deng, C., Wynshaw-Boris, A., Zhou, F., Kuo, A. and Leder, P. (1996) Fibroblast growth factor receptor 3 is a negative regulator of bone growth. *Cell*, **84**, 911-921.

40   Webster, M.K. and Donoghue, D.J. (1996) Constitutive activation of fibroblast growth factor receptor 3 by the transmembrane domain point mutation found in achondroplasia. *EMBO J*, **15**, 520-527.

41   Webster, M.K., D'Avis, P.Y., Robertson, S.C. and Donoghue, D.J. (1996) Profound ligand-independent kinase activation of fibroblast growth factor receptor 3 by the activation loop mutation responsible for a lethal skeletal dysplasia, thanatophoric dysplasia type II. *Mol Cell Biol*, **16**, 4081-4087.

42   Tavormina, P.L., Shiang, R., Thompson, L.M., Zhu, Y.Z., Wilkin, D.J., Lachman, R.S., Wilcox, W.R., Rimoin, D.L., Cohn, D.H. and Wasmuth, J.J. (1995) Thanatophoric dysplasia (types I and II) caused by distinct mutations in fibroblast growth factor receptor 3. *Nat Genet*, **9**, 321-328.

43   Rousseau, F., Saugier, P., Le Merrer, M., Munnich, A., Delezoide, A.L., Maroteaux, P., Bonaventure, J., Narcy, F. and Sanak, M. (1995) Stop codon FGFR3 mutations in thanatophoric dwarfism type 1. *Nat Genet*, **10**, 11-12.

44   Stoilov, I., Kilpatrick, M.W. and Tsipouras, P. (1995) A common FGFR3 gene mutation is present in achondroplasia but not in hypochondroplasia. *Am J Med Genet*, **55**, 127-133.

45   Prinos, P., Costa, T., Sommer, A., Kilpatrick, M.W. and Tsipouras, P. (1995) A common FGFR3 gene mutation in hypochondroplasia. *Hum Mol Genet*, **4**, 2097-2101.

46   Bamshad, M.J., Ng, S.B., Bigham, A.W., Tabor, H.K., Emond, M.J., Nickerson, D.A. and Shendure, J. (2011) Exome sequencing as a tool for Mendelian disease gene discovery. *Nat Rev Genet*, **12**, 745-755.

47   Metzker, M.L. (2010) Sequencing technologies - the next generation. *Nat Rev Genet*, **11**, 31-46.

48   Karaplis, A.C., Luz, A., Glowacki, J., Bronson, R.T., Tybulewicz, V.L., Kronenberg, H.M. and Mulligan, R.C. (1994) Lethal skeletal dysplasia from targeted disruption of the parathyroid hormone-related peptide gene. *Genes Dev*, **8**, 277-289.

49   Otto, F., Thornell, A.P., Crompton, T., Denzel, A., Gilmour, K.C., Rosewell, I.R., Stamp, G.W., Beddington, R.S., Mundlos, S., Olsen, B.R. *et al.* (1997) Cbfa1, a candidate gene for cleidocranial dysplasia syndrome, is essential for osteoblast differentiation and bone development. *Cell*, **89**, 765-771.

50   Mundlos, S., Otto, F., Mundlos, C., Mulliken, J.B., Aylsworth, A.S., Albright, S., Lindhout, D., Cole, W.G., Henn, W., Knoll, J.H. *et al.* (1997) Mutations involving the transcription factor CBFA1 cause cleidocranial dysplasia. *Cell*, **89**, 773-779.

51   Lee, B., Thirunavukkarasu, K., Zhou, L., Pastore, L., Baldini, A., Hecht, J., Geoffroy, V., Ducy, P. and Karsenty, G. (1997) Missense mutations abolishing DNA binding of the osteoblast-specific transcription factor OSF2/CBFA1 in cleidocranial dysplasia. *Nat Genet*, **16**, 307-310.

52   Arikawa-Hirasawa, E., Watanabe, H., Takami, H., Hassell, J.R. and Yamada, Y. (1999) Perlecan is essential for cartilage and cephalic development. *Nat Genet*, **23**, 354-358.

53   Arikawa-Hirasawa, E., Wilcox, W.R., Le, A.H., Silverman, N., Govindraj, P., Hassell, J.R. and Yamada, Y. (2001) Dyssegmental dysplasia, Silverman-Handmaker type, is caused by functional null mutations of the perlecan gene. *Nat Genet*, **27**, 431-434.

54   Nicole, S., Davoine, C.S., Topaloglu, H., Cattolico, L., Barral, D., Beighton, P., Hamida, C.B., Hammouda, H., Cruaud, C., White, P.S. *et al.* (2000) Perlecan, the major proteoglycan of basement membranes, is altered in patients with Schwartz-Jampel syndrome (chondrodystrophic myotonia). *Nat Genet*, **26**, 480-483.

55   Ventura, A., Young, A.G., Winslow, M.M., Lintault, L., Meissner, A., Erkeland, S.J., Newman, J., Bronson, R.T., Crowley, D., Stone, J.R. *et al.* (2008) Targeted deletion reveals essential and overlapping functions of the miR-17 through 92 family of miRNA clusters. *Cell*, **132**, 875-886.

56   Dowdle, W.E., Robinson, J.F., Kneist, A., Sirerol-Piquer, M.S., Frints, S.G., Corbit, K.C., Zaghloul, N.A., van Lijnschoten, G., Mulders, L., Verver, D.E. *et al.* (2011) Disruption of a ciliary B9 protein complex causes Meckel syndrome. *Am J Hum Genet*, **89**, 94-110.

57   Smits, P., Bolton, A.D., Funari, V., Hong, M., Boyden, E.D., Lu, L., Manning, D.K., Dwyer, N.D., Moran, J.L., Prysak, M. *et al.* (2010) Lethal skeletal dysplasia in mice and humans lacking the golgin GMAP-210. *N Engl J Med*, **362**, 206-216.

58   Dauber, A., Lafranchi, S.H., Maliga, Z., Lui, J.C., Moon, J.E., McDeed, C., Henke, K., Zonana, J., Kingman, G.A., Pers, T.H. *et al.* (2012) Novel microcephalic primordial dwarfism disorder associated with variants in the centrosomal protein ninein. *J Clin Endocrinol Metab*, **97**, E2140-2151.

59   Sarig, O., Nahum, S., Rapaport, D., Ishida-Yamamoto, A., Fuchs-Telem, D., Qiaoli, L., Cohen-Katsenelson, K., Spiegel, R., Nousbeck, J., Israeli, S. *et al.* (2012) Short stature, onychodysplasia, facial dysmorphism, and hypotrichosis syndrome is caused by a POC1A mutation. *Am J Hum Genet*, **91**, 337-342.

60   Shaheen, R., Faqeih, E., Shamseldin, H.E., Noche, R.R., Sunker, A., Alshammari, M.J., Al-Sheddi, T., Adly, N., Al-Dosari, M.S., Megason, S.G. *et al.* (2012) POC1A truncation mutation causes a ciliopathy in humans characterized by primordial dwarfism. *Am J Hum Genet*, **91**, 330-336.

61   Thomas, S., Legendre, M., Saunier, S., Bessieres, B., Alby, C., Bonniere, M., Toutain, A., Loeuillet, L., Szymanska, K., Jossic, F. *et al.* (2012) TCTN3 mutations cause Mohr-Majewski syndrome. *Am J Hum Genet*, **91**, 372-378.

62   Perrault, I., Saunier, S., Hanein, S., Filhol, E., Bizet, A.A., Collins, F., Salih, M.A., Gerber, S., Delphin, N., Bigot, K. *et al.* (2012) Mainzer-Saldino syndrome is a ciliopathy caused by IFT140 mutations. *Am J Hum Genet*, **90**, 864-870.

63   Boyden, E.D., Campos-Xavier, A.B., Kalamajski, S., Cameron, T.L., Suarez, P., Tanackovic, G., Andria, G., Ballhausen, D., Briggs, M.D., Hartley, C. *et al.* (2011) Recurrent dominant mutations affecting two adjacent residues in the motor domain of the monomeric kinesin KIF22 result in skeletal dysplasia and joint laxity. *Am J Hum Genet*, **89**, 767-772.

64   Min, B.J., Kim, N., Chung, T., Kim, O.H., Nishimura, G., Chung, C.Y., Song, H.R., Kim, H.W., Lee, H.R., Kim, J. *et al.* (2011) Whole-exome sequencing identifies mutations of KIF22 in spondyloepimetaphyseal dysplasia with joint laxity, leptodactylic type. *Am J Hum Genet*, **89**, 760-766.

65   Bredrup, C., Saunier, S., Oud, M.M., Fiskerstrand, T., Hoischen, A., Brackman, D., Leh, S.M., Midtbo, M., Filhol, E., Bole-Feysot, C. *et al.* (2011) Ciliopathies with skeletal anomalies and renal insufficiency due to mutations in the IFT-A gene WDR19. *Am J Hum Genet*, **89**, 634-643.

66   Mill, P., Lockhart, P.J., Fitzpatrick, E., Mountford, H.S., Hall, E.A., Reijns, M.A., Keighren, M., Bahlo, M., Bromhead, C.J., Budd, P. *et al.* (2011) Human and mouse mutations in WDR35 cause short-rib polydactyly syndromes due to abnormal ciliogenesis. *Am J Hum Genet*, **88**, 508-515.

67   Thiel, C., Kessler, K., Giessl, A., Dimmler, A., Shalev, S.A., von der Haar, S., Zenker, M., Zahnleiter, D., Stoss, H., Beinder, E. *et al.* (2011) NEK1 mutations cause short-rib polydactyly syndrome type majewski. *Am J Hum Genet*, **88**, 106-114.

68   Valente, E.M., Logan, C.V., Mougou-Zerelli, S., Lee, J.H., Silhavy, J.L., Brancati, F., Iannicelli, M., Travaglini, L., Romani, S., Illi, B. *et al.* (2010) Mutations in TMEM216 perturb ciliogenesis and cause Joubert, Meckel and related syndromes. *Nat Genet*, **42**, 619-625.

69   Below, J.E., Earl, D.L., Shively, K.M., McMillin, M.J., Smith, J.D., Turner, E.H., Stephan, M.J., Al-Gazali, L.I., Hertecant, J.L., Chitayat, D. *et al.* (2013) Whole-genome analysis reveals that mutations in inositol polyphosphate phosphatase-like 1 cause opsismodysplasia. *Am J Hum Genet*, **92**, 137-143.

70   Huber, C., Faqeih, E.A., Bartholdi, D., Bole-Feysot, C., Borochowitz, Z., Cavalcanti, D.P., Frigo, A., Nitschke, P., Roume, J., Santos, H.G. *et al.* (2013) Exome sequencing identifies INPPL1 mutations as a cause of opsismodysplasia. *Am J Hum Genet*, **92**, 144-149.

71   Michot, C., Le Goff, C., Goldenberg, A., Abhyankar, A., Klein, C., Kinning, E., Guerrot, A.M., Flahaut, P., Duncombe, A., Baujat, G. *et al.* (2012) Exome sequencing identifies PDE4D mutations as another cause of acrodysostosis. *Am J Hum Genet*, **90**, 740-745.

72   Merrill, A.E., Sarukhanov, A., Krejci, P., Idoni, B., Camacho, N., Estrada, K.D., Lyons, K.M., Deixler, H., Robinson, H., Chitayat, D. *et al.* (2012) Bent bone dysplasia-FGFR2 type, a distinct skeletal disorder, has deficient canonical FGF signaling. *Am J Hum Genet*, **90**, 550-557.

73   Lindhurst, M.J., Sapp, J.C., Teer, J.K., Johnston, J.J., Finn, E.M., Peters, K., Turner, J., Cannons, J.L., Bick, D., Blakemore, L. *et al.* (2011) A mosaic activating mutation in AKT1 associated with the Proteus syndrome. *N Engl J Med*, **365**, 611-619.

74   Le Goff, C., Mahaut, C., Wang, L.W., Allali, S., Abhyankar, A., Jensen, S., Zylberberg, L., Collod-Beroud, G., Bonnet, D., Alanay, Y. *et al.* (2011) Mutations in the TGFbeta binding-protein-like domain 5 of FBN1 are responsible for acromicric and geleophysic dysplasias. *Am J Hum Genet*, **89**, 7-14.

75   Becker, J., Semler, O., Gilissen, C., Li, Y., Bolz, H.J., Giunta, C., Bergmann, C., Rohrbach, M., Koerber, F., Zimmermann, K. *et al.* (2011) Exome sequencing identifies truncating mutations in human SERPINF1 in autosomal-recessive osteogenesis imperfecta. *Am J Hum Genet*, **88**, 362-371.

76   Klopocki, E., Lohan, S., Brancati, F., Koll, R., Brehm, A., Seemann, P., Dathe, K., Stricker, S., Hecht, J., Bosse, K. *et al.* (2011) Copy-number variations involving the IHH locus are associated with syndactyly and craniosynostosis. *Am J Hum Genet*, **88**, 70-75.

77   Foulquier, F., Amyere, M., Jaeken, J., Zeevaert, R., Schollen, E., Race, V., Bammens, R., Morelle, W., Rosnoblet, C., Legrand, D. *et al.* (2012) TMEM165 deficiency causes a congenital disorder of glycosylation. *Am J Hum Genet*, **91**, 15-26.

78   Vissers, L.E., Lausch, E., Unger, S., Campos-Xavier, A.B., Gilissen, C., Rossi, A., Del Rosario, M., Venselaar, H., Knoll, U., Nampoothiri, S. *et al.* (2011) Chondrodysplasia and abnormal joint development associated with mutations in IMPAD1, encoding the Golgi-resident nucleotide phosphatase, gPAPP. *Am J Hum Genet*, **88**, 608-615.

79   Zankl, A., Duncan, E.L., Leo, P.J., Clark, G.R., Glazov, E.A., Addor, M.C., Herlin, T., Kim, C.A., Leheup, B.P., McGill, J. *et al.* (2012) Multicentric carpotarsal osteolysis is caused by mutations clustering in the amino-terminal transcriptional activation domain of MAFB. *Am J Hum Genet*, **90**, 494-501.

80   Clayton-Smith, J., O'Sullivan, J., Daly, S., Bhaskar, S., Day, R., Anderson, B., Voss, A.K., Thomas, T., Biesecker, L.G., Smith, P. *et al.* (2011) Whole-exome-sequencing identifies mutations in histone acetyltransferase gene KAT6B in individuals with the Say-Barber-Biesecker variant of Ohdo syndrome. *Am J Hum Genet*, **89**, 675-681.

81   de Pontual, L., Yao, E., Callier, P., Faivre, L., Drouin, V., Cariou, S., Van Haeringen, A., Genevieve, D., Goldenberg, A., Oufadem, M. *et al.* (2011) Germline deletion of the miR-17 approximately 92 cluster causes skeletal and growth defects in humans. *Nat Genet*, **43**, 1026-1030.

82   Hanson, D., Murray, P.G., O'Sullivan, J., Urquhart, J., Daly, S., Bhaskar, S.S., Biesecker, L.G., Skae, M., Smith, C., Cole, T. *et al.* (2011) Exome sequencing identifies CCDC8

mutations in 3-M syndrome, suggesting that CCDC8 contributes in a pathway with CUL7 and OBSL1 to control human growth. *Am J Hum Genet*, **89**, 148-153.

83   Ogi, T., Walker, S., Stiff, T., Hobson, E., Limsirichaikul, S., Carpenter, G., Prescott, K., Suri, M., Byrd, P.J., Matsuse, M. *et al.* (2012) Identification of the first ATRIP-deficient patient and novel mutations in ATR define a clinical spectrum for ATR-ATRIP Seckel Syndrome. *PLoS Genet*, **8**, e1002945.

84   Miyake, N., Elcioglu, N.H., Iida, A., Isguven, P., Dai, J., Murakami, N., Takamura, K., Cho, T.J., Kim, O.H., Hasegawa, T. *et al.* (2012) PAPSS2 mutations cause autosomal recessive brachyolmia. *J Med Genet*, **49**, 533-538.

85   van Bon, B.W., Gilissen, C., Grange, D.K., Hennekam, R.C., Kayserili, H., Engels, H., Reutter, H., Ostergaard, J.R., Morava, E., Tsiakas, K. *et al.* (2012) Cantu syndrome is caused by mutations in ABCC9. *Am J Hum Genet*, **90**, 1094-1101.

86   Qvist, P., Huertas, P., Jimeno, S., Nyegaard, M., Hassan, M.J., Jackson, S.P. and Borglum, A.D. (2011) CtIP Mutations Cause Seckel and Jawad Syndromes. *PLoS Genet*, **7**, e1002310.

87   Guernsey, D.L., Matsuoka, M., Jiang, H., Evans, S., Macgillivray, C., Nightingale, M., Perry, S., Ferguson, M., LeBlanc, M., Paquette, J. *et al.* (2011) Mutations in origin recognition complex gene ORC4 cause Meier-Gorlin syndrome. *Nat Genet*, **43**, 360-364.

88   Bicknell, L.S., Walker, S., Klingseisen, A., Stiff, T., Leitch, A., Kerzendorfer, C., Martin, C.A., Yeyati, P., Al Sanna, N., Bober, M. *et al.* (2011) Mutations in ORC1, encoding the largest subunit of the origin recognition complex, cause microcephalic primordial dwarfism resembling Meier-Gorlin syndrome. *Nat Genet*, **43**, 350-355.

89   Bicknell, L.S., Bongers, E.M., Leitch, A., Brown, S., Schoots, J., Harley, M.E., Aftimos, S., Al-Aama, J.Y., Bober, M., Brown, P.A. *et al.* (2011) Mutations in the pre-replication complex cause Meier-Gorlin syndrome. *Nat Genet*, **43**, 356-359.

90   Puente, X.S., Quesada, V., Osorio, F.G., Cabanillas, R., Cadinanos, J., Fraile, J.M., Ordonez, G.R., Puente, D.A., Gutierrez-Fernandez, A., Fanjul-Fernandez, M. *et al.* (2011) Exome sequencing and functional analysis identifies BANF1 mutation as the cause of a hereditary progeroid syndrome. *Am J Hum Genet*, **88**, 650-656.

91   He, H., Liyanarachchi, S., Akagi, K., Nagy, R., Li, J., Dietrich, R.C., Li, W., Sebastian, N., Wen, B., Xin, B. *et al.* (2011) Mutations in U4atac snRNA, a component of the minor spliceosome, in the developmental disorder MOPD I. *Science*, **332**, 238-240.

92   Edery, P., Marcaillou, C., Sahbatou, M., Labalme, A., Chastang, J., Touraine, R., Tubacher, E., Senni, F., Bober, M.B., Nampoothiri, S. *et al.* (2011) Association of TALS developmental disorder with defect in minor splicing component U4atac snRNA. *Science*, **332**, 240-243.

93   Glazov, E.A., Zankl, A., Donskoi, M., Kenna, T.J., Thomas, G.P., Clark, G.R., Duncan, E.L. and Brown, M.A. (2011) Whole-exome re-sequencing in a family quartet identifies POP1 mutations as the cause of a novel skeletal dysplasia. *PLoS Genet*, **7**, e1002027.

94   Kawasaki, Y., Kugimiya, F., Chikuda, H., Kamekura, S., Ikeda, T., Kawamura, N., Saito, T., Shinoda, Y., Higashikawa, A., Yano, F. *et al.* (2008) Phosphorylation of GSK-3beta by cGMP-dependent protein kinase II promotes hypertrophic differentiation of murine chondrocytes. *J Clin Invest*, **118**, 2506-2515.

95   Murakami, S., Balmes, G., McKinney, S., Zhang, Z., Givol, D. and de Crombrugghe, B. (2004) Constitutive activation of MEK1 in chondrocytes causes Stat1-independent

achondroplasia-like dwarfism and rescues the Fgfr3-deficient mouse phenotype. *Genes Dev*, **18**, 290-305.

96   Yasoda, A. and Nakao, K. (2010) Translational research of C-type natriuretic peptide (CNP) into skeletal dysplasias. *Endocr J*, **57**, 659-666.

97   Xie, Y., Su, N., Jin, M., Qi, H., Yang, J., Li, C., Du, X., Luo, F., Chen, B., Shen, Y. *et al.* (2012) Intermittent PTH (1-34) injection rescues the retarded skeletal development and postnatal lethality of mice mimicking human achondroplasia and thanatophoric dysplasia. *Hum Mol Genet*, **21**, 3941-3955.

98   Jin, M., Yu, Y., Qi, H., Xie, Y., Su, N., Wang, X., Tan, Q., Luo, F., Zhu, Y., Wang, Q. *et al.* (2012) A novel FGFR3-binding peptide inhibits FGFR3 signaling and reverses the lethal phenotype of mice mimicking human thanatophoric dysplasia. *Hum Mol Genet*, **21**, 5443-5455.

99   Jonquoy, A., Mugniery, E., Benoist-Lasselin, C., Kaci, N., Le Corre, L., Barbault, F., Girard, A.L., Le Merrer, Y., Busca, P., Schibler, L. *et al.* (2012) A novel tyrosine kinase inhibitor restores chondrocyte differentiation and promotes bone growth in a gain-of-function Fgfr3 mouse model. *Hum Mol Genet*, **21**, 841-851.

100   Lorget, F., Kaci, N., Peng, J., Benoist-Lasselin, C., Mugniery, E., Oppeneer, T., Wendt, D.J., Bell, S.M., Bullens, S., Bunting, S. *et al.* (2012) Evaluation of the therapeutic potential of a CNP analog in a Fgfr3 mouse model recapitulating achondroplasia. *Am J Hum Genet*, **91**, 1108-1114.

101   Shukla, V., Coumoul, X., Wang, R.H., Kim, H.S. and Deng, C.X. (2007) RNA interference and inhibition of MEK-ERK signaling prevent abnormal skeletal phenotypes in a mouse model of craniosynostosis. *Nat Genet*, **39**, 1145-1150.

102   Geister, K.A., Brinkmeier, M.L., Hsieh, M., Faust, S.M., Karolyi, I.J., Perosky, J.E., Kozloff, K.M., Conti, M. and Camper, S.A. (2013) A novel loss-of-function mutation in Npr2 clarifies primary role in female reproduction and reveals a potential therapy for acromesomelic dysplasia, Maroteaux type. *Hum Mol Genet*, **22**, 345-357.

103   Krejci, P., Masri, B., Fontaine, V., Mekikian, P.B., Weis, M., Prats, H. and Wilcox, W.R. (2005) Interaction of fibroblast growth factor and C-natriuretic peptide signaling in regulation of chondrocyte proliferation and extracellular matrix homeostasis. *J Cell Sci*, **118**, 5089-5100.

104   Yasoda, A., Komatsu, Y., Chusho, H., Miyazawa, T., Ozasa, A., Miura, M., Kurihara, T., Rogi, T., Tanaka, S., Suda, M. *et al.* (2004) Overexpression of CNP in chondrocytes rescues achondroplasia through a MAPK-dependent pathway. *Nat Med*, **10**, 80-86.

105   Kake, T., Kitamura, H., Adachi, Y., Yoshioka, T., Watanabe, T., Matsushita, H., Fujii, T., Kondo, E., Tachibe, T., Kawase, Y. *et al.* (2009) Chronically elevated plasma C-type natriuretic peptide level stimulates skeletal growth in transgenic mice. *Am J Physiol Endocrinol Metab*, **297**, E1339-1348.

106   Yasoda, A., Kitamura, H., Fujii, T., Kondo, E., Murao, N., Miura, M., Kanamoto, N., Komatsu, Y., Arai, H. and Nakao, K. (2009) Systemic administration of C-type natriuretic peptide as a novel therapeutic strategy for skeletal dysplasias. *Endocrinology*, **150**, 3138-3144.

107   Bartels, C.F., Bukulmez, H., Padayatti, P., Rhee, D.K., van Ravenswaaij-Arts, C., Pauli, R.M., Mundlos, S., Chitayat, D., Shih, L.Y., Al-Gazali, L.I. *et al.* (2004) Mutations in the transmembrane natriuretic peptide receptor NPR-B impair skeletal growth and cause acromesomelic dysplasia, type Maroteaux. *Am J Hum Genet*, **75**, 27-34.

108   Erneux, C., Edimo, W.E., Deneubourg, L. and Pirson, I. (2011) SHIP2 multiple functions: a balance between a negative control of PtdIns(3,4,5)P(3) level, a positive control of PtdIns(3,4)P(2) production, and intrinsic docking properties. *J Cell Biochem*, **112**, 2203-2209.

109   Caputo, V., Cianetti, L., Niceta, M., Carta, C., Ciolfi, A., Bocchinfuso, G., Carrani, E., Dentici, M.L., Biamino, E., Belligni, E. *et al.* (2012) A restricted spectrum of mutations in the SMAD4 tumor-suppressor gene underlies Myhre syndrome. *Am J Hum Genet*, **90**, 161-169.

110   Hirata, M., Kugimiya, F., Fukai, A., Ohba, S., Kawamura, N., Ogasawara, T., Kawasaki, Y., Saito, T., Yano, F., Ikeda, T. *et al.* (2009) C/EBPbeta Promotes transition from proliferation to hypertrophic differentiation of chondrocytes through transactivation of p57. *PLoS One*, **4**, e4543.

111   Kronenberg, H.M. (2006) PTHrP and skeletal development. *Ann N Y Acad Sci*, **1068**, 1-13.

112   Biesecker, L. (2006) The challenges of Proteus syndrome: diagnosis and management. *Eur J Hum Genet*, **14**, 1151-1157.

113   Caux, F., Plauchu, H., Chibon, F., Faivre, L., Fain, O., Vabres, P., Bonnet, F., Selma, Z.B., Laroche, L., Gerard, M. *et al.* (2007) Segmental overgrowth, lipomatosis, arteriovenous malformation and epidermal nevus (SOLAMEN) syndrome is related to mosaic PTEN nullizygosity. *Eur J Hum Genet*, **15**, 767-773.

114   Beier, F. and Loeser, R.F. (2010) Biology and pathology of Rho GTPase, PI-3 kinase-Akt, and MAP kinase signaling pathways in chondrocytes. *J Cell Biochem*, **110**, 573-580.

115   Ford-Hutchinson, A.F., Ali, Z., Lines, S.E., Hallgrimsson, B., Boyd, S.K. and Jirik, F.R. (2007) Inactivation of Pten in osteo-chondroprogenitor cells leads to epiphyseal growth plate abnormalities and skeletal overgrowth. *J Bone Miner Res*, **22**, 1245-1259.

116   Yang, G., Sun, Q., Teng, Y., Li, F., Weng, T. and Yang, X. (2008) PTEN deficiency causes dyschondroplasia in mice by enhanced hypoxia-inducible factor 1alpha signaling and endoplasmic reticulum stress. *Development*, **135**, 3587-3597.

117   Hsieh, S.C., Chen, N.T. and Lo, S.H. (2009) Conditional loss of PTEN leads to skeletal abnormalities and lipoma formation. *Mol Carcinog*, **48**, 545-552.

118   Sleeman, M.W., Wortley, K.E., Lai, K.M., Gowen, L.C., Kintner, J., Kline, W.O., Garcia, K., Stitt, T.N., Yancopoulos, G.D., Wiegand, S.J. *et al.* (2005) Absence of the lipid phosphatase SHIP2 confers resistance to dietary obesity. *Nat Med*, **11**, 199-205.

119   Olsen, J.V., Blagoev, B., Gnad, F., Macek, B., Kumar, C., Mortensen, P. and Mann, M. (2006) Global, in vivo, and site-specific phosphorylation dynamics in signaling networks. *Cell*, **127**, 635-648.

120   Jurynec, M.J. and Grunwald, D.J. (2010) SHIP2, a factor associated with diet-induced obesity and insulin sensitivity, attenuates FGF signaling in vivo. *Dis Model Mech*, **3**, 733-742.

121   Le Goff, C. and Cormier-Daire, V. (2012) From tall to short: the role of TGFbeta signaling in growth and its disorders. *Am J Med Genet C Semin Med Genet*, **160C**, 145-153.

122   Myhre, S.A., Ruvalcaba, R.H. and Graham, C.B. (1981) A new growth deficiency syndrome. *Clin Genet*, **20**, 1-5.

123   Burglen, L., Heron, D., Moerman, A., Dieux-Coeslier, A., Bourguignon, J.P., Bachy, A., Carel, J.C., Cormier-Daire, V., Manouvrier, S. and Verloes, A. (2003) Myhre syndrome: new reports, review, and differential diagnosis. *J Med Genet*, **40**, 546-551.

124   Asakura, Y., Muroya, K., Sato, T., Kurosawa, K., Nishimura, G. and Adachi, M. (2012) First case of a Japanese girl with Myhre syndrome due to a heterozygous SMAD4 mutation. *Am J Med Genet A*, **158A**, 1982-1986.

125   Zhang, J., Tan, X., Li, W., Wang, Y., Wang, J., Cheng, X. and Yang, X. (2005) Smad4 is required for the normal organization of the cartilage growth plate. *Dev Biol*, **284**, 311-322.

126   Wang, Y., Wysocka, J., Perlin, J.R., Leonelli, L., Allis, C.D. and Coonrod, S.A. (2004) Linking covalent histone modifications to epigenetics: the rigidity and plasticity of the marks. *Cold Spring Harbor symposia on quantitative biology*, **69**, 161-169.

127   Bhaumik, S.R., Smith, E. and Shilatifard, A. (2007) Covalent modifications of histones during development and disease pathogenesis. *Nature structural & molecular biology*, **14**, 1008-1016.

128   Bannister, A.J. and Kouzarides, T. (2011) Regulation of chromatin by histone modifications. *Cell research*, **21**, 381-395.

129   Vega, R.B., Matsuda, K., Oh, J., Barbosa, A.C., Yang, X., Meadows, E., McAnally, J., Pomajzl, C., Shelton, J.M., Richardson, J.A. *et al.* (2004) Histone deacetylase 4 controls chondrocyte hypertrophy during skeletogenesis. *Cell*, **119**, 555-566.

130   Williams, S.R., Aldred, M.A., Der Kaloustian, V.M., Halal, F., Gowans, G., McLeod, D.R., Zondag, S., Toriello, H.V., Magenis, R.E. and Elsea, S.H. (2010) Haploinsufficiency of HDAC4 causes brachydactyly mental retardation syndrome, with brachydactyly type E, developmental delays, and behavioral problems. *Am J Hum Genet*, **87**, 219-228.

131   Ducy, P., Zhang, R., Geoffroy, V., Ridall, A.L. and Karsenty, G. (1997) Osf2/Cbfa1: a transcriptional activator of osteoblast differentiation. *Cell*, **89**, 747-754.

132   Kraft, M., Cirstea, I.C., Voss, A.K., Thomas, T., Goehring, I., Sheikh, B.N., Gordon, L., Scott, H., Smyth, G.K., Ahmadian, M.R. *et al.* (2011) Disruption of the histone acetyltransferase MYST4 leads to a Noonan syndrome-like phenotype and hyperactivated MAPK signaling in humans and mice. *J Clin Invest*, **121**, 3479-3491.

133   Feingold, M., Hall, B.D., Lacassie, Y. and Martinez-Frias, M.L. (1997) Syndrome of microcephaly, facial and hand abnormalities, tracheoesophageal fistula, duodenal atresia, and developmental delay. *Am J Med Genet*, **69**, 245-249.

134   Celli, J., van Bokhoven, H. and Brunner, H.G. (2003) Feingold syndrome: clinical review and genetic mapping. *Am J Med Genet A*, **122A**, 294-300.

135   van Bokhoven, H., Celli, J., van Reeuwijk, J., Rinne, T., Glaudemans, B., van Beusekom, E., Rieu, P., Newbury-Ecob, R.A., Chiang, C. and Brunner, H.G. (2005) MYCN haploinsufficiency is associated with reduced brain size and intestinal atresias in Feingold syndrome. *Nat Genet*, **37**, 465-467.

136   Courtens, W., Levi, S., Verbelen, F., Verloes, A. and Vamos, E. (1997) Feingold syndrome: report of a new family and review. *Am J Med Genet*, **73**, 55-60.

137   Fontana, L., Fiori, M.E., Albini, S., Cifaldi, L., Giovinazzi, S., Forloni, M., Boldrini, R., Donfrancesco, A., Federici, V., Giacomini, P. *et al.* (2008) Antagomir-17-5p abolishes the growth of therapy-resistant neuroblastoma through p21 and BIM. *PLoS One*, **3**, e2236.

138   Northcott, P.A., Fernandez, L.A., Hagan, J.P., Ellison, D.W., Grajkowska, W., Gillespie, Y., Grundy, R., Van Meter, T., Rutka, J.T., Croce, C.M. *et al.* (2009) The miR-17/92

polycistron is up-regulated in sonic hedgehog-driven medulloblastomas and induced by N-myc in sonic hedgehog-treated cerebellar neural precursors. *Cancer research*, **69**, 3249-3255.

139   O'Donnell, K.A., Wentzel, E.A., Zeller, K.I., Dang, C.V. and Mendell, J.T. (2005) c-Myc-regulated microRNAs modulate E2F1 expression. *Nature*, **435**, 839-843.

140   Schulte, J.H., Horn, S., Otto, T., Samans, B., Heukamp, L.C., Eilers, U.C., Krause, M., Astrahantseff, K., Klein-Hitpass, L., Buettner, R. *et al.* (2008) MYCN regulates oncogenic MicroRNAs in neuroblastoma. *International journal of cancer. Journal international du cancer*, **122**, 699-704.

141   Loven, J., Zinin, N., Wahlstrom, T., Muller, I., Brodin, P., Fredlund, E., Ribacke, U., Pivarcsi, A., Pahlman, S. and Henriksson, M. (2010) MYCN-regulated microRNAs repress estrogen receptor-alpha (ESR1) expression and neuronal differentiation in human neuroblastoma. *Proc Natl Acad Sci U S A*, **107**, 1553-1558.

142   Nagy, A., Moens, C., Ivanyi, E., Pawling, J., Gertsenstein, M., Hadjantonakis, A.K., Pirity, M. and Rossant, J. (1998) Dissecting the role of N-myc in development using a single targeting vector to generate a series of alleles. *Current biology : CB*, **8**, 661-664.

143   Moens, C.B., Auerbach, A.B., Conlon, R.A., Joyner, A.L. and Rossant, J. (1992) A targeted mutation reveals a role for N-myc in branching morphogenesis in the embryonic mouse lung. *Genes Dev*, **6**, 691-704.

144   Ota, S., Zhou, Z.Q., Keene, D.R., Knoepfler, P. and Hurlin, P.J. (2007) Activities of N-Myc in the developing limb link control of skeletal size with digit separation. *Development*, **134**, 1583-1592.

145   Klingseisen, A. and Jackson, A.P. (2011) Mechanisms and pathways of growth failure in primordial dwarfism. *Genes Dev*, **25**, 2011-2024.

146   Growth Hormone Research, S. (2000) Consensus guidelines for the diagnosis and treatment of growth hormone (GH) deficiency in childhood and adolescence: summary statement of the GH Research Society. GH Research Society. *J Clin Endocrinol Metab*, **85**, 3990-3993.

147   Bongers, E.M., Opitz, J.M., Fryer, A., Sarda, P., Hennekam, R.C., Hall, B.D., Superneau, D.W., Harbison, M., Poss, A., van Bokhoven, H. *et al.* (2001) Meier-Gorlin syndrome: report of eight additional cases and review. *Am J Med Genet*, **102**, 115-124.

148   de Munnik, S.A., Bicknell, L.S., Aftimos, S., Al-Aama, J.Y., van Bever, Y., Bober, M.B., Clayton-Smith, J., Edrees, A.Y., Feingold, M., Fryer, A. *et al.* (2012) Meier-Gorlin syndrome genotype-phenotype studies: 35 individuals with pre-replication complex gene mutations and 10 without molecular diagnosis. *Eur J Hum Genet*, **20**, 598-606.

149   O'Driscoll, M., Ruiz-Perez, V.L., Woods, C.G., Jeggo, P.A. and Goodship, J.A. (2003) A splicing mutation affecting expression of ataxia-telangiectasia and Rad3-related protein (ATR) results in Seckel syndrome. *Nat Genet*, **33**, 497-501.

150   Kalay, E., Yigit, G., Aslan, Y., Brown, K.E., Pohl, E., Bicknell, L.S., Kayserili, H., Li, Y., Tuysuz, B., Nurnberg, G. *et al.* (2011) CEP152 is a genome maintenance protein disrupted in Seckel syndrome. *Nat Genet*, **43**, 23-26.

151   Al-Dosari, M.S., Shaheen, R., Colak, D. and Alkuraya, F.S. (2010) Novel CENPJ mutation causes Seckel syndrome. *J Med Genet*, **47**, 411-414.

152   Griffith, E., Walker, S., Martin, C.A., Vagnarelli, P., Stiff, T., Vernay, B., Al Sanna, N., Saggar, A., Hamel, B., Earnshaw, W.C. *et al.* (2008) Mutations in pericentrin cause

Seckel syndrome with defective ATR-dependent DNA damage signaling. *Nat Genet*, **40**, 232-236.

153   Rauch, A., Thiel, C.T., Schindler, D., Wick, U., Crow, Y.J., Ekici, A.B., van Essen, A.J., Goecke, T.O., Al-Gazali, L., Chrzanowska, K.H. *et al.* (2008) Mutations in the pericentrin (PCNT) gene cause primordial dwarfism. *Science*, **319**, 816-819.

154   Wang, X., Tsai, J.W., Imai, J.H., Lian, W.N., Vallee, R.B. and Shi, S.H. (2009) Asymmetric centrosome inheritance maintains neural progenitors in the neocortex. *Nature*, **461**, 947-955.

155   Piel, M., Meyer, P., Khodjakov, A., Rieder, C.L. and Bornens, M. (2000) The respective contributions of the mother and daughter centrioles to centrosome activity and behavior in vertebrate cells. *J Cell Biol*, **149**, 317-330.

156   Knoblich, J.A. (2010) Asymmetric cell division: recent developments and their implications for tumour biology. *Nat Rev Mol Cell Biol*, **11**, 849-860.

157   Hemerly, A.S., Prasanth, S.G., Siddiqui, K. and Stillman, B. (2009) Orc1 controls centriole and centrosome copy number in human cells. *Science*, **323**, 789-793.

158   Hossain, M. and Stillman, B. (2012) Meier-Gorlin syndrome mutations disrupt an Orc1 CDK inhibitory domain and cause centrosome reduplication. *Genes Dev*, **26**, 1797-1810.

159   Kuo, A.J., Song, J., Cheung, P., Ishibe-Murakami, S., Yamazoe, S., Chen, J.K., Patel, D.J. and Gozani, O. (2012) The BAH domain of ORC1 links H4K20me2 to DNA replication licensing and Meier-Gorlin syndrome. *Nature*, **484**, 115-119.

160   Stiff, T., Alagoz, M., Alcantara, D., Outwin, E., Brunner, H.G., Bongers, E.M., O'Driscoll, M. and Jeggo, P.A. (2013) Deficiency in origin licensing proteins impairs cilia formation: implications for the aetiology of Meier-Gorlin syndrome. *PLoS Genet*, **9**, e1003360.

161   Nigg, E.A. and Stearns, T. (2011) The centrosome cycle: Centriole biogenesis, duplication and inherent asymmetries. *Nature cell biology*, **13**, 1154-1160.

162   Ishikawa, H. and Marshall, W.F. (2011) Ciliogenesis: building the cell's antenna. *Nat Rev Mol Cell Biol*, **12**, 222-234.

163   Wallingford, J.B. and Mitchell, B. (2011) Strange as it may seem: the many links between Wnt signaling, planar cell polarity, and cilia. *Genes Dev*, **25**, 201-213.

164   Fry, A.M., O'Regan, L., Sabir, S.R. and Bayliss, R. (2012) Cell cycle regulation by the NEK family of protein kinases. *J Cell Sci*, **125**, 4423-4433.

165   Venoux, M., Tait, X., Hames, R.S., Straatman, K.R., Woodland, H.R. and Fry, A.M. (2013) Poc1A and Poc1B act together in human cells to ensure centriole integrity. *J Cell Sci*, **126**, 163-175.

166   Alazami, A.M., Al-Owain, M., Alzahrani, F., Shuaib, T., Al-Shamrani, H., Al-Falki, Y.H., Al-Qahtani, S.M., Alsheddi, T., Colak, D. and Alkuraya, F.S. (2012) Loss of function mutation in LARP7, chaperone of 7SK ncRNA, causes a syndrome of facial dysmorphism, intellectual disability, and primordial dwarfism. *Hum Mutat*, **33**, 1429-1434.

167   Zitano, L., Loder, R.T., Cohen, M.D. and Weaver, D.D. (2012) Severe lateral tibial bowing with short stature in two siblings--a provisionally novel syndrome. *Am J Med Genet A*, **158A**, 2309-2316.

168   Murphy-Ryan, M., Kirmani, S., Thompson, D.M., Binkovitz, L.A., Thomas, K.B. and Babovic-Vuksanovic, D. (2012) A novel sclerosing skeletal dysplasia with mixed

sclerosing bone dysplasia, characteristic syndromic features, and clinical and radiographic evidence of male-male transmission. *Am J Med Genet A*, **158A**, 2292-2296.

169   Abdel-Salam, G.M., Abdel-Hamid, M.S., Saleem, S.N., Ahmed, M.K., Issa, M., Effat, L.K., Kayed, H.F., Zaki, M.S. and Gaber, K.R. (2012) Profound microcephaly, primordial dwarfism with developmental brain malformations: a new syndrome. *Am J Med Genet A*, **158A**, 1823-1831.

170   Baratela, W.A., Bober, M.B., Tiller, G.E., Okenfuss, E., Ditro, C., Duker, A., Krakow, D., Stabley, D.L., Sol-Church, K., Mackenzie, W. *et al.* (2012) A newly recognized syndrome with characteristic facial features, skeletal dysplasia, and developmental delay. *Am J Med Genet A*, **158A**, 1815-1822.

171   Shalev, S.A., Spiegel, R. and Borochowitz, Z.U. (2012) A distinctive autosomal recessive syndrome of severe disproportionate short stature with short long bones, brachydactyly, and hypotrichosis in two consanguineous Arab families. *Eur J Med Genet*, **55**, 256-264.

172   Perrin, L., Fenneteau, O., Ilharreborde, B., Capri, Y., Gerard, M., Quoc, E.B., Passemard, S., Ghoumid, J., Caillaud, C., Froissart, R. *et al.* (2012) A new lysosomal storage disorder resembling Morquio syndrome in sibs. *Eur J Med Genet*, **55**, 157-162.

173   Grigelioniene, G., Papadogiannakis, N., Conner, P., Geiberger, S., Nishikawa, M. and Nakayama, M. (2011) Extending the phenotype of lethal skeletal dysplasia type al Gazali. *Am J Med Genet A*, **155A**, 1404-1408.

174   McAbee, G.N., Santilli, A.M., Stone, J. and Schnur, R.E. (2011) Ectodermal, skeletal, and genitourinary abnormalities with neonatal hyperekplexia. *Pediatric neurology*, **44**, 381-384.

175   Phadke, S.R., Sharda, S., Urquhart, J., Jenkinson, E., Chawala, S. and Trump, D. (2011) Report of two brothers with short stature, microcephaly, mental retardation, and retinoschisis-A new mental retardation syndrome? *Am J Med Genet A*, **155A**, 9-13.

176   Shastry, S., Simha, V., Godbole, K., Sbraccia, P., Melancon, S., Yajnik, C.S., Novelli, G., Kroiss, M. and Garg, A. (2010) A novel syndrome of mandibular hypoplasia, deafness, and progeroid features associated with lipodystrophy, undescended testes, and male hypogonadism. *J Clin Endocrinol Metab*, **95**, E192-197.

177   Lango Allen, H., Estrada, K., Lettre, G., Berndt, S.I., Weedon, M.N., Rivadeneira, F., Willer, C.J., Jackson, A.U., Vedantam, S., Raychaudhuri, S. *et al.* (2010) Hundreds of variants clustered in genomic loci and biological pathways affect human height. *Nature*, **467**, 832-838.

CHAPTER 2

A Novel Loss-of-Function Mutation in *Npr2* Clarifies Primary Role in Female Reproduction and Reveals a Potential Therapy for Acromesomelic Dysplasia, Maroteaux Type

Abstract

We discovered a new spontaneous mutant allele of *Npr2* named *peewee* (*pwe*) that exhibits severe disproportionate dwarfism and female infertility. The *pwe* phenotype is caused by a 4 base-pair deletion in exon three that generates a premature stop codon at codon 313 (L313X). The *Npr2*^pwe/pwe mouse is a model for the human skeletal dysplasia acromesomelic dysplasia, Maroteaux type (AMDM). We conducted a thorough analysis of the female reproductive tract and report that the primary cause of *Npr2*^pwe/pwe female infertility is premature oocyte meiotic resumption, while the pituitary and uterus appear normal. *Npr2* is expressed in chondrocytes and osteoblasts. We determined that loss of *Npr2* causes a reduction in the hypertrophic and proliferative zones of the growth plate but mineralization of skeletal elements is normal. Mutant tibiae have increased levels of the activated form of ERK1/2, consistent with the idea that NPR2 signaling inhibits the activation of the MEK/ERK MAPK pathway.

Treatment of fetal tibiae explants with MEK1/2 inhibitors U0126 and PD325901 rescues the

Npr2[pwe/pwe] growth defect, providing a promising foundation for skeletal dysplasia therapeutics.

Introduction

Disruptions in skeletal development and growth are classified as skeletal dysplasias and are an important contributor to severe short stature, occurring in approximately 1 out of every 5000 births (1). The effects on individuals with skeletal dysplasia can range from relatively minor to lethality (1-3) and multiple organ systems can be affected (1). The advent and improved accessibility to high-throughput sequencing technologies has brought forth a wealth of information regarding the genetic causes of skeletal dysplasias (1, 4). According to the most recent nosology, there are 456 forms of skeletal dysplasia, of which 316 have been associated with mutations in one or more of 226 genes (4). This means that approximately 70% of the skeletal dysplasias have known genetic causes (4). The genetic causes of the remaining forms are currently unknown (1, 3, 4), and even those forms that have a known genetic cause may not have a clear molecular mechanism (1). Animal models of skeletal dysplasia have been useful in understanding the mechanisms by which these genes regulate proper skeletal development and growth and contribute to the pathology of skeletal dysplasia (1, 5-7).

Some disorders of the skeleton also affect the reproductive organs (8-11). Infertility is estimated to affect 15% of the global population and 25% of these cases are idiopathic (12). There has been a surge of interest in the mechanisms of female infertility and sub-fertility with respect to reproductive aging, as many women in developed countries are delaying their age of first conception past their early 20s, when female fertility is at its zenith (13). Mouse models of female infertility have offered much in the way of understanding the genetic regulation of female fertility (14, 15).

We have discovered a novel recessive, mutant allele of *Npr2*, the gene that encodes natriuretic peptide receptor type 2 (NPR2), that we have named *peewee* (*pwe*). The mutant mice have growth insufficiency, skeletal dysplasia, and female infertility. Mutations in *NPR2* cause a rare form of recessive skeletal dysplasia in humans, Acromesomelic Dysplasia, Maroteaux Type (AMDM) (16), which affects the middle and distal portions of limbs and the shape of vertebrae (16, 17). *Npr2* encodes a membrane-bound guanylyl cyclase that generates the secondary messenger cyclic GMP upon binding its ligand, C-Type natriuretic peptide (CNP) (18).

We report a comprehensive analysis of the role of *Npr2* in the regulation of female fertility, and evidence that pharmacological inhibition of MEK1/2 is sufficient to rescue the *peewee* growth defect in tibial explants. These findings offer promising clues as to signaling pathways that could be therapeutic targets in the treatment of AMDM and other forms of skeletal dysplasia.

Results

The *peewee* Growth Defect

The *peewee* (*pwe*) mouse arose on the NAW/WI background, was outcrossed to obtain hybrid vigor, and was maintained as a stock by breeding heterozygotes. Only 12% of the progeny were mutant, which is lower than expected for autosomal recessive inheritance. Outcrossing to *Mus castaneus* supported homozygote viability. Mutants constituted 27% of the progeny of this F1 x F1 intercross (28/103), consistent with the expected Mendelian ratio for an autosomal recessive allele.

pwe homozygous mutants exhibit growth delay and disproportionate dwarfism that is evident at two weeks of age (Figure 2.1). Body weight and crown-rump length of mutants are
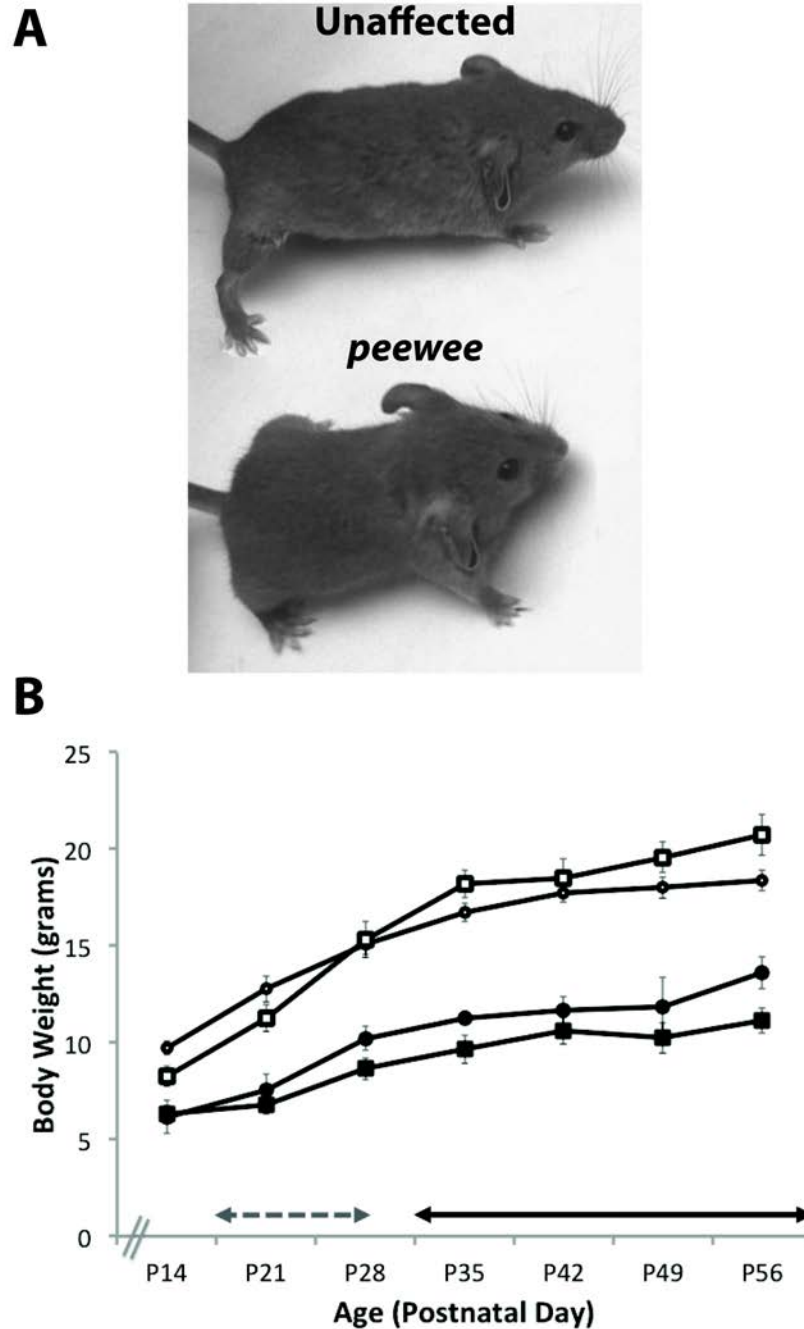
Figure 2.1. Decreased body size and growth delay in *peewee* mice. Panel A: Comparison of an unaffected littermate and a *peewee* mutant reveal decreased body size and cranial dysmorphology by 2 weeks of age (P14). Panel B: Growth curve (unaffected males: open squares, unaffected females: open circles; affected males: closed squares; affected females: closed circles) showing significant decrease in body weight in mutants by P14. Arrows below indicate range of ages at vaginal opening in unaffected (dashed arrow, n=11) and affected (solid arrow, n=6) females.

54% and 77%, respectively, of their unaffected littermates (Table 2.1). *pwe* mice have a

characteristic cranial dysmorphology that includes a domed skull and short snout (Figure 2.1A).

Malocclusion is frequent, but incompletely penetrant. All bones formed through endochondral

ossification are significantly reduced in length (Table 2.1 and Figure 2.2A, Panels A-L).

Table 2.1. Disproportionate Dwarfism in *peewee* Mutants				
	unaffected	*peewee*	**ratio[1]**	**p-value**
body weight (g)	25±1	16±1	0.54	0.001
Length of body and skeletal elements (mm)[2]				
crown to rump	71.05±0.96	54.43±0.94	0.77	0.0003
radius	10.40±0.19	5.28±0.13	0.51	<0.0001
ulna	12.83±0.25	7.16±0.18	0.56	<0.0001
femur	15.12±0.19	8.49±0.21	0.56	<0.0001
humerus	11.52±0.17	7.36±0.17	0.64	<0.0001
tibia	15.84±1.01	10.28±0.29	0.65	0.001
illium	17.09±0.39	12.59±0.13	0.74	<0.0001
scapula	10.93±0.15	8.22±0.15	0.75	<0.0001
skull	23.38±0.31	19.89±0.41	0.85	0.0003
Width of skeletal elements (mm)[2]				
L6 vertebrae	3.51±0.09	2.48±0.08	0.71	0.001
femur[3] (a)	2.08±0.04	1.83±0.03	0.88	0.0005
femur[3] (b)	1.47±0.04	1.36±0.04	0.93	NS
skull	11.52±0.22	11.28±0.35	0.98	NS
rib	0.78±0.05	0.83±0.03	1.06	NS

[1]*Ratio of peewee to unaffected*
[2]*Individual skeletal elements are listed from most affected to least affected*
[3]*Femurs were measured in the thicker (a) and thinner (b) dimensions*

The proximal skeletal elements of the appendicular skeleton (femur and humerus) are the

most severely affected in the *pwe* mouse (Table 2.1 and Figure 2.2A, Panels C and E). All

skeletal elements formed through endochondral ossification are ≤ 75% the length of unaffected

skeletal elements (Table 2.1 and Figure 2.2A, Panels A-L). There is no reduction in the width of

the skull, femur (thinner dimension) or ribs (Table 2.1). A fully penetrant aspect of the

phenotype is a notch on the dorsal surface of the atlas (Figure 2.2A, Panel K).
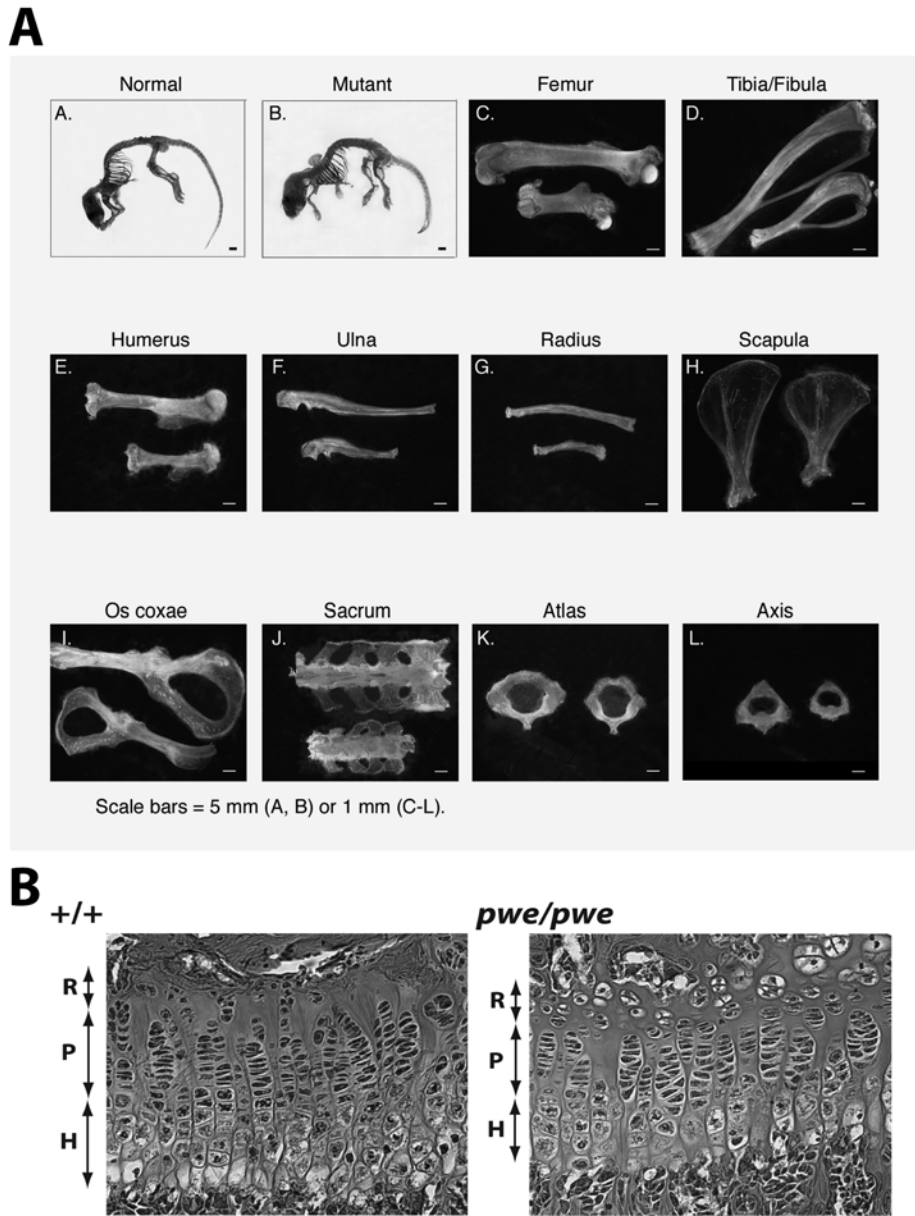
Figure 2.2. Skeletal phenotype of *peewee* mice. Panel A: Whole skeletal preparations individual skeletal elements from mutants and normal littermates. Unaffected (A.) and affected whole skeletons (B.) are shown. Individual skeletal elements from unaffected and affected animals were dissected from whole skeletons (C.-L.). K: C2, or the atlas: Mutant C2 vertebrae have an abnormal notch on the dorsal side. Panel B: Bone histology. Sections through 5-week old male proximal tibiae at the level of the growth plate (40X Magnification). Arrows indicate hypertrophic (H), proliferative (P) and resting zones (R).

Sections through 5-week old male tibial growth plates suggest that the skeletal growth defect in *pwe* mice stems from a disruption in the regulation of chondrocyte differentiation, and potentially proliferation, due to the reduction in the height of the hypertrophic and proliferative zones of the growth plate (Figure 2.2B). However, all zones of the growth plate are present, and their organization is maintained, meaning that the disturbance in skeletal growth may be due to a disruption in the number or rate in which the chondrocytes progress through the zones of the growth plate (Figure 2.2B).

Molecular Identification of the *peewee* mutation

Analysis of DNA samples from fifteen affected animals from a [(*pwe/+)* X CAST/Ei$^{+/+}$] F1 X F1 intercross with a SNP mapping panel (19) placed the locus in a region on proximal mouse chromosome 4. Analysis of additional animals with more markers confirmed this location and narrowed the interval. The genotype of affected mice placed the mutation distal to the microsatellite marker *D4Mit93* (Figure 2.3A), and analysis of unaffected animals narrowed the critical interval to a 3 Mb region between *D4Mit212* and *D4Mit109* (Figure 2.3A, 1 animal per marker), that contains more than 80 genes and corresponds to human chromosome 9p13.3. A search for skeletal dysplasias associated with this region of human chromosome 9 identified Acromesomelic Dysplasia, Maroteaux Type, which is caused by loss-of-function mutations of *Npr2* in humans (16, 17). Sequencing of *Npr2* in known *pwe* mutants revealed a four base-pair deletion in exon 3 of *Npr2* (Figure 2.3B). This deletion results in a frameshift that generates a premature stop codon at codon 313, which encodes a leucine residue in the wild type and reference open reading frame (ORF) (L313X, Figure 2.3B). Genotyping this mutation revealed that one apparently affected animal was actually a runted heterozygote, explaining the erroneous exclusion of *Npr2* as a potential candidate gene early in our analysis (Figure 2.3A, asterisk).
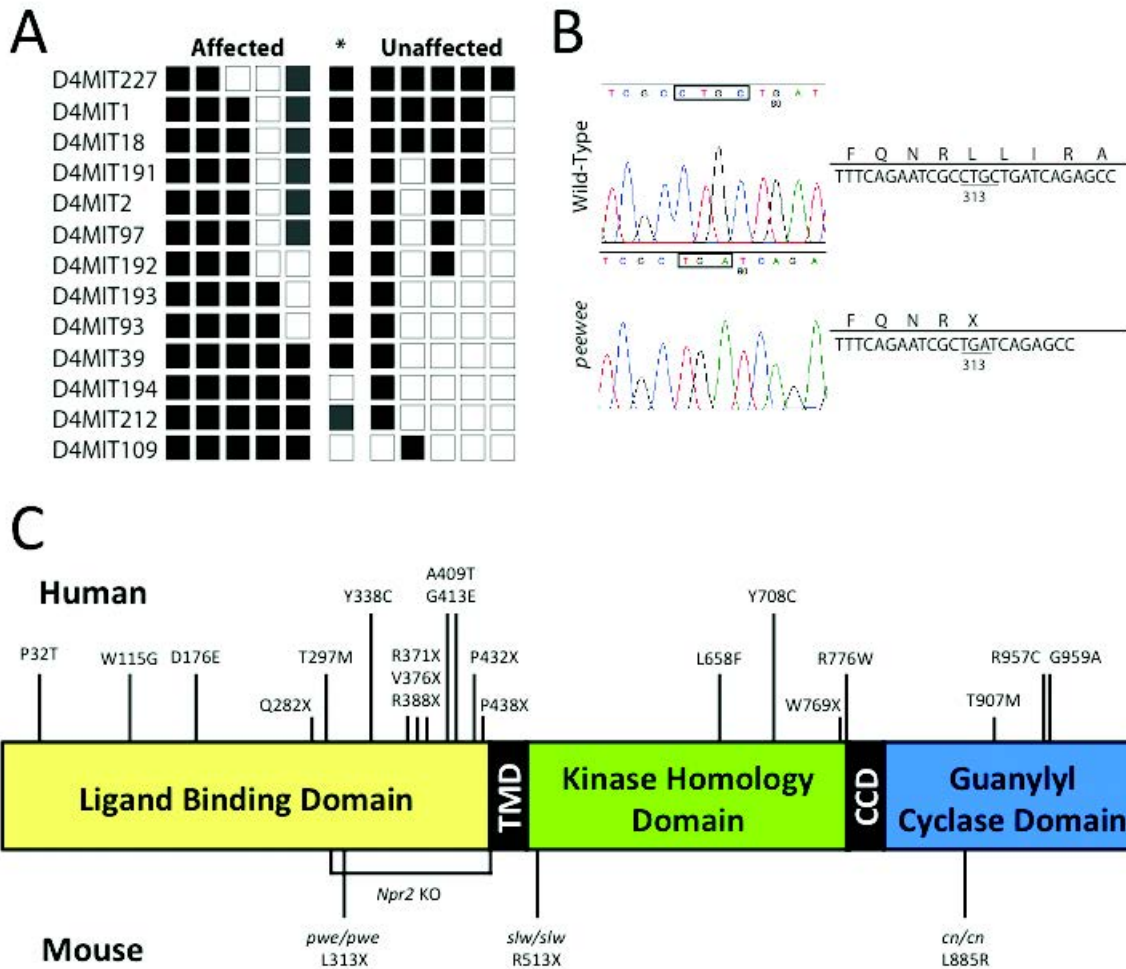
Figure 2.3. The *peewee* phenotype is caused by a mutation in *Npr2*. Panel A. Mapping of the *peewee* critical interval in progeny of an F1 X F1 cross with *Mus castaneus*. Haplotypes are shown for selected mice, and genotypes indicating homozygous or heterozygous *Mus castaneus* alleles are open boxes, homozygous *peewee* stock are black boxes, and gray boxes indicate data are unavailable. The critical interval is limited to the region between *D4MIT212* and *D4MIT109*. A single animal that appeared affected genotypes as a heterozygote in the critical interval (*). Panel B: DNA sequencing of genomic DNA reveals that *peewee* animals have a 4 bp deletion in exon 3 of *Npr2*. This generates a premature stop codon at codon 313 (L313X). Panel C: Missense and nonsense mutations (true nonsense and those formed from frame shift mutations) in NPR2 are found in AMDM patients (16, 20-22), spontaneous mutant *Npr2*[slw/slw] and *Npr2*[cn/cn] mice (23-25), and a targeted knock out (KO) animal (26). (TMD: Transmembrane domain, CCD: Coiled-coil domain)

Npr2 encodes a membrane-bound guanylyl cyclase that is present at the plasma membrane as a dimer (18). Mutations in human AMDM patients occur throughout the length of the encoded NPR2 protein (16, 21) (Figure 2.3C). The premature stop codon at codon 313 in *Npr2*[pwe/pwe] mice truncates NPR2 within the ligand-binding domain (18) (Figure 2.3C). Without an intact ligand binding domain or any of the domains C-terminal to the premature stop codon, any translated protein from the *pwe* allele is predicted to be non-functional, generating a null allele (Figure 2.3C). The growth insufficiency of *pwe* mutants is indistinguishable from that reported for other mouse null alleles of *Npr2* (23-26).

Npr2[pwe/pwe] Female Infertility

We tested fertility by mating wild-type mice with *Npr2*[pwe/pwe] mutants. Males were sub-fertile, but had no obvious abnormalities in the penian bone or testis histology (data not shown). Over a three-month period, all unaffected females (n=3) bore litters, while none of the *Npr2*[pwe/pwe] females (n=3) bore litters (data not shown). *Npr2* is expressed at all levels of the female reproductive tract in the rodent (18, 27-30). Thus, *Npr2*[pwe/pwe] female infertility could be due to defects in any or all of these organs. We undertook a systematic approach to uncover critical sites of *Npr2* action in the female reproductive tract.

We tested whether *Npr2*[pwe/pwe] females experienced puberty normally by observing the date of vaginal opening as an indicator of the onset of puberty in mice (31-33). The control animals experienced vaginal opening on average at postnatal day 21 (P21) as expected (Figure 2.1B, range: P18-P28, n=11), while *Npr2*[pwe/pwe] females experienced vaginal opening from P33-P84 (Figure 2.1B, n=6). The extensive delay in puberty in individual *Npr2*[pwe/pwe] females appears to correlate with their body weight (Appendix 2.1). Body weight is a known predictor of the onset of puberty in mice (32, 33) and humans (34).

To determine whether post-pubertal $Npr2^{pwe/pwe}$ females were capable of cycling through estrus, vaginal smears were taken for 20 consecutive days and estrous stage was assigned by vaginal cytology (31). Control (n=7) and $Npr2^{pwe/pwe}$ (n=4) females cycled normally through all stages of the estrous cycle during this 20-day period (Figure 2.4A). The amount of time spent in each of stage of the cycle did not differ between mutants and controls (Figure 2.4A). Thus, while $Npr2^{pwe/pwe}$ females have a delay in the onset of puberty, they are capable of cycling through estrus normally, suggesting that the hypothalamus and pituitary are functioning properly to regulate the estrous cycle (31, 35). The diestrus uterine histology of $Npr2^{pwe/pwe}$ females is normal at 12 weeks of age, indicating that the uterine tissues, including the endometrium, myometrium, and stromal glands, are intact (Figure 2.4C).

To assess ovarian follicle development in the $Npr2^{pwe/pwe}$ female, we stimulated pre-pubertal females with PMSG, which stimulates follicle growth to the pre-ovulatory stage. Oocytes are arrested around birth at prophase I, and this is morphologically distinguished by the presence of a germinal vesicle (13, 15, 36-38). The germinal vesicle is normally maintained until the pre-ovulatory follicle receives the surge of LH that promotes meiotic resumption and ovulation (13, 15, 36-38). At this point, the germinal vesicle will break down, the meiotic spindle is formed, and the first meiotic division is completed with the extrusion of the first polar body (13, 15, 36-38). Pre-ovulatory follicles in the ovaries of PMSG-primed control females contained oocytes (either released from ovarian follicles or in sections of whole ovaries) with intact germinal vesicles (Figure 2.5A). However, $Npr2^{pwe/pwe}$ oocytes had progressed prematurely through meiosis; virtually all oocytes examined underwent premature germinal vesicle breakdown (GVBD) (Figure 2.5A). Some had formed meiotic spindles, or extruded one or even two polar bodies (Figure 2.5A). Cyclic GMP (cGMP), which is generated by NPR2, is
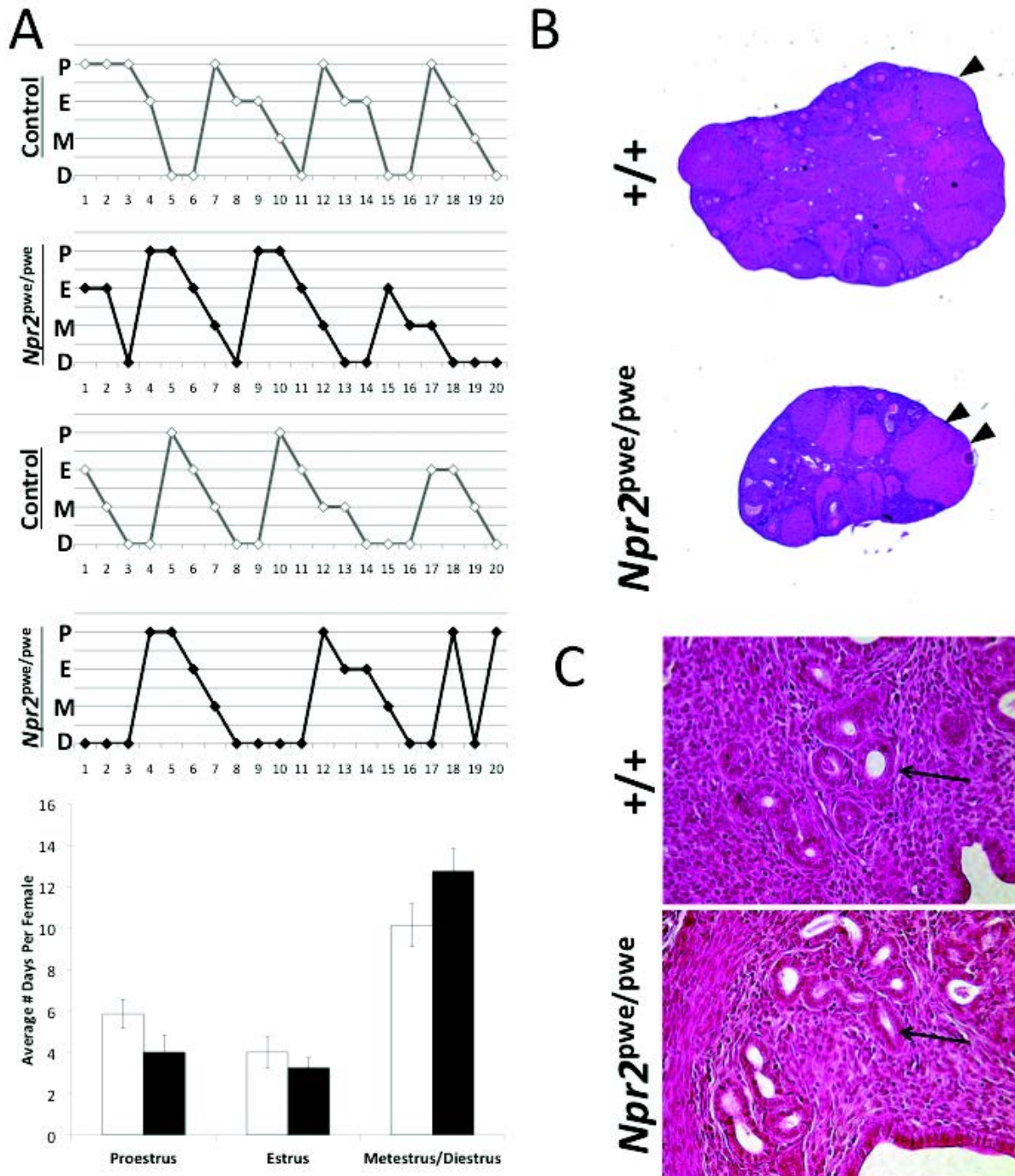
Figure 2.4. *Npr2*^{pwe/pwe} **females cycle through estrus, have normal levels of estradiol and FSH, form corpora lutea, and have normal uterine histology.** Panel A: Estrous cycles of two representative *Npr2*^{pwe/pwe} females (black symbols and lines) and controls (white symbols and grey lines) over a 20-day consecutive period show all stages of the estrous cycle (P=proestrus, E=estrus, M=metestrus, and D=diestrus, top panel). *Npr2*^{pwe/pwe} females spend similar amounts of time in each stage of the estrous cycle as controls. Panel B: 8 week *Npr2*^{pwe/pwe} ovaries contain corpora lutea at metestrus (arrowheads). Panel C: 12 week *Npr2*^{pwe/pwe} uterine histology at diestrus is normal, including the presence of stromal glands (arrows).

70

Figure 2.5. ***Npr2*^{pwe/pwe} female infertility is caused by a failure in meiotic arrest, leading to the release of oocytes that are not viable**. Panel A: Oocytes from unaffected (+/-) and *Npr2*^{pwe/pwe} mice were released from pre-pubertal PMSG-primed antral follicles by needle puncture and examined by light microscopy with DIC optics (left). Almost all unaffected oocytes had a single pronucleus while most oocytes from *Npr2*^{pwe/pwe} follicles exhibited GVBD (Germinal Vesicle Breakdown) and premature formation of polar bodies. The percentage of oocytes that underwent GVBD is shown at the far right (top). Data are the mean ± SEM of three separate experiments. Histological sections from fixed ovary tissues from the same mice (center panels) revealed premature meiotic spindle formation in mutants. Extracts from pre-pubertal PMSG-primed antral follicles had measurable levels of cGMP in controls, but undetectable levels in mutants (far right, bottom). Data are the mean ± SEM of three separate experiments. Panel B: Superovulated pre-pubertal wild type (+/+) mice released normal eggs whereas nearly all mutant oocytes underwent fragmentation. When wild-type and *Npr2*^{pwe/pwe} females were superovulated and mated with wild-type males, *Npr2*^{pwe/pwe} females (black bars) released fewer oocytes compared with the wild type (white bars). Most of the mutant oocytes were not fertilized and mutant zygotes failed to develop to 2-cell embryos. Data are the mean ± SEM (Control, n=6; Mutant, n=4)
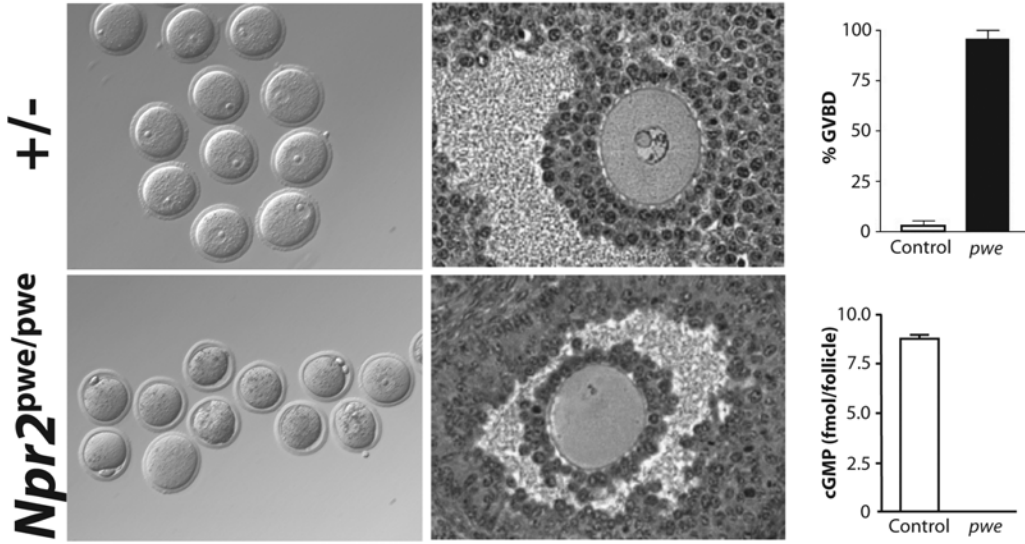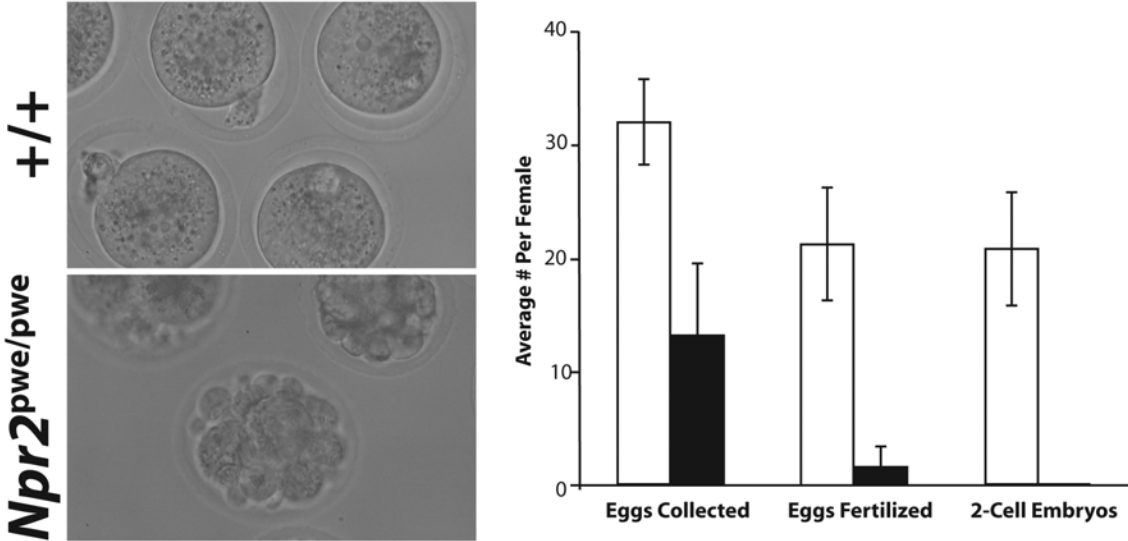
known to inhibit progression through meiosis (39, 40). The level of cGMP in $Npr2^{pwe/pwe}$ antral follicles was reduced to undetectable levels (Figure 2.5A).   Thus, $Npr2$ is essential for cGMP production and maintenance of meiotic arrest in the oocyte.

To determine whether $Npr2^{pwe/pwe}$ females were capable of releasing fertilizable oocytes into the oviducts, we superovulated pre-pubertal $Npr2^{pwe/pwe}$ females as described in the Methods and mated them with a proven wild-type male. $Npr2^{pwe/pwe}$ females ovulated fewer oocytes than controls (Figure 2.5B), and they underwent oocyte fragmentation, a precursor to oocyte cell death (41). None of the $Npr2^{pwe/pwe}$ oocytes progressed to the two-cell embryo stage.

We tested the natural ability of $Npr2^{pwe/pwe}$ females to ovulate by conducting natural mating experiments with mature, post-pubertal animals. $Npr2^{pwe/pwe}$ females released similar numbers of oocytes when compared to controls ($Npr2^{pwe/pwe}$, n=6 and control, n=6), data not shown). We measured levels of FSH and estradiol. Levels of both hormones at diestrus were normal (Table 2.2). Levels of LH and FSH from individual male and female pituitaries determined by RIA were also normal (data not shown). Sections through $Npr2^{pwe/pwe}$ ovaries at 8 and 12 weeks revealed the presence of corpora lutea (Figure 2.4B), consistent with ovulation (35, 42). Together, these data indicate that the hypothalamus and pituitary of $Npr2^{pwe/pwe}$ females are functioning well enough to support ovulation and the ovary responds with appropriate steroid hormone production (35, 42).

Table 2.2. Normal Hormone Levels In *peewee* Females		
Hormone	**Unaffected**	*peewee*
FSH* (ng/mL)	16.9±10.8	17.8±8.6
Estradiol** (pg/mL)	16.4±4.7	15.1±3.8

*Multiplex testing on serum samples collected at diestrus (Control, n=8; *peewee*, n=8)
**ELISA on serum samples collected at diestrus (Control, n=8; *peewee*, n=8)

***Npr2* and Bone Tissue Mineral Density**

      Npr2 is expressed in osteoblasts as well as chondrocytes (43), and data suggest that CNP-NPR2 signaling may augment osteoblast differentiation in combination with other factors (44). It is hypothesized that many disruptions in the growth plate also affect the normal function of osteoblasts or osteoclasts (7). We assessed whether bone was defective in mineralization or integrity by microscopic computed tomography (microCT) scans of 12-week old male femurs and L4 vertebrae (Control, n=6; mutant, n=7). No major deficits in the mineralization of trabecular and cortical bone of *Npr2^pwe/pwe^* males were observed (Appendix 2.1). Therefore, while *Npr2* is expressed in osteoblasts, the loss of *Npr2* in this cell type does not appear to affect proper mineralization of long bones and vertebral elements.

Elevated levels of phosphorylated ERK1/2 in *Npr2*^pwe/pwe^ tibiae

      The fibroblast growth factor (FGF) signaling axis is a potent activator of the MEK/ERK MAPK pathway in the growth plate (45, 46) (Figure 2.6A). Gain-of-function mutations in the gene that encodes FGF receptor 3 (FGFR3) cause achondroplasia in humans (1, 6, 7, 46, 47). In cultured chondrocytes, activation of MEK/ERK leads to a reduction in the production of extracellular matrix proteins, differentiation, and possibly proliferation (45, 46). The cGMP generated by NPR2 upon binding CNP activates cGMP-dependent protein kinase II (PKGII), which goes on to inhibit the activation of RAF-1, the activator of MEK1/2 (45). Thus, NPR2 signaling halts the MEK/ERK MAPK cascade at the level of RAF-1 (Figure 2.6A) through its activation of PKGII (45) *in vitro*.

      We hypothesized that if *Npr2*^pwe/pwe^ mice lack the critical receptor required for MEK/ERK inhibition, they should have increased levels of phosphorylated ERK1/2. Western blot analysis was performed using postnatal day three (P3) tibial lysates. Higher levels of

phosphorylated ERK1/2 were observed in lysates prepared from mutant tibiae relative to wild type (Figure 2.6B). Thus, signaling through NPR2 inhibits the activation of the MEK/ERK MAPK pathway in intact bone.

Therapy for the *Npr2^{pwe/pwe}* growth defect

We reasoned that treatment of *Npr2*^{pwe/pwe} mice with a pharmacological inhibitor of the MEK/ERK MAPK pathway might improve bone growth. We cultured fetal tibiae harvested at embryonic day 16.5 for six days as explants in the presence of vehicle (DMSO) or the MEK1/2 inhibitors U0126 and PD325901 (Figure 2.7A) (26, 48-52). PD325901 is a potent MEK1/2 inhibitor (52), and has been used to study mouse cancers (48, 49). After the culture period, the tibiae were photographed and measured (Figure 2.7). Mutant tibiae were shorter than wild type after treatment with vehicle, and both inhibitors induced growth of wild type and mutant tibiae. PD235901 induced more growth than U0126. Two-way ANOVA and Bonferroni post-hoc analysis confirmed that the effects of both treatments were highly significant (Figure 2.7B, $p<0.0001$, n=16 of both genotypes for U0126, n=7 of both genotypes for PD325901). Drug-induced growth of the normal tibiae suggests that CNP signaling is rate limiting in normal mice. Western blots revealed reduced phosphorylated ERK1/2 in U0126-treated animals, demonstrating that the drug effectively inhibited MEK/ERK activation in explants from normal and mutant mice (Figure 2.7C).

The histology of sections from cultured tibiae suggested that the primary effect of U0126 on wild type and mutant tibiae was to expand the size of the hypertrophic zone (Figure 2.7A). *In situ* hybridization was performed to assess expression of *Col10a1* (53) (collagen 10, alpha subunit), a marker of hypertrophic chondrocytes (Figure 2.7A). The cells in this expanded zone
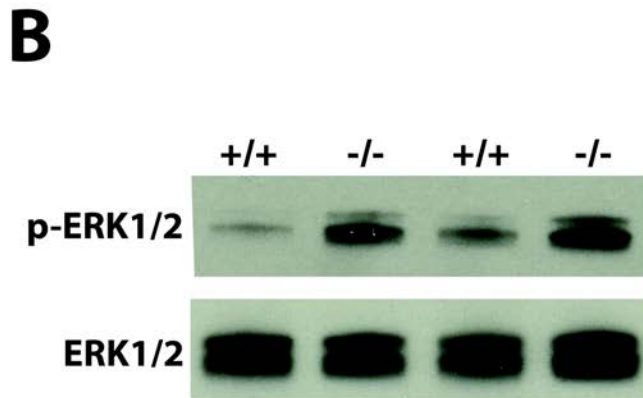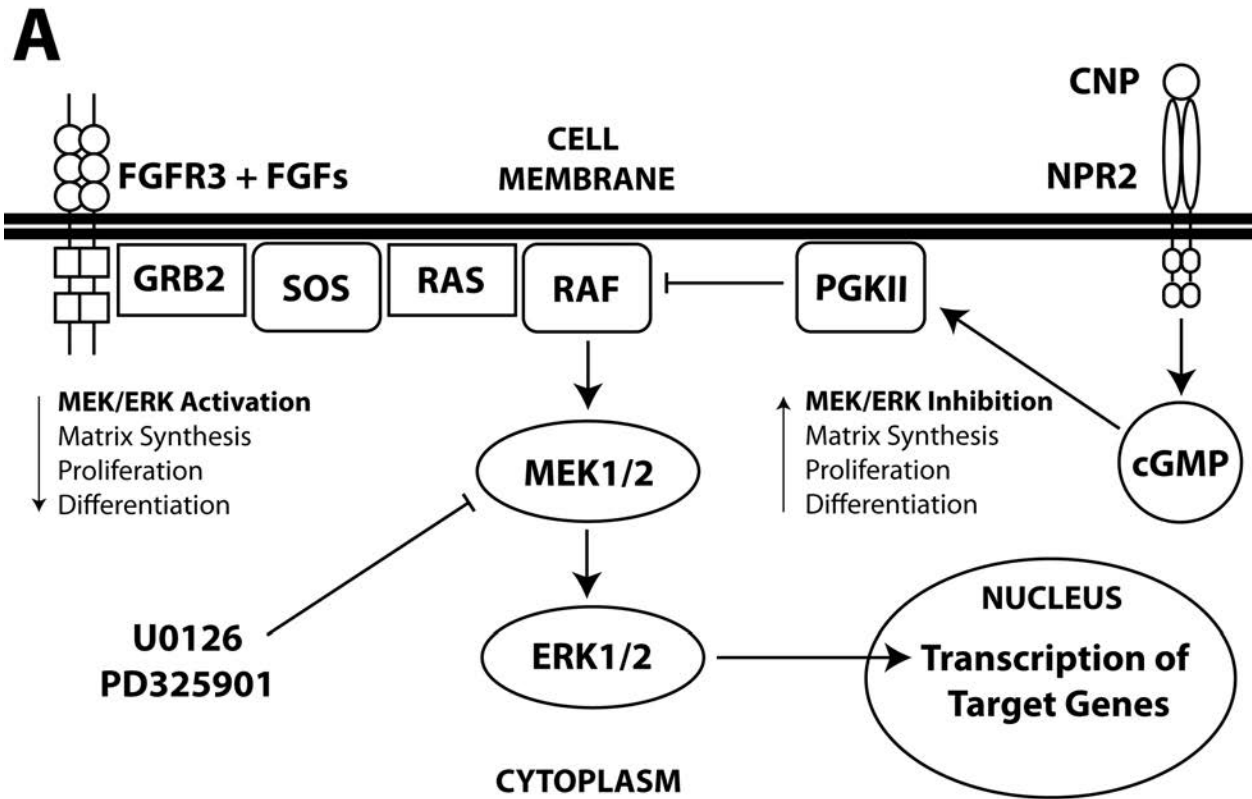
Figure 2.6. FGF and CNP signaling pathways converge at the MEK/ERK pathway and *Npr2*[pwe/pwe] mutants have elevated phosphorylated ERK1/2. Panel A: Diagram detailing the key components involved in the FGF and CNP pathways in the growth plate, and the outcomes of activation of these pathways (7, 45, 46, 51, 54, 55). Panel B: Western blots on postnatal day 3 individual tibial lysates (1 tibia per lane) indicate that *Npr2*[pwe/pwe] tibiae (-/-) have elevated levels of phosphorylated ERK1/2 (p-ERK1/2) relative to wild type (+/+) but similar levels of total ERK1/2. Blot images are representative exposures of membranes incubated first with p-ERK1/2 primary antibody, stripped, and incubated with total ERK1/2 primary antibody.

Figure 2.7. **MEK1/2 inhibitors rescue the *Npr2*^{pwe/pwe} growth defect in explants.** Panel A: Treatment with the inhibitor U0126 increases the length of mutant and wild type tibiae by increasing the hypertrophic zone. Both wild type and mutant whole tibiae are obviously longer than their DMSO (vehicle) treated contralateral controls. Sections stained with nuclear fast red and alcian blue show the expansion of the hypertrophic zone (vertical arrows) upon treatment. *In situ* hybridization reveals *Col10a1* transcripts in the hypertrophic zone of all samples. Panel B: Quantification of tibial length in U0126 (n=16 for both genotypes) and PD325901 (901) (n=7 for both genotypes) treated mutants (-/-) relative to wild type (+/+). Treatment of both genotypes with either inhibitor leads to a highly significant increase in length ($p<0.0001$). The PD325901-treated cohort is significantly longer than those treated with U0126 ($p<0.01$). Letters indicate groups that are significantly different from one another (a,b,c), while the superscript numbers indicate the two different treatment groups (1: U0126, 2: PD325901) Panel C: Western blot of phosphorylated ERK1/2 conducted on U0126-treated tibiae of both genotypes harvested at E16.5 and cultured in the presence of vehicle (DMSO) or U0126 for 6 days indicates that U0126 inhibits activation of ERK1/2 without altering levels of total ERK1/2 protein. Each lane contains lysates pooled from 4 individual tibiae of each genotype and treatment. Blot images are representative exposures of membranes incubated first with p-ERK1/2 primary antibody, stripped, and incubated with total ERK1/2 primary antibody.
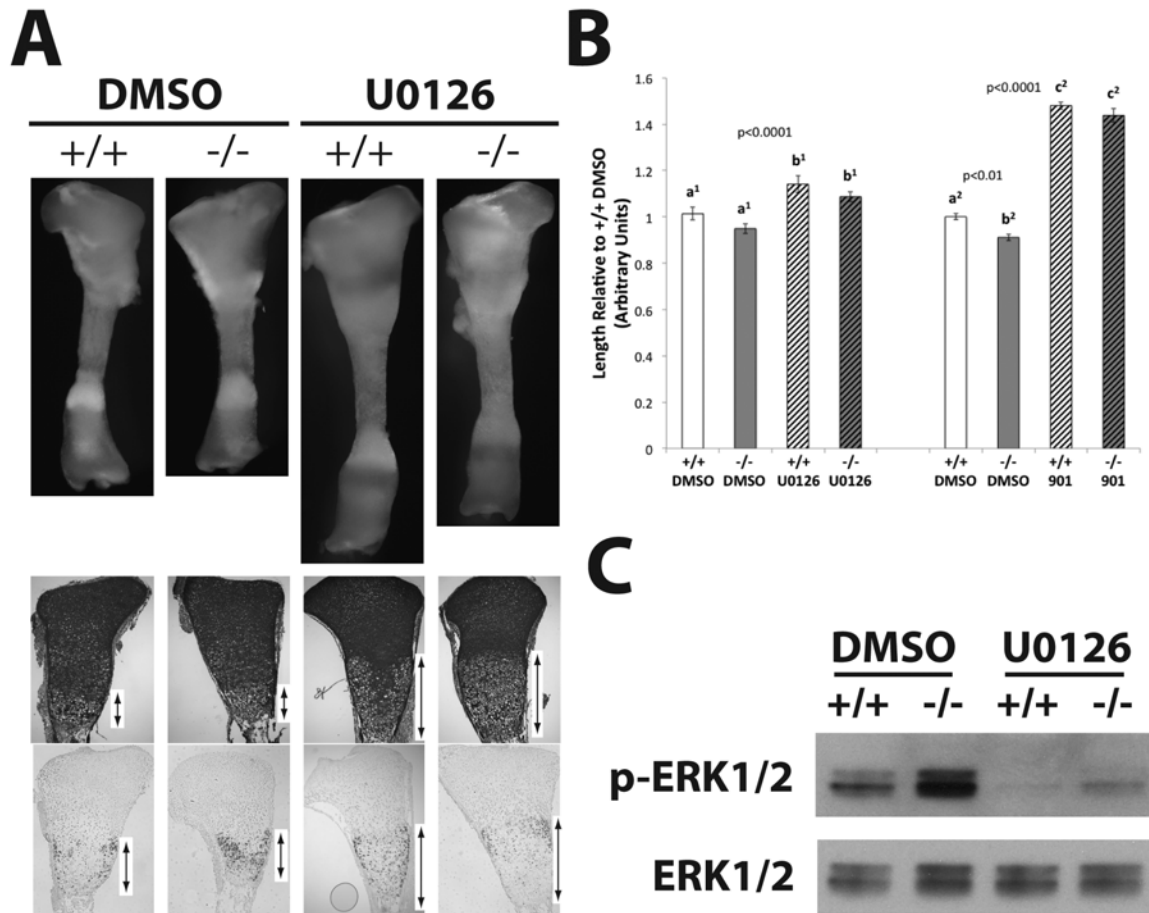
of the growth plate are marked with *Col10a1* transcripts, confirming that these are hypertrophic chondrocytes.

Discussion

We have identified the genetic defect in *peewee*, a new spontaneous mutant allele of *Npr2*, with growth insufficiency and female infertility. The phenotype is caused by a 4-bp deletion in exon 3 of *Npr2* that generates a premature stop codon at codon 313. This leads to truncation of the receptor within the ligand-binding domain and a predicted null allele due to the loss of all domains C-terminal to the mutation. Other null alleles of *Npr2* with similar skeletal and growth insufficiencies have been reported, but previous characterization focused on other

aspects of *Npr2* function including blood pressure regulation and gastrointestinal tract function (25, 26). Here we report a comprehensive analysis of female infertility and a bone growth in response to pharmacotherapy.

Since *Npr2* is expressed in all the major organs of the female reproductive tract (18, 27-30), we addressed the possibility that multiple organs could contribute to *peewee* female infertility. We show for the first time that *Npr2*-deficient females exhibit a delay in puberty, and this delay correlates with the body size (32, 33). Once *Npr2*$^{pwe/pwe}$ females reach puberty, they progress through all stages of the estrous cycle and are capable of ovulating in response to exogenous and natural stimulation. Our results differ from previous reports that the *Npr2* knock out allele caused loss of cycling, uterine atrophy, reduced endometrial and myometrial layers, and absent stromal glands (26). The differences are likely due to genetic background effects. We characterized *Npr2*$^{pwe/pwe}$ on a mixed background that supports viability, but the mutation has reduced viability on other backgrounds, similar to reports for other *Npr2* alleles. Susceptible background strains may offer less compensation for *Npr2* deficiency in a variety of organs that express *Npr2*, including the uterus and pituitary gland. Genetic compensation could involve variable cross talk between other natriuretic peptide receptors and ligands.

Npr2$^{pwe/pwe}$ females have normal serum levels of FSH and estradiol at diestrus and naturally ovulate, indicating that hypothalamic stimulation of the pituitary by pulsatile GnRH secretion and pituitary secretion of FSH and LH (35) are occurring. This is surprising, given that *Npr2* is expressed at all points of the female HPG axis (18, 27-30), and natriuretic peptide signaling through NPR2 was proposed to play a role in gonadotropin production (29). Importantly, this work and the work of others (56) clearly demonstrate that *Npr2* signaling is not required for HPG axis function in the female in the context of this genetic background.

The primary cause of female infertility in $Npr2^{pwe/pwe}$ females is premature oocyte meiotic resumption. We show that in $Npr2^{pwe/pwe}$ mice, impaired cGMP production in ovarian follicles is associated with premature oocyte maturation and impaired embryonic development. Our findings support the requirement for NPR2 to maintain the production of cGMP in ovarian follicles to ensure oocyte meiotic arrest (27). Although $Npr2^{pwe/pwe}$ females are able to ovulate in response to exogenous or endogenous gonadotropin stimulation, the oocytes undergo fragmentation (41). This has been reported in $Npr2^{cn/cn}$ mutants, mice with reduced levels of CNP ($Nppc^{lbab/lbab}$), and in the G-protein coupled receptor 3 mutant mouse ($Gpr3^{-/-}$) (56). $Gpr3^{-/-}$ oocytes have reduced levels of cAMP, leading to premature meiotic resumption and oocyte fragmentation (41). Taken together, the primary site of $Npr2^{pwe/pwe}$ female infertility is the oocyte. None of the descriptions of people affected with AMDM discuss female fertility (16, 17, 20-22). Our studies suggest that if AMDM female patients are infertile due to a failure to maintain oocyte meiotic arrest, they may be able to bear children using donor eggs, provided that uterine and placental function are normal.

Endochondral bone ossification involves the differentiation of condensed mesenchymal cells into chondrocytes that will proliferate and undergo terminal hypertrophic differentiation to ultimately promote the vascularization, mineralization, and recruitment of osteoclasts and osteoblasts into the nascent element (1, 5, 6). The trabecular and cortical tissue mineral density of femurs and L4 vertebral elements are normal in $Npr2^{pwe/pwe}$ mice, even though the receptor is expressed in osteoblasts (43). It is clear that the main role of the CNP-NPR2 signaling axis in skeletal elements is to regulate their longitudinal growth through action in the growth plate. Without $Npr2$, chondrocyte hypertrophy is compromised, so the bones of mutant animals will

never reach a normal adult length, although the bone tissue laid down is normal in its composition.

Both the proliferative and hypertrophic zones of the growth plates in $Npr2^{pwe/pwe}$ animals appear reduced in size, consistent with the $Npr2$ knock-out mouse (26) and other spontaneous mutant alleles of $Npr2$ (23, 24). Loss of $Npr2$ does not affect the overall organization of the growth plate, but probably affects either the overall number of chondrocytes recruited to undergo hypertrophic differentiation, the rate in which they commit to this fate, and/or the rate in which they proliferate. We observed elevated activation of ERK1/2 in whole mutant tibial lysates, which demonstrates that NPR2 is required for ERK1/2 inhibition *in vivo*, as predicted by *in vitro* cell culture studies (45).

Treatment for skeletal dysplasia involves multiple lengthening surgeries for the long bones (1, 47). These surgeries are expensive, time consuming, fraught with many possible complications, and ultimately result in only a modest increase in bone length (1, 47). In general, the acceptance of short stature is advocated in the USA by patients, their families, and advocacy groups for individuals with severe short stature (1). There are currently no effective pharmacological therapies for individuals with skeletal dysplasia (1). Growth hormone treatment has been attempted in achondroplasia patients without much success (1, 47). C-Type Natriuretic peptide (CNP), the ligand of NPR2, is a very promising new therapeutic candidate that has been shown to rescue growth defects in mouse models of achondroplasia both genetically and pharmacologically (7, 51, 54, 57). While this therapeutic approach could offer hope for achondroplasia patients and their families, this form of therapy would be ineffective in AMDM patients that lack the receptor for CNP (16).

There are no reports of growth promoting pharmacotherapy for *Npr2* mutants. Here we report successful elongation of *Npr2*^{pwe/pwe} mutant tibiae and inhibition of MEK/ERK MAPK signaling within these tibial explants through utilization of the MEK1/2 inhibitors U0126 and PD325901. We also show that MEK1/2 inhibitor treatment extends the length of the hypertrophic zone, consistent with the proposed role of ERK1/2 inhibition in the promotion of hypertrophic differentiation (7, 45, 51, 58). PD325901 treatment led to a more dramatic increase in tibial length compared to U0126. This could be due to the fact that PD325901 is known to be a more potent MEK1/2 inhibitor, and has been successfully administered to the whole animal in cancer studies (42, 49). PD325901 has also been administered orally in clinical trials (52, 59). Thus PD325901 as well as other structurally related agents that are currently undergoing clinical evaluation in cancer are promising therapeutic candidates for growth defects associated with excess MEK1/2 signaling, including patients with AMDM, achondroplasia or other appropriate skeletal dysplasias. We have administered U0126 to *Npr2*^{pwe/pwe} mice, as another group had done with a mouse model of Apert Syndrome (50), but the results were difficult to reproduce in *Npr2*^{pwe/pwe} animals (data not shown). We leave this avenue of future study open to experts in pharmacotherapy. The key to moving skeletal dysplasia therapeutics forward will be to deliver this class of agents specifically to the growth plate, and individuals with expertise in the realm of pharmacology will be better suited to address this issue.

We have identified a novel null allele of *Npr2* and characterized the effect on long bone growth and female fertility. In addition, we have established a proof of principle for pharmacotherapy to correct poor bone growth. The next challenge is to develop efficacious delivery methods and treatment regimes in intact animals, minimizing effects on other tissues.

Materials and Methods

Generation of *peewee* mice and mapping of the mutation. The *peewee* mutation arose

spontaneously on the NAW/WI strain in Glen Wolfe's laboratory at the University of Kansas

(Lawrence, Kansas). The mice were then transferred to Andrzej Bartke's laboratory at Southern

Illinois University (SIU, Carbondale, Illinois). The line was maintained at SIU by outcrossing

for hybrid vigor. Upon transfer to the University of Michigan in vitro fertilization was carried

out with oocytes from C57BL/6J females (The Jackson Laboratory, Bar Harbor, Maine) and

sperm from a single homozygous *peewee* male from a mixed background including contributions

from the NAW/WI, C57BL/6, and C3H/HeJ strains. The fertilized eggs were transferred to

surrogate mothers yielding *pwe* heterozygotes that were a mixture of all these backgrounds.

Heterozygotes were bred to (C57BL/6J X C3H/HeJ) F1 mice (The Jackson Laboratory, Bar

Harbor, Maine), and the heterozygous progeny of this cross were intercrossed to generate mutant

animals for analysis. These *pwe* heterozygotes were also crossed to *Mus castaneus* and F1

progeny were intercrossed to map the mutation by genotyping SNPs (19) and microsatellite

markers.

All mice were housed in a specific pathogen free facility with 12-h light, 12-h dark cycle in

ventilated cages with unlimited access to tap water and Purina 5020 chow. All procedures using

mice were approved by the University of Michigan Committee on Use and Care of Animals

(UCUCA), and all experiments were conducted in accordance with the principles and procedures

outlined in the National Institutes of Health Guidelines of the Care and Use of Experimental

Animals.

Skeletal preparation and histology. Skeletal preparations of whole, skinned adult mice were

prepared by fixation in 95% ethanol overnight, stained with Alcian Blue, treated with 2% KOH,

stained with Alizarin Red, and stored in glycerol. Bones from affected and unaffected animals were measured with calipers for determination of disproportionate dwarfism. Five week old male tibiae were fixed overnight in 4% formaldehyde in PBS, decalcified as described previously (60), dehydrated through an ethanol series, and embedded in paraffin. Tibiae were sectioned and stained with hemotoxylin and eosin.

Analysis of the onset of puberty and estrous cyclicity. Females were observed for date of vaginal opening daily from P18-P28, and estrous cycles were monitored by vaginal cytology every day for a 20-day period between 8 and 12 weeks of age as described (31).

Hormone measurements. Females were sacrificed at 12 weeks of age at diestrus. Serum was prepared from blood samples after clotting for 90 minutes at room temperature, running a wooden toothpick along the sides of the collection tube, and spinning the samples at 2,000Xg for 15 min. The serum supernatant was removed and stored at -20°C until analysis. Analysis was performed by the University of Virginia Ligand Core.

Analysis of oocytes, ovaries, and uterus. Prepubertal female mice were stimulated with 5 IU pregnant mare's serum gonadotropin (PMSG) to stimulate follicle growth to the preovulatory follicle stage and euthanized 46 hours later (61). Oocytes were released from antral follicles from one ovary by needle puncture. The other ovary was fixed overnight in Bouin's fixative (Ricca Chemicals), dehydrated in an ethanol series, followed by n-butanol, and embedded in paraffin. Sections were stained with Mayer's hemotoxylin and eosin. Uteri were dissected from 12-week old females at diestrus, fixed for 1 hour in 4% PFA, dehydrated through an ethanol series and embedded in paraffin. Sections were stained with hemotoxylin and eosin.

cGMP Quantification. Intact antral follicles were dissected from PMSG-primed ovaries of mutant and control females as previously described (62). The follicles were processed for cGMP

quantification according to the manufacturer's instructions (Cyclic GMP EIA Assay, Cayman Chemical # 581021).

Superovulation. Prepubertal females were stimulated with 5 IU PMSG followed 46 hours later by 5 IU human chorionic gonadotropin (hCG) to induce the superovulation of oocytes (61) and placed with an experienced wild-type male overnight. The morning after hCG administration, females were observed for a copulation plug, and fertilized eggs were collected, counted and cultured in M16 media at 37°C in 5% CO_2 for 4 days to observe normal early embryonic development (61).

Natural mating experiments. 12 week old mutant and control females were placed with an experienced hybrid male (C57BL/6J X C3H/HeJ F1, The Jackson Laboratory, Bar Harbor, Maine) for a week and observed daily for evidence of a copulation plug. The day of the plug, females were euthanized and their oviducts were flushed with a blunted needle filled with a 6% BSA/1 X PBS solution. Oocytes were counted under a dissection microscope.

Micro-computed tomography. Specimens were dissected free of soft tissue and analyzed by micro-computed tomography (μCT, eXplore Locus SP, GE Healthcare Pre-Clinical Imaging, London, ON, Canada). Specimens were immersed in water and scanned 4 (femora) or 12 (vertebrae) at a time using the Parker method (180 degrees plus a 20 degree fan angle) of rotation at 80 kVp and 80μA and added filtration in the form of both an acrylic beam flattener and a 0.02 inch aluminum filter. Images were reconstructed at an isotropic voxel size of 18μm and calibrated for densitometry. A region of interest 20 and 25 percent of the mid-diaphysis was isolated from the femora for trabecular and cortical analysis, respectively. A region of interest including centrum of the vertebrae and excluding the spinal processes was segmented out for trabecular analysis. Manufacturer software (MicroView v2.2, GE Healthcare Pre-Clinical

Imaging, London, ON, Canada) was used to calculate trabecular bone volume fraction (BV/TV), bone surface-to-volume ratio (BS/BV), thickness (Tb.Th), number (N), and spacing (Tb.Sp) along with bone mineral content (BMC), tissue mineral density (TMD), and periosteal and endosteal perimeters after applying a uniform threshold of 1200 Hounsfield Units (HU) for trabecular analyses and 2000 HU for cortical analyses.

Tibial cultures and analysis. Tibial cultures were performed as previously described (26). U0126 was purchased from Promega (#V1121), and PD325901 was purchased from LC Laboratories (#P-9688). Both of these inhibitors were used at a final concentration of 10 μM. On the sixth day of culture, tibiae were photographed under a 2.5X objective lens under a dissection microscope and used for histological analysis or frozen at -80°C for protein analysis. Enlarged photographs were printed and measured with a ruler in centimeters to determine their lengths in arbitrary units. For histological analysis, cultured tibiae were fixed overnight in 4% formaldehyde in PBS, dehydrated through and ethanol series, and embedded in paraffin. Nuclear Fast Red/Alcian Blue staining was performed as previously described (63). In situ hybridizations were performed as previously described (64). The *Col10a1* probe (53) was a generous gift from Ernestina Schipani (Indiana University).

Western blotting. Total protein from cultured tibiae and P3 tibiae was extracted in T-PER^® buffer (Thermo/Pierce #78510) and Halt™ Protease and Phosphatase Inhibitor Cocktail (Thermo/Pierce #78440). Total protein was quantified using a BCA Protein Assay Kit (Thermo/Pierce #23225). Proteins and ladder (BIO-RAD #161-0375) were run on 4-20% Mini-Protean^® TGX™ Gels from BIO-RAD (#456-1093S (10 well)) and transferred to an Amersham Hybond™-P membrane (GE Healthcare). Membranes were washed with a standard Tris-buffered saline solution with Tween-20 (TBS-Tween). ERK antibodies were purchased from

Cell Signaling Technology (phospho-ERK1/2: #4370, total ERK1/2: #4695) and diluted as per

the manufacturer's instructions. Anti-beta actin was obtained from Abcam and used at a 1:2500

dilution. Goat-anti-rabbit conjugated to horseradish peroxidase (HRP) secondary antibody was

purchased from Thermo Scientific (#31462) and was diluted 1:25,000. Membranes were

blocked and incubated with antibody in a 1% BSA/TBS-Tween solution. BSA was purchased

from Cell Signaling Technology (#9998S). Membranes were developed with the SuperSignal$^{®}$

West Pico Chemiluminescent Substrate (Thermo/Pierce #34080) and stripped with Restore™

Western Blot Stripping Buffer (Thermo/Pierce #21059).

Author Contributions

Geister: intellectual force in identification of the mutation, concept and execution of

pharmacotherapy; histology of the skeleton, uterus and ovary; puberty and estrus assessments;

wrote the manuscript with editing by Camper. Brinkmeier: sequenced several candidate genes.

 Hsieh and Conti: meiotic arrest. Faust: male fertility assessment. Karolyi: skeletal preparations

and measurements, intersubspecific cross for genetic mapping. Perosky and Kozloff: MicroCT

analysis.

References

1   Krakow, D. and Rimoin, D.L. (2010) The skeletal dysplasias. *Genet Med*, **12**, 327-341.
2   Dighe, M., Fligner, C., Cheng, E., Warren, B. and Dubinsky, T. (2008) Fetal skeletal dysplasia: an approach to diagnosis with illustrative cases. *Radiographics*, **28**, 1061-1077.
3   Superti-Furga, A. and Unger, S. (2007) Nosology and classification of genetic skeletal disorders: 2006 revision. *Am J Med Genet A*, **143**, 1-18.
4   Warman, M.L., Cormier-Daire, V., Hall, C., Krakow, D., Lachman, R., LeMerrer, M., Mortier, G., Mundlos, S., Nishimura, G., Rimoin, D.L. *et al.* (2011) Nosology and classification of genetic skeletal disorders: 2010 revision. *Am J Med Genet A*, **155A**, 943-968.
5   Mackie, E.J., Tatarczuch, L. and Mirams, M. (2011) The skeleton: a multi-functional complex organ: the growth plate chondrocyte and endochondral ossification. *J Endocrinol*, **211**, 109-121.
6   Karsenty, G., Kronenberg, H.M. and Settembre, C. (2009) Genetic control of bone formation. *Annu Rev Cell Dev Biol*, **25**, 629-648.
7   Baldridge, D., Shchelochkov, O., Kelley, B. and Lee, B. (2010) Signaling pathways in human skeletal dysplasias. *Annu Rev Genomics Hum Genet*, **11**, 189-217.
8   Lee, H., Graham, J.M., Jr., Rimoin, D.L., Lachman, R.S., Krejci, P., Tompson, S.W., Nelson, S.F., Krakow, D. and Cohn, D.H. (2012) Exome sequencing identifies PDE4D mutations in acrodysostosis. *Am J Hum Genet*, **90**, 746-751.
9   Sybert, V.P. and McCauley, E. (2004) Turner's syndrome. *N Engl J Med*, **351**, 1227-1238.
10   Velagaleti, G.V., Bien-Willner, G.A., Northup, J.K., Lockhart, L.H., Hawkins, J.C., Jalal, S.M., Withers, M., Lupski, J.R. and Stankiewicz, P. (2005) Position effects due to chromosome breakpoints that map approximately 900 Kb upstream and approximately 1.3 Mb downstream of SOX9 in two patients with campomelic dysplasia. *Am J Hum Genet*, **76**, 652-662.
11   Arboleda, V.A., Lee, H., Parnaik, R., Fleming, A., Banerjee, A., Ferraz-de-Souza, B., Delot, E.C., Rodriguez-Fernandez, I.A., Braslavsky, D., Bergada, I. *et al.* (2012) Mutations in the PCNA-binding domain of CDKN1C cause IMAGe syndrome. *Nat Genet*, **44**, 788-792.
12   Matzuk, M.M. and Lamb, D.J. (2002) Genetic dissection of mammalian fertility pathways. *Nat Cell Biol*, **4 Suppl**, s41-49.
13   Tatone, C., Amicarelli, F., Carbone, M.C., Monteleone, P., Caserta, D., Marci, R., Artini, P.G., Piomboni, P. and Focarelli, R. (2008) Cellular and molecular aspects of ovarian follicle ageing. *Hum Reprod Update*, **14**, 131-142.
14   Matzuk, M.M. and Lamb, D.J. (2008) The biology of infertility: research advances and clinical challenges. *Nat Med*, **14**, 1197-1213.

15   Barnett, K.R., Schilling, C., Greenfeld, C.R., Tomic, D. and Flaws, J.A. (2006) Ovarian follicle development and transgenic mouse models. *Hum Reprod Update*, **12**, 537-555.

16   Bartels, C.F., Bukulmez, H., Padayatti, P., Rhee, D.K., van Ravenswaaij-Arts, C., Pauli, R.M., Mundlos, S., Chitayat, D., Shih, L.Y., Al-Gazali, L.I. *et al.* (2004) Mutations in the transmembrane natriuretic peptide receptor NPR-B impair skeletal growth and cause acromesomelic dysplasia, type Maroteaux. *Am J Hum Genet*, **75**, 27-34.

17   Kant, S.G., Polinkovsky, A., Mundlos, S., Zabel, B., Thomeer, R.T., Zonderland, H.M., Shih, L., van Haeringen, A. and Warman, M.L. (1998) Acromesomelic dysplasia Maroteaux type maps to human chromosome 9. *Am J Hum Genet*, **63**, 155-162.

18   Potter, L.R. (2011) Guanylyl cyclase structure, function and regulation. *Cell Signal*, **23**, 1921-1926.

19   Moran, J.L., Bolton, A.D., Tran, P.V., Brown, A., Dwyer, N.D., Manning, D.K., Bjork, B.C., Li, C., Montgomery, K., Siepka, S.M. *et al.* (2006) Utilization of a whole genome SNP panel for efficient genetic mapping in the mouse. *Genome Res*, **16**, 436-440.

20   Khan, S., Hussain Ali, R., Abbasi, S., Nawaz, M., Muhammad, N. and Ahmad, W. (2012) Novel mutations in natriuretic peptide receptor-2 gene underlie acromesomelic dysplasia, type maroteaux. *BMC Med Genet*, **13**, 44.

21   Hachiya, R., Ohashi, Y., Kamei, Y., Suganami, T., Mochizuki, H., Mitsui, N., Saitoh, M., Sakuragi, M., Nishimura, G., Ohashi, H. *et al.* (2007) Intact kinase homology domain of natriuretic peptide receptor-B is essential for skeletal development. *J Clin Endocrinol Metab*, **92**, 4009-4014.

22   Olney, R.C., Bukulmez, H., Bartels, C.F., Prickett, T.C., Espiner, E.A., Potter, L.R. and Warman, M.L. (2006) Heterozygous mutations in natriuretic peptide receptor-B (NPR2) are associated with short stature. *J Clin Endocrinol Metab*, **91**, 1229-1232.

23   Tsuji, T. and Kunieda, T. (2005) A loss-of-function mutation in natriuretic peptide receptor 2 (Npr2) gene is responsible for disproportionate dwarfism in cn/cn mouse. *J Biol Chem*, **280**, 14288-14292.

24   Sogawa, C., Tsuji, T., Shinkai, Y., Katayama, K. and Kunieda, T. (2007) Short-limbed dwarfism: slw is a new allele of Npr2 causing chondrodysplasia. *J Hered*, **98**, 575-580.

25   Sogawa, C., Abe, A., Tsuji, T., Koizumi, M., Saga, T. and Kunieda, T. (2010) Gastrointestinal tract disorder in natriuretic peptide receptor B gene mutant mice. *Am J Pathol*, **177**, 822-828.

26   Tamura, N., Doolittle, L.K., Hammer, R.E., Shelton, J.M., Richardson, J.A. and Garbers, D.L. (2004) Critical roles of the guanylyl cyclase B receptor in endochondral ossification and development of female reproductive organs. *Proc Natl Acad Sci U S A*, **101**, 17300-17305.

27   Zhang, M., Su, Y.Q., Sugiura, K., Xia, G. and Eppig, J.J. (2010) Granulosa cell ligand NPPC and its receptor NPR2 maintain meiotic arrest in mouse oocytes. *Science*, **330**, 366-369.

28   Fowkes, R.C. and McArdle, C.A. (2000) C-type natriuretic peptide: an important neuroendocrine regulator? *Trends Endocrinol Metab*, **11**, 333-338.

29   Thompson, I.R., Chand, A.N., Jonas, K.C., Burrin, J.M., Steinhelper, M.E., Wheeler-Jones, C.P., McArdle, C.A. and Fowkes, R.C. (2009) Molecular characterisation and

functional interrogation of a local natriuretic peptide system in rodent pituitaries, alphaT3-1 and LbetaT2 gonadotroph cells. *J Endocrinol*, **203**, 215-229.

30   Dos Reis, A.M., Fujio, N., Dam, T.V., Mukaddam-Daher, S., Jankowski, M., Tremblay, J. and Gutkowska, J. (1995) Characterization and distribution of natriuretic peptide receptors in the rat uterus. *Endocrinology*, **136**, 4247-4253.

31   Caligioni, C.S. (2009) Assessing reproductive status/stages in mice. *Curr Protoc Neurosci*, **Appendix 4**, Appendix 4I.

32   Daftary, S.S. and Gore, A.C. (2005) IGF-1 in the brain as a regulator of reproductive neuroendocrine function. *Exp Biol Med (Maywood)*, **230**, 292-306.

33   Chandrashekar, V., Zaczek, D. and Bartke, A. (2004) The consequences of altered somatotropic system on reproduction. *Biol Reprod*, **71**, 17-27.

34   DiVall, S.A. and Radovick, S. (2008) Pubertal development and menarche. *Ann N Y Acad Sci*, **1135**, 19-28.

35   Cone, R.D., Low, M.J., Elmquist, J.K. and Cameron, J.L. (2003) Larsen, P.R., Kronenberg, H.M., Melmed, S. and Polonsky, K.S. (eds.), In *Williams Textbook of Endocrinology*. Saunders, Philadelphia, pp. 81-176.

36   Zhang, M., Ouyang, H. and Xia, G. (2009) The signal pathway of gonadotrophins-induced mammalian oocyte meiotic resumption. *Mol Hum Reprod*, **15**, 399-409.

37   Mehlmann, L.M. (2005) Stops and starts in mammalian oocytes: recent advances in understanding the regulation of meiotic arrest and oocyte maturation. *Reproduction*, **130**, 791-799.

38   Sun, Q.Y., Miao, Y.L. and Schatten, H. (2009) Towards a new understanding on the regulation of mammalian oocyte meiosis resumption. *Cell Cycle*, **8**, 2741-2747.

39   Vaccari, S., Weeks, J.L., 2nd, Hsieh, M., Menniti, F.S. and Conti, M. (2009) Cyclic GMP signaling is involved in the luteinizing hormone-dependent meiotic maturation of mouse oocytes. *Biol Reprod*, **81**, 595-604.

40   Norris, R.P., Ratzan, W.J., Freudzon, M., Mehlmann, L.M., Krall, J., Movsesian, M.A., Wang, H., Ke, H., Nikolaev, V.O. and Jaffe, L.A. (2009) Cyclic GMP from the surrounding somatic cells regulates cyclic AMP and meiosis in the mouse oocyte. *Development*, **136**, 1869-1878.

41   Ledent, C., Demeestere, I., Blum, D., Petermans, J., Hamalainen, T., Smits, G. and Vassart, G. (2005) Premature ovarian aging in mice deficient for Gpr3. *Proc Natl Acad Sci U S A*, **102**, 8922-8926.

42   Bulun, S.E. and Adashi, E.Y. (2003) Larsen, P.R., Kronenberg, H.M., Melmed, S. and Polonsky, K.S. (eds.), In *Williams Textbook of Endocrinology*. Saunders, Philadelphia, pp. 587-664.

43   Kaneki, H., Kurokawa, M. and Ide, H. (2008) The receptor attributable to C-type natriuretic peptide-induced differentiation of osteoblasts is switched from type B- to type C-natriuretic peptide receptor with aging. *J Cell Biochem*, **103**, 753-764.

44   Yeh, L.C., Zavala, M.C. and Lee, J.C. (2006) C-type natriuretic peptide enhances osteogenic protein-1-induced osteoblastic cell differentiation via Smad5 phosphorylation. *J Cell Biochem*, **97**, 494-500.

45   Krejci, P., Masri, B., Fontaine, V., Mekikian, P.B., Weis, M., Prats, H. and Wilcox, W.R. (2005) Interaction of fibroblast growth factor and C-natriuretic peptide signaling in regulation of chondrocyte proliferation and extracellular matrix homeostasis. *J Cell Sci*, **118**, 5089-5100.

46   Horton, W.A. and Degnin, C.R. (2009) FGFs in endochondral skeletal development. *Trends Endocrinol Metab*, **20**, 341-348.

47   Shirley, E.D. and Ain, M.C. (2009) Achondroplasia: manifestations and treatment. *J Am Acad Orthop Surg*, **17**, 231-241.

48   Lauchle, J.O., Kim, D., Le, D.T., Akagi, K., Crone, M., Krisman, K., Warner, K., Bonifas, J.M., Li, Q., Coakley, K.M. *et al.* (2009) Response and resistance to MEK inhibition in leukaemias initiated by hyperactive Ras. *Nature*, **461**, 411-414.

49   Lyubynska, N., Gorman, M.F., Lauchle, J.O., Hong, W.X., Akutagawa, J.K., Shannon, K. and Braun, B.S. (2011) A MEK inhibitor abrogates myeloproliferative disease in Kras mutant mice. *Sci Transl Med*, **3**, 76ra27.

50   Shukla, V., Coumoul, X., Wang, R.H., Kim, H.S. and Deng, C.X. (2007) RNA interference and inhibition of MEK-ERK signaling prevent abnormal skeletal phenotypes in a mouse model of craniosynostosis. *Nat Genet*, **39**, 1145-1150.

51   Yasoda, A., Komatsu, Y., Chusho, H., Miyazawa, T., Ozasa, A., Miura, M., Kurihara, T., Rogi, T., Tanaka, S., Suda, M. *et al.* (2004) Overexpression of CNP in chondrocytes rescues achondroplasia through a MAPK-dependent pathway. *Nat Med*, **10**, 80-86.

52   Barrett, S.D., Bridges, A.J., Dudley, D.T., Saltiel, A.R., Fergus, J.H., Flamme, C.M., Delaney, A.M., Kaufman, M., LePage, S., Leopold, W.R. *et al.* (2008) The discovery of the benzhydroxamate MEK inhibitors CI-1040 and PD 0325901. *Bioorg Med Chem Lett*, **18**, 6501-6504.

53   Araldi, E., Khatri, R., Giaccia, A.J., Simon, M.C. and Schipani, E. (2011) Lack of HIF-2alpha in limb bud mesenchyme causes a modest and transient delay of endochondral bone development. *Nat Med*, **17**, 25-26; author reply 27-29.

54   Yasoda, A. and Nakao, K. (2010) Translational research of C-type natriuretic peptide (CNP) into skeletal dysplasias. *Endocr J*, **57**, 659-666.

55   Agoston, H., Khan, S., James, C.G., Gillespie, J.R., Serra, R., Stanton, L.A. and Beier, F. (2007) C-type natriuretic peptide regulates endochondral bone growth through p38 MAP kinase-dependent and -independent pathways. *BMC Dev Biol*, **7**, 18.

56   Kiyosu, C., Tsuji, T., Yamada, K., Kajita, S. and Kunieda, T. (2012) NPPC/NPR2 signaling is essential for oocyte meiotic arrest and cumulus oophorus formation during follicular development in the mouse ovary. *Reproduction*.

57   Yasoda, A., Kitamura, H., Fujii, T., Kondo, E., Murao, N., Miura, M., Kanamoto, N., Komatsu, Y., Arai, H. and Nakao, K. (2009) Systemic administration of C-type natriuretic peptide as a novel therapeutic strategy for skeletal dysplasias. *Endocrinology*, **150**, 3138-3144.

58   Foldynova-Trantirkova, S., Wilcox, W.R. and Krejci, P. (2012) Sixteen years and counting: the current understanding of fibroblast growth factor receptor 3 (FGFR3) signaling in skeletal dysplasias. *Hum Mutat*, **33**, 29-41.

59   Boasberg, P.D., Redfern, C.H., Daniels, G.A., Bodkin, D., Garrett, C.R. and Ricart, A.D. (2011) Pilot study of PD-0325901 in previously treated patients with advanced melanoma, breast cancer, and colon cancer. *Cancer Chemother Pharmacol*, **68**, 547-552.

60   Song, B., Haycraft, C.J., Seo, H.S., Yoder, B.K. and Serra, R. (2007) Development of the post-natal growth plate requires intraflagellar transport proteins. *Dev Biol*, **305**, 202-216.

61   Nagy, A., Gertsenstein, M., Vinterstein, K. and Behringer, R. (2003) *Manipulating the Mouse Embryo: A Laboratory Manual*. Cold Spring Harbor Laboratory Press, Cold Spring Harbor.

62   Panigone, S., Hsieh, M., Fu, M., Persani, L. and Conti, M. (2008) Luteinizing hormone signaling in preovulatory follicles involves early activation of the epidermal growth factor receptor pathway. *Mol Endocrinol*, **22**, 924-936.

63   Retting, K.N., Song, B., Yoon, B.S. and Lyons, K.M. (2009) BMP canonical Smad signaling through Smad1 and Smad5 is required for endochondral bone formation. *Development*, **136**, 1093-1104.

64   Cushman, L.J., Watkins-Chow, D.E., Brinkmeier, M.L., Raetzman, L.T., Radak, A.L., Lloyd, R.V. and Camper, S.A. (2001) Persistent Prop1 expression delays gonadotrope differentiation and enhances pituitary tumor susceptibility. *Hum Mol Genet*, **10**, 1141-1153.
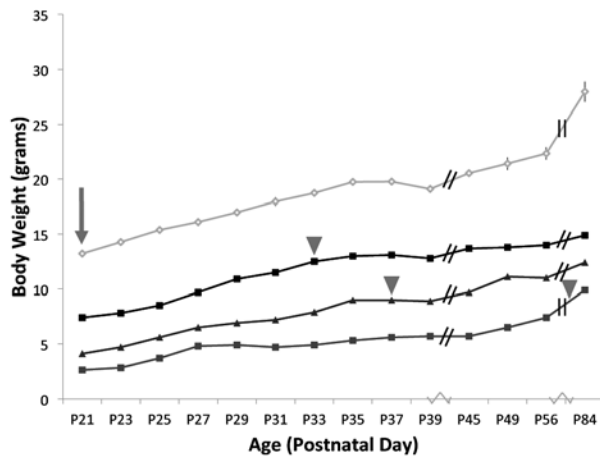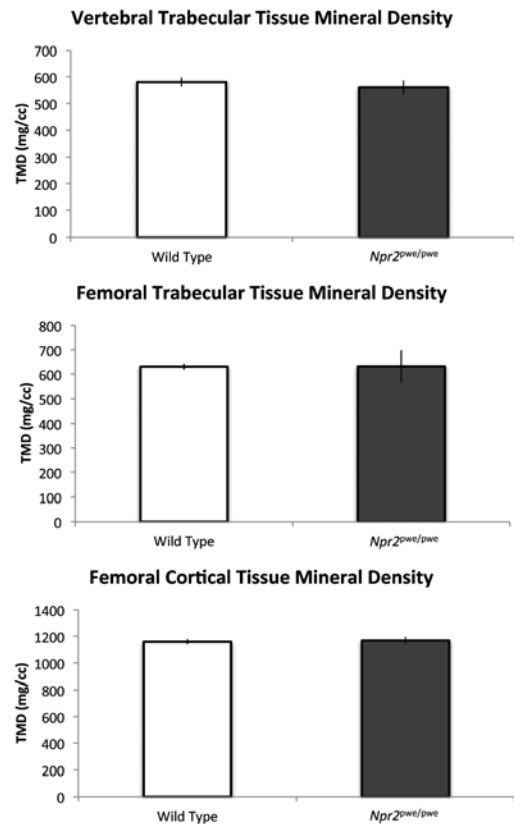
Appendix 2.1. *Npr2*[pwe/pwe] **female pubertal delay coincides with lower body weight, and** *Npr2*[pwe/pwe] **bones exhibit normal tissue mineral density.** Panel A: Growth curve of a representative litter of *Npr2*[pwe/pwe] females (n=3 shown individually) with dates of vaginal opening indicated with arrowheads. Control females (n=6) are graphed as an average and average vaginal opening is indicated with an arrow. Panel B: Trabecular tissue mineral densities of *Npr2*[pwe/pwe] male L4 vertebrae and femurs are normal, as is the cortical tissue mineral density of the femur in the same males (Control, n=6; *Npr2*[pwe/pwe], n=7)

CHAPTER 3

chagun, a Hypomorphic Allele of *Poc1a,* Models Primordial Dwarfism

Abstract

Skeletal dysplasias are a common, genetically heterogeneous cause of severe short stature. Disruptions in many pathways can cause skeletal dysplasia, including signal transduction, extracellular matrix components, control of protein trafficking and glycosylation, and control of gene expression at the levels of transcription, RNA processing and translation. An emerging new group includes genes involved in the development and function of centromeres and cilia. Using exome and genomic sequencing we identified a hypomorphic mutation in the mouse *Poc1a* gene, which encodes a protein of the centriole and cilia. Affected mice have skeletal dysplasia, severe growth insufficiency, and male infertility. While *Poc1a* is broadly expressed, strong expression is evident in sperm and the proliferative zone of the growth plate. We show that growth insufficiency results from cellular disorganization at the growth plate. Infertility is due to progressive germ cell loss and reciprocal spermatagonial stem cell transplants indicate Sertoli cell dysfunction. Genome variation influences the viability of the mutant mice, and humans with hypomorphic *POC1A* mutations have severe short stature and variable associated features. This mouse model will be invaluable for identifying the genes that modify the clinical features, understanding the pathophysiology of ciliopathies that cause growth insufficiency and developing therapeutics.

Introduction

Normal adult stature in humans is achieved primarily through regulation of long bone growth, which occurs through a process known as endochondral ossification (1, 2). This process begins early in embryonic development and results in the differentiation of mesenchymal cells into chondrocytes throughout the body where skeletal elements will eventually reside. Hypertrophic differentiation of these chondrocytes directs the vascularization of the forming element, allowing osteoblasts to enter and mineralize the cartilage-based template.

Pools of cells at the epiphyses of the long bones retain their cartilage identity as a means to secure the progressive addition of bone matrix throughout the period of skeletal growth (1). These structures are the epiphyseal growth plates. Tight control of chondrocyte proliferation and terminal hypertrophic differentiation, allows new bone tissue to be laid down in the place of dying chondrocytes in a spatially and temporally regulated manner, ensuring the proper growth of the skeletal elements and the individual overall (2).

The growth plate maintains a highly ordered architecture to carry out its function and it is divided into several distinct zones (1, 2). In the resting zone, lesser-differentiated chondrocytes await further direction to undergo rounds of cell division and enter the proliferative zone of the growth plate. These cells are guided to undergo terminal hypertrophic differentiation in the hypertrophic zone of the growth plate. Perturbation of growth plate organization can result in profound growth defects in mice and humans (3-5). Major orchestrators of growth plate architecture include the WNT-planar cell polarity pathway (6), the TGFβ/BMP signaling pathways (4), and the primary cilium (3).

These disorganization phenotypes are particularly evident in the proliferative zone of the growth plate, where a process known as chondrocyte rotation occurs (3, 6, 7). The proliferative

zone forms distinctive columns of disc-shaped chondrocytes that resemble stacks of coins. These columns form through the directed cell division of chondrocytes perpendicular to the plane of the growth plate, followed by sliding of the newly formed daughter cells over one another. It is not known what advantage this process grants the growth plate, but disruption of chondrocyte rotation results in impaired longitudinal growth of the long bones (3).

Primordial dwarfisms are a subset of growth insufficiency disorders caused by defects intrinsic to the skeleton that are classified as forms of skeletal dysplasia (8, 9). Rather than exhibiting a disproportionate reduction of long bone length, where elements are affected differentially, primordial dwarfism causes a proportionate reduction in longitudinal growth that commences early in fetal life (8). The proportionate reduction in growth and onset of the growth defect in these patients highly resembles insulin-like growth factor type 1 (IGF-1) deficiency. Primordial dwarfisms result in profound reductions in height, with some patients only reaching an adult height of 1 meter.

The primordial dwarfisms include Seckel Syndrome, Microcephalic Osteodysplastic Primordial Dwarfism I-III (MOPD I-III), and Meier-Gorlin Syndrome (MGS) (8). The genetic causes of the primordial dwarfisms do not appear to cause endocrine disturbances, but rather interfere with processes that are intimately connected to the cell cycle (8). Common pathways that are disrupted in primordial dwarfism patients include: DNA repair (10-13), DNA replication (14-17), centrosome-mediated processes (13-16, 18-23), and splicing of specific subsets of introns in mRNA transcripts (24, 25).

A novel form of microcephalic primordial dwarfism in humans, was recently shown to be caused by mutations in the gene that encodes protein of centriole 1A (*POC1A*) (22, 23). Human patients exhibit intrauterine growth retardation, severe short stature throughout their lives, and a

distinctive, triangular-shaped face. Variable incidences of developmental delay, failure to thrive, sparse hair, and delayed bone age have been reported. Patients homozygous for a nonsense mutation (R81X) exhibit read-through translation that results in expression of 50-85% of the normal level of POC1A protein in fibroblasts, when it is expected that little to no protein would be present (23). This has led to a hypothesis that mutations in *POC1A* may actually represent hypomorphic alleles as opposed to true null alleles.

We recently discovered the gene responsible for skeletal dysplasia and male infertility in the *chagun* mouse, a previously described, spontaneous, recessive mouse mutation (26). The mutation is a hypomorphic allele of *Poc1a* that produces normal levels of POC1A protein that lacks 23 amino acids. This domain is clearly necessary for normal growth plate architecture. We also show that the infertility of male $Poc1a^{cha/cha}$ mice is due to progressive loss of germ cells, which is likely caused by Sertoli cell dysfunction. Thus, this animal model has clarified the molecular basis for the clinical features in human patients with POC1A mutations.

Results

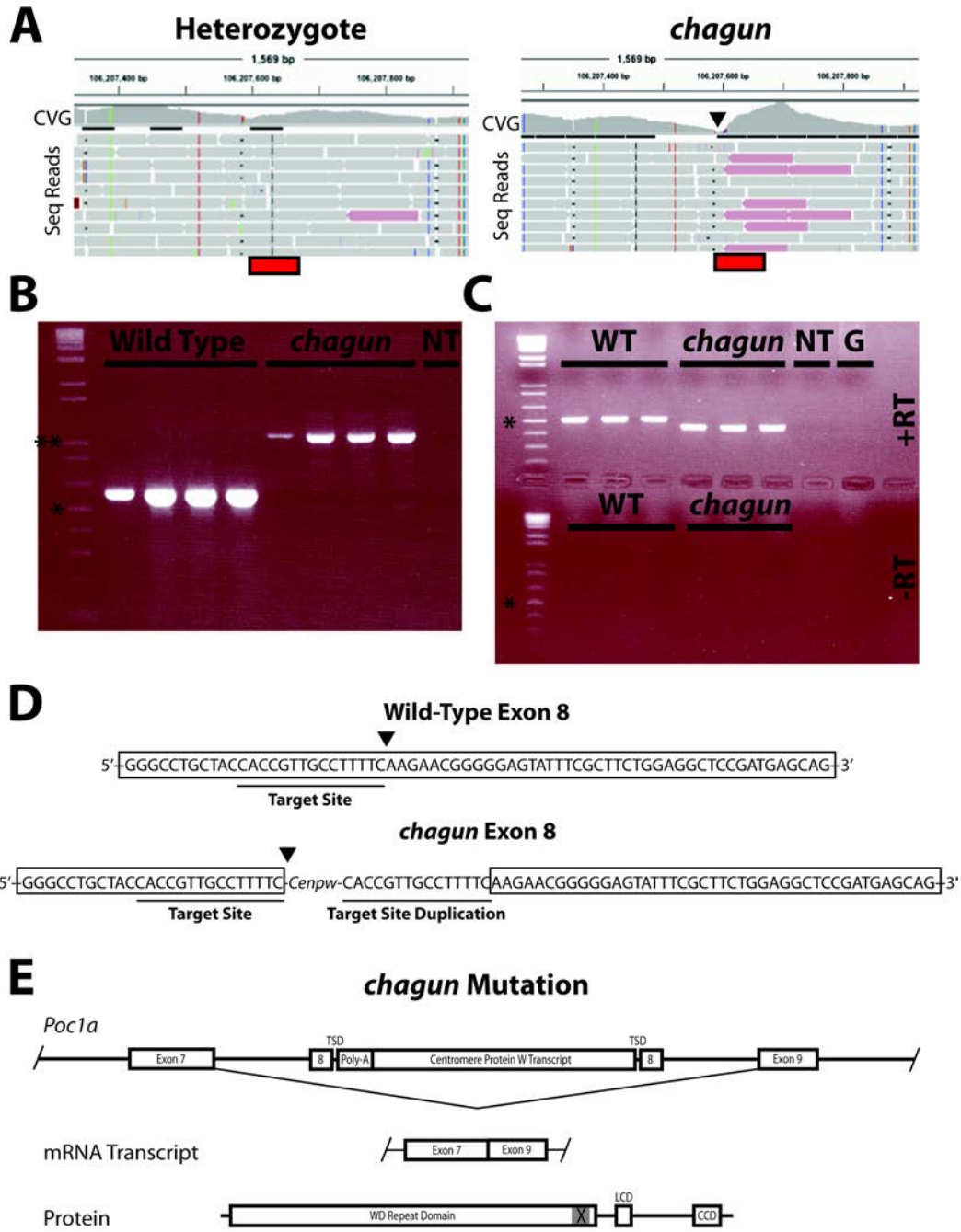***chagun* is caused by a mutation in *Poc1a***

The *chagun* mutation arose on DBA/2J and was mapped to Chr 9 in 129 progeny of an F1 x F1 intercross with CAST/Ei to a 6 cM region of mouse Chr 9 (26). We arranged for genome wide exome capture and high throughput sequencing of a *chagun* genomic DNA sample (Mutant Mouse Resequencing Project, The Broad Institute of MIT and Harvard, Cambridge, MA). At least 2X coverage was obtained from the exons in the critical interval. No nonsense mutations or disruptions in consensus splice sites were uncovered in the critical interval using this approach. There were some synonymous changes and a single missense mutation that encoded an amino acid normally present in other species. Some variants were detected in

intronic regions captured with the exons, but none appeared likely to disrupt splicing or create ectopic splice donors or acceptors (Appendix 3.1).

Having found no obvious deleterious mutations with exome sequencing, we turned to regional DNA capture to enrich for non-repetitive genomic DNA in the most broadly defined 8.5 Mb *chagun* critical region (*D9Mit183-D9Mit212*). We captured genomic DNA from an obligate carrier (*cha/+*) and a known mutant (*cha/cha*). We obtained high throughput sequence with at least 20X coverage for approximately 90% of the bases sequenced from both samples. We detected five new insertions of transposable elements that are not present in the 16 mouse reference genomes (Appendix 3.2).

We observed a steep decrease in coverage in the middle of exon 8 of the gene that encodes protein of centriole 1A (*Poc1a*) (Figure 3.1A). Reduced coverage is more obvious in the mutant than the heterozygote. In addition, many sequencing reads that map to exon 8 in the mutant have paired ends that map to other locations in the genome: chromosomes 5, 10, and 12, rather than chromosome 9. Together, these data suggest that an element repeated on three chromosomes is inserted in *Poc1a* exon 8. PCR amplification of exon 8 and flanking intronic regions using *chagun* genomic DNA as the template amplified a product 500 bp larger than the product generated from unaffected animals (Figure 3.1B). Sanger sequencing of the genomic amplification products indicated that exon 8 is disrupted by the insertion of a partial transcript of centromere protein W (*Cenpw*) that has approximately 30 nucleotides of poly-A. *Cenpw* is located on mouse chromosome 10, and there are two locations in the mouse genome that also contain complementary sequence on chromosomes 5 and 12, which are most likely pseudogenes, due to the fact that they are also complementary to the *Cenpw* mRNA transcript. The insertion

Figure 3.1. The *chagun* phenotype is caused by a LINE-1 mediated insertion of a processed transcript into exon 8 of *Poc1a*. Panel A. Screenshots from the Broad Institute's Integrative Genomics Viewer (IGV) show a drop in paired end sequence coverage within exon 8 of *Poc1a*. Pink reads indicate that the other end of the mate pair maps a different region of the genome. The location of exon 8 is indicated by the red rectangles under the sequence reads. (CVG: coverage) Panel B. PCR amplification of genomic DNA with primers designed to intronic regions 5' and 3' of exon 8 generates an approximately 1100 bp product from the *chagun* genomic DNA samples (right) and the predicted product 613 bp in wild-type genomic DNA (left). NT: No template. Panel C. RT-PCR amplification of *Poc1a* exons 5-10 produces a 526 bp product in cDNA from wild-type testis and bone, but the *chagun Poc1a* transcript is only ~450 bp. (NT: No template, G: Genomic DNA, +/-RT: +/- Reverse Transcriptase). Panel D. Sequence of exon 8 in wild type and *chagun* animals. The cleavage site targeted by LINE-1 is indicated as an arrowhead in the wild type and *chagun* sequences. The target site and its duplication are underlined. Panel E. Schematic diagram illustrating the disruption of *chagun* genomic DNA by an insertion of a transcript complementary to *Cenpw* (centromere protein W) complete with a poly-A tail. Skipping of exon 8 is diagrammed. The skipping of exon 8 would lead to the deletion of 23 amino acids in the WD repeat domain (loss delineated by the X and gray shading, LCD: Low complexity domain, CCD: Coiled-coil domain, TSD: Target site duplication). *Indicates 500 bp standard, **Indicates 1000 bp standard.

A Heterozygote   *chagun*

CVG

Seq Reads

B Wild Type   *chagun*   NT

C WT   *chagun* NT G   +RT

WT   *chagun*   -RT

D

Wild-Type Exon 8

5'-GGGCCTGCTACCACCGTTGCCTTTTCAAGAACGGGGGAGTATTTCGCTTCTGGAGGCTCCGATGAGCAG-3'

Target Site

***chagun* Exon 8**

5'-GGGCCTGCTACCACCGTTGCCTTTTC-*Cenpw*-CACCGTTGCCTTTTCAAGAACGGGGGAGTATTTCGCTTCTGGAGGCTCCGATGAGCAG-3'

Target Site   Target Site Duplication

E ***chagun* Mutation**

Poc1a

Exon 7   TSD   8   Poly-A   Centromere Protein W Transcript   TSD   8   Exon 9

mRNA Transcript   Exon 7   Exon 9

Protein   WD Repeat Domain   X   LCD   CCD

100

of the *Cenpw* processed transcript is unique to the *chagun* mutants—it is not present in any of the 16 additional strains analyzed (data not shown).

All of exon 8 is present, and the insertion point of the processed transcript is flanked by short (15 bp) stretches of identical *Poc1a* sequence, consistent with target-site duplications characteristic of a LINE-1 mediated event. Furthermore, there is a LINE-1 retrotransposon ORF-2 excision site (arrowheads, Figure 3.1D) present in exon 8 that occurs just before the insertion of the transcript. These observations have led us to conclude that this is a LINE-1 retrotransposon-mediated insertion of a mature mRNA transcript of *Cenpw*.

The *chagun* phenotype is caused by a hypomorphic allele of *Poc1a*

Tibia RNA was prepared for RT-PCR analysis of *Poc1a* transcripts. The *chagun* cDNA produced a smaller amplification product than that detected in normal tibia (Figure 3.1C). Sanger sequencing of the mutant RT-PCR product revealed that exon 8 of *Poc1a* is skipped precisely (Figure 3.1E). Additional RT-PCR analyses did not detect any splicing into exon 8 in *chagun* mutants (Figure 3.2A). Quantitative RT-PCR was carried out using probes designed to amplify exon 2-3 at the 5' end of the *Poc1a* transcript and exon 11-12 at the 3' end of the transcript. The same level of transcripts were detected in wild type and *chagun* mutants using probes for both the 5' or 3' ends of the transcript. This suggests that exon 8 is cleanly skipped and that the mutant transcript is equal in stability to the wild type (Figure 3.2B). Skipping exon 8 preserves the reading frame, and these mutant transcripts are predicted to produce a POC1A protein that lacks 23 amino acids in the WD40 repeat domain (Figure 3.1E).

Western blots were carried out to assess the level of POC1A protein in tibia. The polyclonal antibody was generated against full-length human POC1A, which is highly conserved
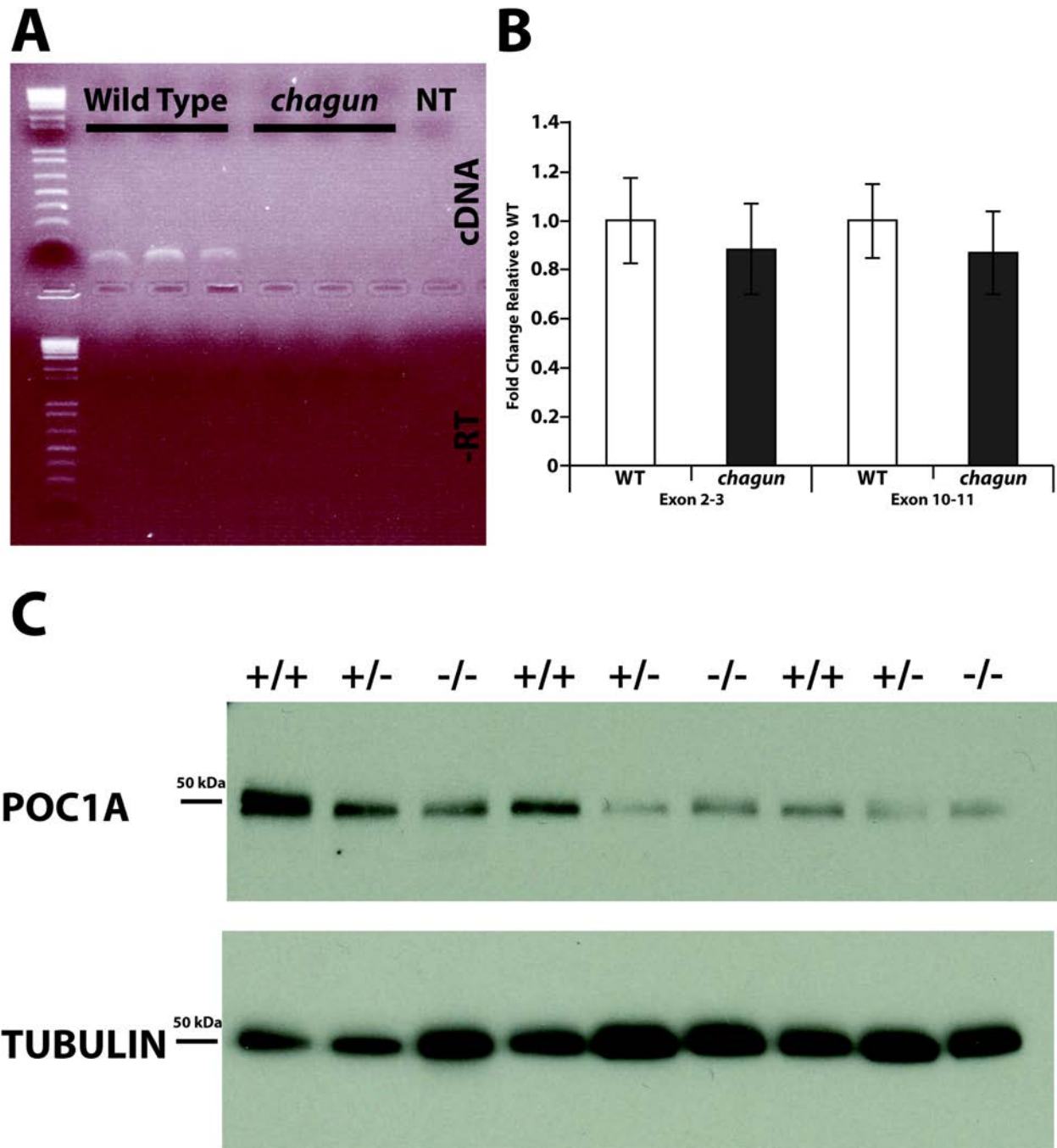
Figure 3.2. *chagun* is likely a hypomorphic allele of *Poc1a*. Panel A. RT-PCR amplification using primers to detect splicing of exon 7 into exon 8 yields no amplification product from cDNA generated from *Poc1a*^cha/cha P3 tibiae. Panel B. Real-Time PCR amplification to detect splicing from exon 2-3 at the 5' end of the transcript and splicing from exon 10-11 at the 3' end of the transcript reveals no significant change in transcript level after the skipping of exon 8 in *Poc1a*^cha/cha P3 tibiae cDNA samples compared to wild type (WT). Panel C. Western blots with primary antibodies raised against POC1A and Tubulin were conducted on lysates from wild type (+/+), heterozygotes (+/-) and *Poc1a*^cha/cha (-/-) P3 tibiae run on a 12% SDS-PAGE gel. Both images are exposures taken from the same blot.

between human and mouse. A single band was detected in wild type and mutant tibia, consistent with a single POC1A protein product. The level of POC1A protein was normalized against α-tubulin, and the POC1A protein is present in *chagun* mutant tibia at comparable levels to unaffected (heterozygotes and wild-type) animals.

POC1A is expressed in tibial growth plates and seminiferous tubules

If the 23 amino acid deletion in *Poc1a* is responsible for the *chagun* phenotype, then *Poc1a* must normally be expressed in the affected tissues, namely the skeleton and the testis. Immunohistochemistry using a primary antibody against POC1A on sections through two-week (postnatal day 14; P14) tibial growth plates (Figure 3.3) show expression in the proliferative zone of the growth plate. The discoid chondrocytes in this zone have robust staining toward one side of the cell, which is also seen with markers of the Golgi apparatus (GM130) in the proliferative zone (3). POC1A is expressed in the seminiferous tubules of the testis, and particularly intense staining is evident in the region closest to the lumen of the tubule where spermatozoa and spermatids are located (Figure 3.3). This is consistent with strong POC1A expression in the post-pachytene stages of germ cell development. Spermatogenesis is arrested at the pachytene stage in *chagun* mutants (26). POC1A staining is punctate in the region farthest from the lumen near the basement membrane. Spermatogonia and myeloid cells are located near and within the basement membrane, respectively, and spermatocytes are in an intermediate position. Sertoli cells nourish the maturation of sperm, and their nuclei are found above the basement membrane and spermatogonia at the level of the tight junctions that form the blood testis barrier. Co-localization studies with antibodies for POC1A and a specific testis cell markers will be necessary to determine whether POC1A is expressed in Sertoli cells and spermatogonia, in addition to the strong expression in later germ cell development.   .
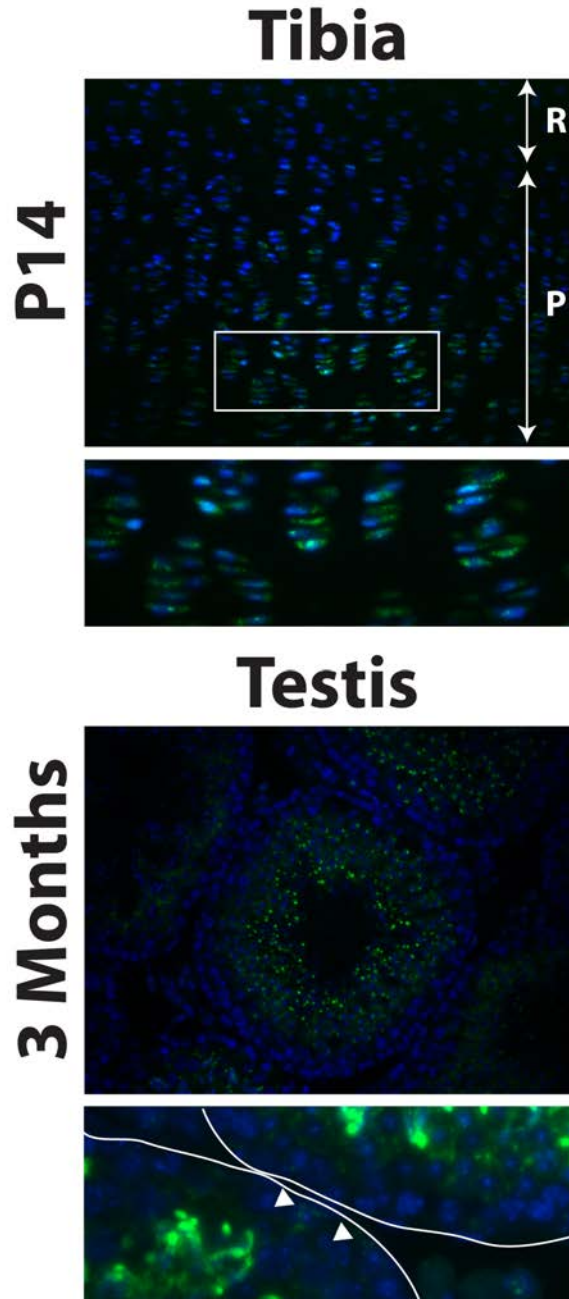
Figure 3.3. POC1A is expressed in the growth plate and seminiferous tubules.
Immunohistochemistry using an anti-POC1A primary antibody demonstrates expression of
POC1A (green) in wild-type testis at 3 months and in wild-type tibial growth plates at two weeks
of age (P14). In the growth plate, POC1A is heavily expressed in the proliferative zone, which is
evident by the discoid shape of the chondrocytes. The white box in the top panel indicates the
area represented in the lower image (R: resting zone, P: proliferative zone). In the testis,
expression is robust in the inner layers near the lumen of the seminiferous tubule, and punctate
staining is observed in cells near the basement membrane (lower panel, arrowheads). Both
images were acquired using a 40X objective lens.

The *chagun* growth defect is due to a loss of growth plate organization

The growth plates of vertebrae and long bones of adult *chagun* mice were examined previously, and the disorganization of the vertebral growth plate was obvious (26). The weight bearing nature of the long bones could have contributed to abnormalities reported in the growth plate of the long bones. Using genotyping for *Poc1a* exon 8 we examined younger mice. Histology of 3-week old tibial growth plates reveals severely disorganized growth plates in these long bones (Figure 3.4).
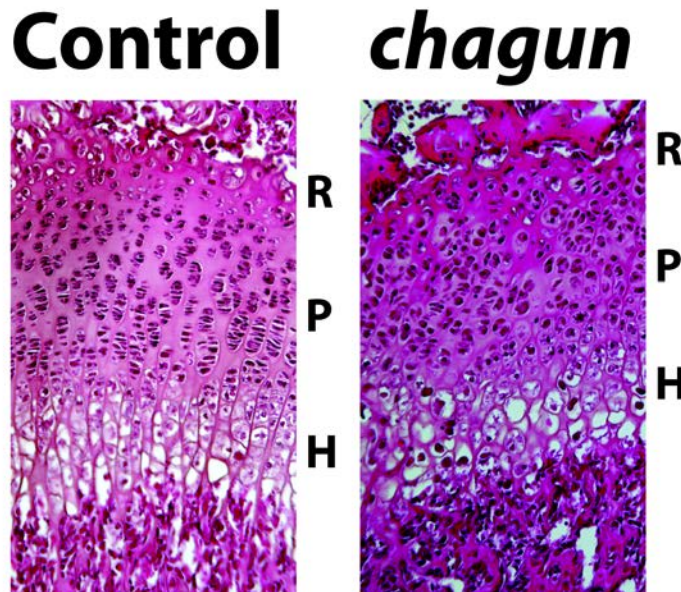

Figure 3.4. The *chagun* long bone growth plates are severely disorganized. Standard hematoxylin and eosin histological staining on paraffin sections through 3-week old tibial growth plates demonstrates profound disorganization of the proliferative zone of the growth plate in *chagun* animals. Both images were acquired using a 40X objective lens. (R: resting zone, P: proliferative zone, H: hypertrophic zone)

***chagun* males exhibit a progressive germ cell loss**

chagun males are infertile (26). No mature sperm were noted in young adult males, and there were fewer germ cells. Older males had more severe germ cell deficiency. Mutants had to be identified phenotypically as growth insufficient and hypogonadal, making it difficult to assess

the onset of hypogonadism and to determine whether the mutant testis initially had a normal number of germ cells. We conducted histological analysis of the testis during development in normal and *chagun* mutant newborns through adulthood using the *Poc1a* exon 8 genotyping to identify mutants. Periodic acid-Schiff (PAS) histological staining of testis sections was conducted on mice from postnatal day 1 (P1), P7, P14, P21, and 3 months (Figure 3.5). The reduced size of the mutant tubules and reduction in germ cells are both highly progressive, with the phenotype manifesting as early as P7 (Figure 3.5). Near birth (P1), the number of nuclei per tubule and the size of the seminiferous tubules of *chagun* males are indistinguishable from wild type, suggesting that germ cell migration to the testis occurred normally. By P7, the mutant tubules appear smaller in diameter. By P14, the testis is already beginning to exhibit the hallmarks of the adult *chagun* testis phenotype, with obviously smaller tubules, a highly vaculolated appearance, and lack of maturing sperm. The testis of sexually mature 12 wk old mice normally contain all stages of sperm development, but the *chagun* testis has only a single layer of cells lining the inner face of the basement membrane, with open spaces spanned by Sertoli cell projections giving the tubules the appearance of Sertoli only syndrome due to the near absence of germ cells in the tubule (26).

chagun males have spermatogonial stem cells at P7 and three months of age

The progressive loss of germ cells could have many etiologies including depletion of spermatogonial stem cells because of a failure in asymmetric cell division, proliferation or cell death. To differentiate between these possibilities, we conducted immunohistochemistry using a primary antibody against PLZF (promyelocytic leukemia zinc finger protein), a transcriptional regulator of spermatogenic stem cell maintenance and marker for that cell type (27). At P7 spermatogenic stem cells begin to express PLZF, and *chagun* testes have a comparable number
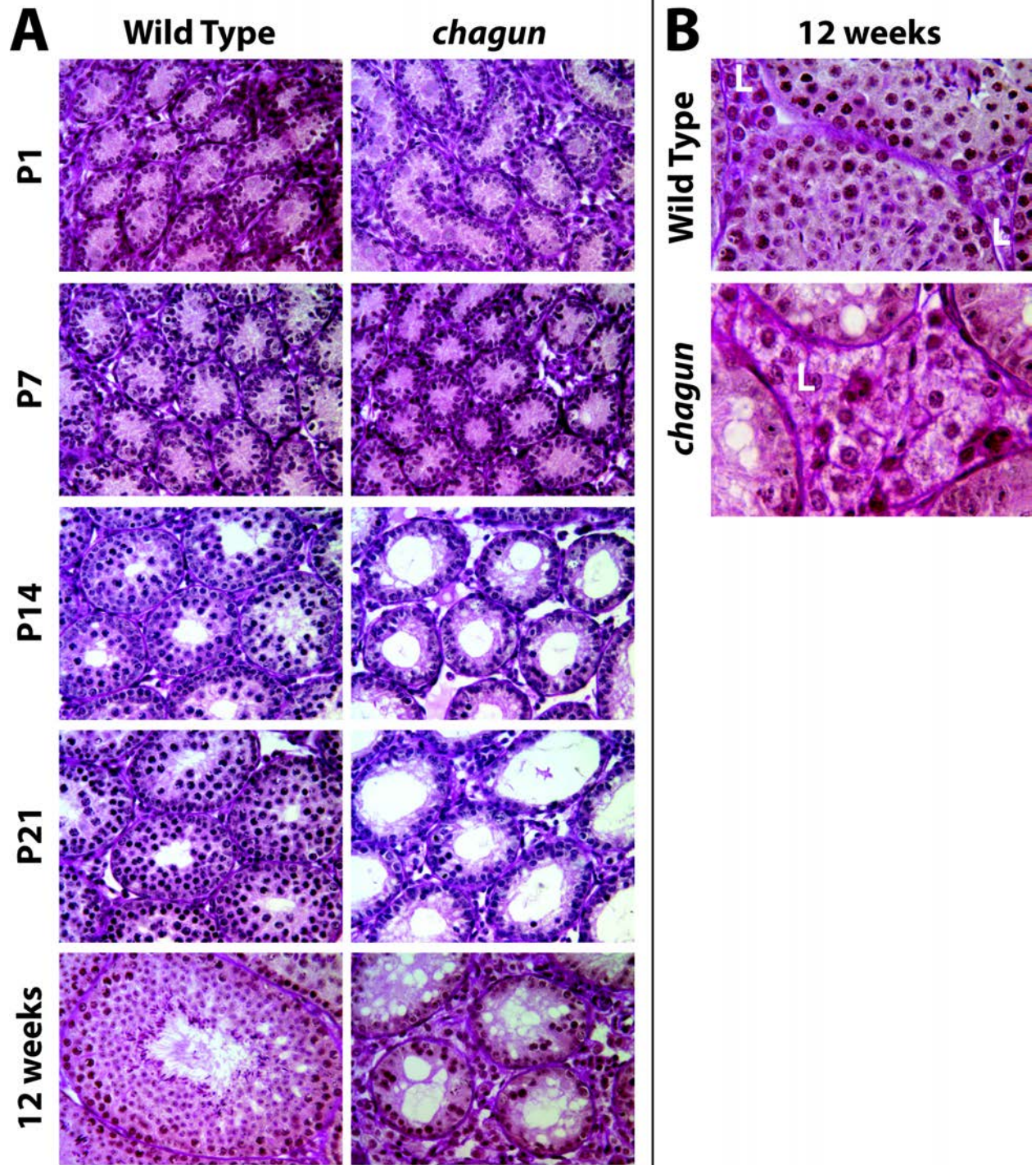
106

Figure 3.5. *chagun* males exhibit progressive germ cell loss. Panel A. Periodic acid-Schiff histological staining of paraffin sections through testes at the ages indicated emphasize the progressive nature of the *chagun* testis phenotype. Near birth, *chagun* tubules resemble wild-type seminiferous tubules, but by sexual maturity, the *Poc1a*[cha/cha] tubules are practically devoid of germ cells. (N=3 animals of each genotype at all timepoints) Panel B. Leydig cells of chagun animals appear normal (N=3 of each genotype at 3 months, L=Leydig cells). All images acquired using a 63X objective lens.

of PLZF+ cells to the controls (Figure 3.6). At 3 months of age, the number of PLZF+ cells per

tubule is indistinguishable in *chagun* and control seminiferous tubules, suggesting normal cell

division and cell death of stem cells. Increased numbers of pyknotic nuclei suggest increased

cell death at later stages of germ cell development (26). Experiments are underway to assess cell

death and proliferation directly using TUNEL staining and EdU incorporation, respectively.
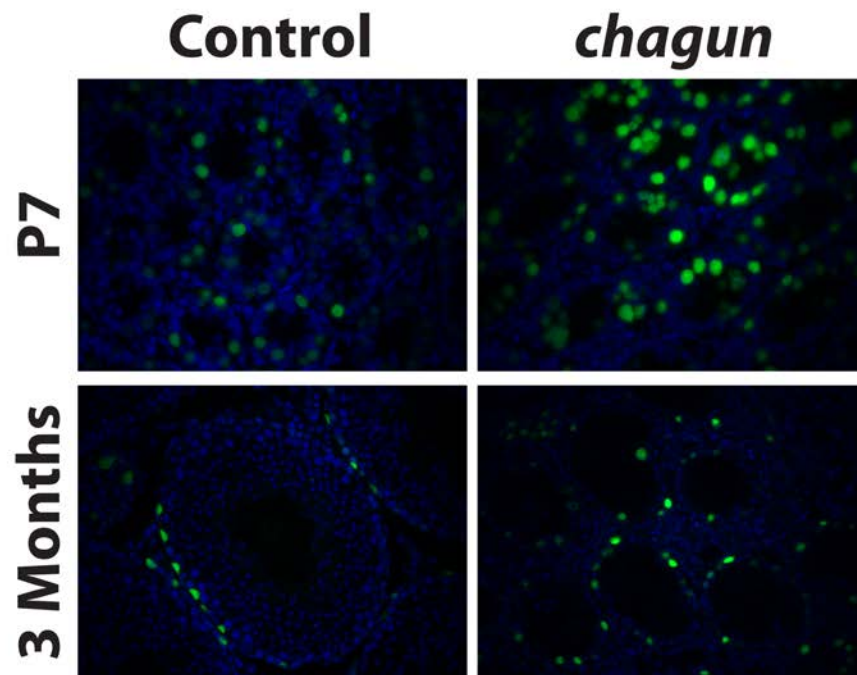

Figure 3.6. *chagun* testes retain spermatogenic stem cells at sexual maturity.
Immunohistochemistry was carried out with a primary antibody against PLZF, a marker of
spermatogenic stem cells, and developed with TSA-FITC Kit from Perkin-Elmer. Testis sections
are shown for wild type and *chagun* mutants at postnatal day 7 and 3 months. DAPI counterstain
identifies the nuclei (blue) All images acquired using a 63X objective lens. (N=3 animals of
each genotype at both timepoints).

The Sertoli cell contributes to the *chagun* testis phenotype

Defects in the germ cells or a class of somatic cells of the testis, the Sertoli cells, can lead

to testis phenotypes like the one observed in *chagun* males. In order to address the function of

the *chagun* microenvironment established by the Sertoli cells, we conducted testis stem cell

transplantation assays (28). Busulfan is a chemotherapeutic alkylating agent that causes

irreparable adenine-guanine crosslinks leading to death of rapidly dividing cells. Doses of busulfan have been determined that will kill spermatogenic stem cells, but preserve the ability of the testis to be re-colonized with normal donor spermatogenic cells, although there may be some variability in the doses that can be tolerated.

Rosa-LacZ labeled spermatogenic stem cells from a normal, immuno-compatible donor male were transplanted into four *chagun* recipients and four busulfan treated controls (Jon Oatley, Ph.D., Washington State University). After allowing two months for the donor cells to colonize the recipient testes and resume the spermatogenic program, the recipients were assessed for X-gal staining to detect engraftment of the Rosa-LacZ labeled donor cells. In the control animals, spermatogenic colonies positive for LacZ expression (dark blue) were observed (Figure 3.7) (N=4). No donor-derived colonies were observed in mutant animals (N=4). These preliminary data suggest that the *chagun* Sertoli cell-generated microenvironment is incapable of supporting repopulation by wild-type spermatogenic stem cells.

Discussion

Here we report the discovery of the genetic basis of skeletal dysplasia, growth insufficiency, and progressive germ cell loss in *chagun* mutants. A LINE-1 retrotransposon-mediated insertion of a processed transcript into the gene that encodes protein of centriole 1A (*Poc1a*) causes elimination of the C-terminal end of a highly conserved WD-40 domain and reduced function. We conclude this based on: 1) identification of an insertion that causes exon-skipping in *Poc1a,* 2) co-segregation of this *Poc1a* mutation with the *chagun* mutant phenotype, 3) the lack of mutations in coding regions of any other genes within the *chagun* critical interval,
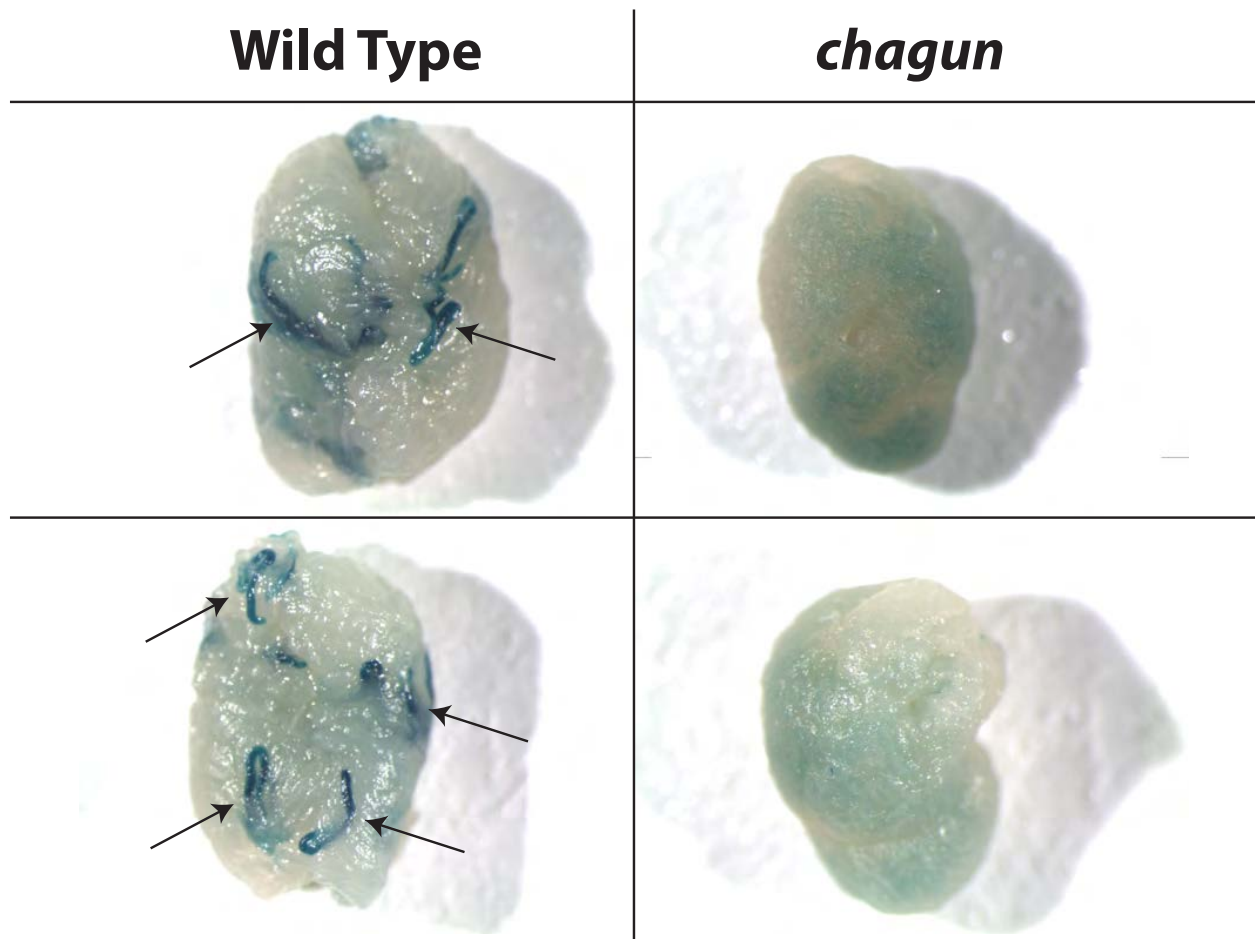
Figure 3.7 The *chagun* Sertoli cells fail to support colonization of wild-type spermatogenic stem cells. Whole testis were removed, stained with X-gal, and photographed. X-gal stained spermatogenic colonies (arrows, dark blue color) of labeled wild-type germ cells are present in the busulfan-treated control recipient testes (top panel), but no colonies were noted in *chagun* recipient testes (lower panel).

4) expression of *Poc1a* in the affected tissues, and 5) the report of independent families with severe short stature and either a missense or nonsense mutation in *POC1A* that appear to cause partial loss of function. Taken together, this provides compelling evidence that the insertion in *Poc1a* causes the *chagun* phenotype.

This mutant allele of *Poc1a* is caused by a LINE-1 mediated insertion of a processed transcript from the gene that encodes centromere protein w (*Cenpw*) into exon 8 of *Poc1a*. The insertion increases the size of exon 8 by approximately 500 bp. This is the likely cause of exon

skipping, as increasing the size of exons can lead to exon skipping (29). Transcripts that skip

exon 8 maintain the open reading frame and are predicted to produce a mutant protein that lacks

23 amino acids in the WD40 repeat domain in POC1A. There are normal levels of *Poc1a*

transcript and protein in mutant tibia, suggesting that the mutant transcript and protein are stable.

The 23 amino acids missing in the mutant are 71% conserved down to *Tetraurelia*

(paramecium), meaning that they are likely critical for the optimal function of *Poc1a*. Taken

together, we conclude that this mutant allele of *Poc1a* is a hypomorphic or reduced function

allele, rather than a null allele.

Two mutations in *POC1A* (p.Arg81stop and p.Leu171Pro) were found in consanguineous

pedigrees with severe short stature (22, 23). The associated clinical features, including viability

and the effects on hair, nails and intellectual ability, varied amongst the affected individuals in

the families. Sarig, Sprecher and colleagues labeled the syndrome a primordial dwarfism called

SOFT (short stature, onychodysplasia, facial dysmorphism and hypotrichosis) Syndrome (22),

although it is not clear that this acronym is appropriate for all patients with *POC1A* mutations.

The fertility of the subjects was not discussed, although some were still children. Alkurava and

colleagues showed that the patient's skin-derived fibroblasts exhibit disruptions in mitotic

spindle orientation and polarity, shortened primary cilia, and a lower frequency of primary cilia

formation (23). Golgi trafficking is disrupted in patient fibroblasts with the point mutation

(p.Leu171Pro) (22), although it is possible that the mutant protein itself is causing Golgi stress.

This possibility was not explored in these patient fibroblasts. The basis for the patient's variable

features is not clear, nor is the mechanism by which *POC1A* mutations cause growth

insufficiency.

Cell division in the growth plate is an intriguing process in which chondrocytes rotate and move to form the coin-stack structure after polarized cell division in the plane perpendicular to the axis of the growth plate (6). The primary cilium has been implicated in maintaining growth plate organization (3). Conditional loss of intraflagellar transport machinery, which is required for the maintenance of the primary cilium, in mouse chondrocytes results in growth insufficiency and disorganized growth plates that resemble the $Poc1a^{cha/cha}$ growth plate. Deficiencies in mitotic spindle orientation and primary cilium formation suggest the mechanism leading to growth defects in humans and mice with POC1A mutations.

We considered the possibility that a defect in the hypothalamus or pituitary could contribute to the infertility of $Poc1a$ mutants. Testosterone levels in $Poc1a^{cha/cha}$ animals are normal, seminal vesicles appear well developed, and Leydig cells appear normal (26). This suggests that the neuroendocrine portion of the male reproductive axis is working properly, implicating defects in germ cells and/or Sertoli cells as the cause of infertility. There are no data that prove that precisely oriented cell division or primary cilia are required for spermatogenesis. POC1A regulates centrosome maturation *in vitro* (30). If the centrosome fails to mature in $Poc1a^{cha/cha}$ germ cells, it could lead to spermatogenic arrest and/or a high rate of spermatogenic cell death due to faulty cell division. First, we must complete reciprocal testis transplantation assays (28) to determine whether $Poc1a^{cha/cha}$ spermatogenic stem cells are capable of establishing a spermatogenic program in a wild-type Sertoli cell microenvironment. If they are not capable of colonizing wild-type testes, then further characterization will be necessary, including, but not limited to, molecular analysis of centrosome maturation, cell proliferation, and cell death in $Poc1a^{cha/cha}$ germ cells, both *in vivo* and *in vitro*. These analyses would determine if

any or all of these cellular processes are leading to the development of the testis phenotype in $Poc1a^{cha/cha}$ animals.

Preliminary results suggest that $Poc1a^{cha/cha}$ Sertoli cells are dysfunctional (Figure 3.7). If this is clearly confirmed in additional experiments, the role of $Poc1a$ in Sertoli cells will be pursued. SOX9, an HMG family transcription factor and marker of Sertoli cells, appears to be expressed normally in $Poc1a^{cha/cha}$ testes, as assessed by immunostaining (data not shown). POC1A may regulate the Sertoli cell microtubule network, and/or it may be required for formation and function of the Sertoli cell primary cilium. Sertoli cells are required for the formation of a supportive spermatogenic microenviroment.

Why does the $Poc1a^{cha/cha}$ mutation seem to affect only skeletal growth and male fertility? $Poc1a$ and the related $Poc1b$ gene are broadly expressed, and, knock-down of both genes by siRNA is necessary to cause defects in mitotic spindle orientation in cell lines (HeLa) (30). The overlapping functions of these genes could provide compensation in tissues where both genes are expressed. Further work is necessary to determine whether or not $Poc1b$ is also expressed in testis and bone. Alternatively, the affected tissues may have a requirement for both $Poc1a$ and $Poc1b$.

The $Poc1a^{cha/cha}$ mutant phenotype may stem from a sensitivity of specific cells to compromises in mitotic spindle formation. Human patients with mutations in $POC1A$ exhibit a wide range of phenotypes. Skin, hair, and fingernails can be affected (22). Some of the patients with failure to thrive have difficulty feeding early in life (23). These features are not seen in $Poc1a^{cha/cha}$ animals on the FVB/NJ strain. Any organ system that has high cellular turnover (the growth plate, seminiferous epithelium, intestinal epithelium, the skin, hair, and fingernails) could be particularly vulnerable to a partial loss of $Poc1a$ function.

On the C57BL/6J genetic background, $Poc1a^{cha/cha}$ animals are sickly. In fact, if the mutation is backcrossed for six generations onto this genetic background, no mutant animals are detected at weaning (data not shown). It is highly likely that one or more genetic modifiers sensitize the C57BL/6J strain to effects of the $Poc1a$ mutation. For example, strain specific allelic variation in genes that encode other components of the cilia and/or centromere could enhance or suppress the effects of the $Poc1a$ mutation. Future work will be centered on understanding how the C57BL/6J genetic background contributes to lethality and failure to thrive.

Like the human cases (23), the causative mutation in the $Poc1a^{cha/cha}$ mouse likely causes a hypomorphic allele of $Poc1a$ that leads to the deletion of 23 amino acids in the translated protein. The loss of these residues could alter the ability of POC1A to localize to the centrosome (31). We show evidence that the protein is expressed in the growth plate of long bones and the seminiferous tubules of the testis (Figure 3.3), which are the tissues with the most obvious cellular phenotype (Figure 3.4 and 3.5). More work is necessary to determine the molecular bases of the growth defect and male infertility in this mouse model of SOFT Syndrome, but we provide much information as to the potential roles that $Poc1a$ plays *in vivo*. Additional work utilizing the $Poc1a^{cha/cha}$ mouse could provide highly valuable information on the molecular mechanism behind the many facets of the SOFT Syndome phenotype. This mouse model also highlights male fertility as a potential area of future interest for clinicians examining adult male SOFT Syndrome patients.

The $Poc1a^{cha/cha}$ mouse serves as a model of primordial dwarfism. Many novel genetic causes of the various forms of primordial dwarfism have been reported in the recent literature. There is also a high likelihood that these disorders, depending on their genetic causes, could be

considered skeletal ciliopathies. SOFT Syndrome and Meier-Gorlin Syndrome are two examples

of primordial dwarfisms that also lead to defects in the primary cilium (23, 32), but not much is

known about the molecular mechanism underlying these conditions. It is for this reason that

mouse models like the $Poc1a^{cha/cha}$ mouse, are an incredibly valuable resource for geneticists.

Materials and Methods

Discovery and husbandry of *chagun* mice. The *chagun* phenotype arose spontaneously on the

DBA/2J strain in Linda Siracusa's laboratory at the Thomas Jefferson University (Philadelphia,

Pennsylvania). The mice were transferred to the University of Michigan (Ann Arbor, Michigan).

Recently they have been maintained on a hybrid background consisting of C57BL/6J and

DBA/2J background strains, and also outcrossed to the FVB/NJ strain, and maintained.

All mice were housed in a specific pathogen free facility with 12-h light, 12-h dark cycle in

ventilated cages with unlimited access to tap water and Purina 5020 chow. All procedures using

mice were approved by the University of Michigan Committee on Use and Care of Animals

(UCUCA), and all experiments were conducted in accordance with the principles and procedures

outlined in the National Institutes of Health Guidelines of the Care and Use of Experimental

Animals.

chagun **Genotyping Protocol.** Before the mutation was uncovered, primers were used to

amplify regions around SNPs by conventional PCR methods that differed between the mutant

(DBA/2J) and the wild-type (FVB/NJ) backgrounds (SNPs: rs30174769, rs29637716) that are

within the critical interval. These amplification products were then digested with Bsr1

endonuclease and run on a 2% agarose/tris-boric acid-EDTA gel to visualize the different bands

that segregated differentially between the two background strains. C57BL/6J alleles matched

that of the wild-type background, FVB/NJ, so if any residual C57BL/6J background remained,

we could still determine which mice were heterozygous or homozygous for the mutant (DBA/2J) background. Once the mutation was uncovered, primers designed to detect the presence of the insertion from flanking sequence (two potential products; a small wild-type allele, and the larger *chagun* allele with the insertion) were used to distinguish mutants, heterozygous, and wild-type animals. All primers anneal optimally at 60°C. Primer sequences:

rs30174769 Fwd: 5'-TGAGCGCCAACACAGTAAAAA-3'

rs30174769 Rev: 5'-GTGGGAGCAAGAGACAAAGAGAT-3'

rs29637716 Fwd: 5'-GCGGGGTGCCTGGGTCTCC-3'

rs29637716 Rev: 5'-TCATACAGCACACGCACTTACACA-3'

WT and *chagun* allele Fwd: 5'-TGTCCCACTGCCACTGCCACTCA-3'

WT and *chagun* allele Rev: 5'-GGAAGACTCGCCCCACAGGACTCA-3'

Capture of the *chagun* critical interval. Targeted enrichment libraries corresponding to the *chagun* critical interval were generated by Daniel Burgess, Ph.D. at Roche/Nimblegen (Madison, Wisconsin). Genomic DNA samples from both a heterozygote (known carrier) and a *chagun* mutant were supplied to generate the libraries, which were indexed separately to allow for simultaneous sequencing. The libraries were sequenced by the University of Michigan DNA Sequencing Core led by Robert Lyons, Ph.D. (Department of Biological Chemistry). Bioinformatic analyses of the sequence data were performed by James Calvalcoli, Ph.D. (Department of Computational Medicine and Bioinformatics, University of Michigan, Ann Arbor, Michigan). The Broad Institute's Integrative Genomics Viewer was utilized to visualize and evaluate the DNA sequence data.

PCR Amplification of Genomic DNA. The region around *Poc1a* exon 8 was amplified by PCR of genomic DNA using the following primer sequences: Forward primer: 5'-

TGTCCCACTGCCACTGCCACTCA-3', and Reverse Primer: 5'-

GGAAGACTCGCCCCACAGGACTCA-3'. Optimal annealing temperature: 60°C. PCR was

conducted with the GoTaq DNA Polymerase and buffers provided by the distributor (Promega).

Extraction of RNA and Generation of cDNA via Reverse Transcription. Extraction of total

RNA was completed with the RNAqueous 4-PCR Kit (Ambion) according to the manufacturer's

instructions. The total RNA was utilized to generate cDNA with Oligo dT Primers

(Invitrogen/Life Technologies) and Superscript II Reverse Transcriptase (Invitrogen/Life

Technologies) according to the manufacturer's instructions. The cDNA was used as a template

in standard PCR reactions using GoTaq DNA Polymerase (Promega) and the following primers

to amplify two regions in the *Poc1a* cDNA:

Exon 5-10 Forward Primer: 5'-CAAGACCAGCCGGGAATGTATC-3'

Exon 5-10 Reverse Primer: CTGGGGCTCGCCTTGAACTGACTC-3'

Optimal annealing temperature: 60°C.

Exon 7-8 Forward Primer: 5'- CCATCGGGAAACTACCTCATCAC-3'

Exon 7-8 Reverse Primer: 5'-AAATACTCCCCCGTTCTTG-3'

Optimal annealing temperature: 55°C. Sequencing was completed by the University of Michigan

DNA Sequencing Core.

Real-Time Quantitative PCR. Real-time quantitative PCR was conducted using cDNA

generated in the manner stated in the previous Methods section. TaqMan® Universal PCR

Master Mix (Applied Biosystems/Life Technologies) was used according to the manufacturer's

instructions. The following TaqMan® probes were included to test expression levels of *Poc1a*:

Exon 2-3 Assay ID: Mm01235877_m1. Exon 10-11 Assay ID: Mm01235875_m1. Reactions

were loaded into MicroAmp® Optical 96-well reaction plates (Applied Biosystems/Life Technologies) and run using an Applied Biosystems 7500 Real-Time PCR System.

POC1A Western Blot Analysis. Isolation of protein from postnatal day 3 tibiae and western blot analyses were carried out as previously described (33). The blot was incubated with a 1:500 dilution of a mouse anti-human POC1A primary antibody (Abcam, ab67698) overnight at 4°C. The blot was incubated with a 1:5000 dilution of a goat anti-mouse IgG secondary antibody (Jackson ImmunoResearch Laboratories, Inc. #115-035-003) for one hour at room temperature. The blot was stripped and incubated with a 1:5000 dilution of a rat anti-yeast tubulin antibody (Abcam, ab6160) overnight at 4°C. The blot was incubated with a 1:10,000 dilution of a goat anti-Rat IgG secondary antibody (Jackson ImmunoResearch Laboratories, # 112-035-102) for one hour at room temperature. All antibodies were diluted in a blocking solution made up of 1% weight:volume Bovine Serum Albumin;Tris-buffered saline with Tween-20.

Bone and Testis Histology. Tibiae were dissected from two and three-week old male animals, fixed overnight in 4% PFA, rinsed in PBS, and decalcified in 14% EDTA solution (weight:volume) for approximately 30 days. Testes were removed from mice of the listed ages, fixed overnight in Bouin's Fixative Solution (Sigma). Both the testes and tibiae were then dehydrated through an ethanol series and embedded in paraffin. Sections were stained with hematoxylin and eosin (tibiae) or periodic acid-Schiff's reagent (testes) according to standard protocols.

POC1A Immunohistochemistry. Immunohistochemistry was conducted by deparaffinization of the slides in xylenes and rehydration in an ethanol series to 1X PBS. Afterward, the testis sections were boiled in a 100 mM solution of citric acid (pH 6.0) for 10 minutes to expose epitopes, and cooled. Tibia sections were fixed for 7 minutes in 4% PFA, washed in PBS, and

were not subjected to heat-induced epitope unmasking in citric acid. Both testis and tibia

sections were incubated for 20 minutes in solution of 3% hydrogen peroxide diluted in methanol

to quench endogenous peroxidase activity. The slides were blocked in a solution included in the

Tyramide Signal Amplification (TSA) Kit (Perkin-Elmer) for one hour at room temperature.

This was followed by an overnight incubation with a rabbit anti-rat POC1A primary antibody

(Abcam, ab135361) diluted 1:100 in TSA Block solution at 4°C. Sections were washed in PBS,

and incubated with a goat anti-rabbit biotin-conjugated secondary antibody (Jackson

ImmunoResearch Laboratories Inc., #111-067-003) for 1 hour at room temperature. The

subsequent steps were carried out according to the instructions provided in the TSA Fluorescein

Tyramide Kit (TSA-FITC Kit) by Perkin-Elmer. Sections were counterstained with DAPI to

reveal nuclei, cover slipped and photographed with a Leica Leitz DMRB/E compound

microscope.

PLZF Immunohistochemistry. The POC1A primary antibody was used in

immunohistochemical analysis of testis sections from the ages listed. The rabbit anti-human

PLZF primary antibody (Santa Cruz Biotechnology Inc., sc-22839) was incubated at a 1:50

dilution in the TSA Block Solution overnight at 4°C, and treated in the same manner as the

sections incubated with the POC1A primary antibody (TSA-FITC Kit, Perkin-Elmer).

Testis Cell Transplantation Assays. Assays were performed at Washington State University

(Pullman, Washington) in the laboratory of Jon Oatley, Ph.D. as previously described (34).

Acknowledgments

All of the experiments done to produce figures 3.1 through 3.6 were done by KAG.

References

1   Karsenty, G., Kronenberg, H.M. and Settembre, C. (2009) Genetic control of bone formation. *Annual review of cell and developmental biology*, **25**, 629-648.
2   Krakow, D. and Rimoin, D.L. (2010) The skeletal dysplasias. *Genetics in medicine : official journal of the American College of Medical Genetics*, **12**, 327-341.
3   Song, B., Haycraft, C.J., Seo, H.S., Yoder, B.K. and Serra, R. (2007) Development of the post-natal growth plate requires intraflagellar transport proteins. *Developmental biology*, **305**, 202-216.
4   Zhang, J., Tan, X., Li, W., Wang, Y., Wang, J., Cheng, X. and Yang, X. (2005) Smad4 is required for the normal organization of the cartilage growth plate. *Developmental biology*, **284**, 311-322.
5   Thiel, C., Kessler, K., Giessl, A., Dimmler, A., Shalev, S.A., von der Haar, S., Zenker, M., Zahnleiter, D., Stoss, H., Beinder, E. *et al.* (2011) NEK1 mutations cause short-rib polydactyly syndrome type majewski. *Am J Hum Genet*, **88**, 106-114.
6   Li, Y. and Dudley, A.T. (2009) Noncanonical frizzled signaling regulates cell polarity of growth plate chondrocytes. *Development*, **136**, 1083-1092.
7   Romereim, S.M. and Dudley, A.T. (2011) Cell polarity: The missing link in skeletal morphogenesis? *Organogenesis*, **7**, 217-228.
8   Klingseisen, A. and Jackson, A.P. (2011) Mechanisms and pathways of growth failure in primordial dwarfism. *Genes & development*, **25**, 2011-2024.
9   Warman, M.L., Cormier-Daire, V., Hall, C., Krakow, D., Lachman, R., LeMerrer, M., Mortier, G., Mundlos, S., Nishimura, G., Rimoin, D.L. *et al.* (2011) Nosology and classification of genetic skeletal disorders: 2010 revision. *American journal of medical genetics. Part A*, **155A**, 943-968.
10   O'Driscoll, M., Ruiz-Perez, V.L., Woods, C.G., Jeggo, P.A. and Goodship, J.A. (2003) A splicing mutation affecting expression of ataxia-telangiectasia and Rad3-related protein (ATR) results in Seckel syndrome. *Nature genetics*, **33**, 497-501.

11   Ogi, T., Walker, S., Stiff, T., Hobson, E., Limsirichaikul, S., Carpenter, G., Prescott, K., Suri, M., Byrd, P.J., Matsuse, M. *et al.* (2012) Identification of the first ATRIP-deficient patient and novel mutations in ATR define a clinical spectrum for ATR-ATRIP Seckel Syndrome. *PLoS Genet*, **8**, e1002945.

12   Qvist, P., Huertas, P., Jimeno, S., Nyegaard, M., Hassan, M.J., Jackson, S.P. and Borglum, A.D. (2011) CtIP Mutations Cause Seckel and Jawad Syndromes. *PLoS Genet*, **7**, e1002310.

13   Kalay, E., Yigit, G., Aslan, Y., Brown, K.E., Pohl, E., Bicknell, L.S., Kayserili, H., Li, Y., Tuysuz, B., Nurnberg, G. *et al.* (2011) CEP152 is a genome maintenance protein disrupted in Seckel syndrome. *Nature genetics*, **43**, 23-26.

14   Bicknell, L.S., Bongers, E.M., Leitch, A., Brown, S., Schoots, J., Harley, M.E., Aftimos, S., Al-Aama, J.Y., Bober, M., Brown, P.A. *et al.* (2011) Mutations in the pre-replication complex cause Meier-Gorlin syndrome. *Nature genetics*, **43**, 356-359.

15   Bicknell, L.S., Walker, S., Klingseisen, A., Stiff, T., Leitch, A., Kerzendorfer, C., Martin, C.A., Yeyati, P., Al Sanna, N., Bober, M. *et al.* (2011) Mutations in ORC1, encoding the largest subunit of the origin recognition complex, cause microcephalic primordial dwarfism resembling Meier-Gorlin syndrome. *Nature genetics*, **43**, 350-355.

16   de Munnik, S.A., Bicknell, L.S., Aftimos, S., Al-Aama, J.Y., van Bever, Y., Bober, M.B., Clayton-Smith, J., Edrees, A.Y., Feingold, M., Fryer, A. *et al.* (2012) Meier-Gorlin syndrome genotype-phenotype studies: 35 individuals with pre-replication complex gene mutations and 10 without molecular diagnosis. *Eur J Hum Genet*, **20**, 598-606.

17   Guernsey, D.L., Matsuoka, M., Jiang, H., Evans, S., Macgillivray, C., Nightingale, M., Perry, S., Ferguson, M., LeBlanc, M., Paquette, J. *et al.* (2011) Mutations in origin recognition complex gene ORC4 cause Meier-Gorlin syndrome. *Nature genetics*, **43**, 360-364.

18   Al-Dosari, M.S., Shaheen, R., Colak, D. and Alkuraya, F.S. (2010) Novel CENPJ mutation causes Seckel syndrome. *Journal of medical genetics*, **47**, 411-414.

19   Griffith, E., Walker, S., Martin, C.A., Vagnarelli, P., Stiff, T., Vernay, B., Al Sanna, N., Saggar, A., Hamel, B., Earnshaw, W.C. *et al.* (2008) Mutations in pericentrin cause Seckel syndrome with defective ATR-dependent DNA damage signaling. *Nature genetics*, **40**, 232-236.

20   Rauch, A., Thiel, C.T., Schindler, D., Wick, U., Crow, Y.J., Ekici, A.B., van Essen, A.J., Goecke, T.O., Al-Gazali, L., Chrzanowska, K.H. *et al.* (2008) Mutations in the pericentrin (PCNT) gene cause primordial dwarfism. *Science*, **319**, 816-819.

21   Dauber, A., Lafranchi, S.H., Maliga, Z., Lui, J.C., Moon, J.E., McDeed, C., Henke, K., Zonana, J., Kingman, G.A., Pers, T.H. *et al.* (2012) Novel microcephalic primordial dwarfism disorder associated with variants in the centrosomal protein ninein. *J Clin Endocrinol Metab*, **97**, E2140-2151.

22   Sarig, O., Nahum, S., Rapaport, D., Ishida-Yamamoto, A., Fuchs-Telem, D., Qiaoli, L., Cohen-Katsenelson, K., Spiegel, R., Nousbeck, J., Israeli, S. *et al.* (2012) Short stature, onychodysplasia, facial dysmorphism, and hypotrichosis syndrome is caused by a POC1A mutation. *Am J Hum Genet*, **91**, 337-342.

23   Shaheen, R., Faqeih, E., Shamseldin, H.E., Noche, R.R., Sunker, A., Alshammari, M.J., Al-Sheddi, T., Adly, N., Al-Dosari, M.S., Megason, S.G. *et al.* (2012) POC1A truncation mutation causes a ciliopathy in humans characterized by primordial dwarfism. *Am J Hum Genet*, **91**, 330-336.

24   Edery, P., Marcaillou, C., Sahbatou, M., Labalme, A., Chastang, J., Touraine, R., Tubacher, E., Senni, F., Bober, M.B., Nampoothiri, S. *et al.* (2011) Association of TALS developmental disorder with defect in minor splicing component U4atac snRNA. *Science*, **332**, 240-243.

25   He, H., Liyanarachchi, S., Akagi, K., Nagy, R., Li, J., Dietrich, R.C., Li, W., Sebastian, N., Wen, B., Xin, B. *et al.* (2011) Mutations in U4atac snRNA, a component of the minor spliceosome, in the developmental disorder MOPD I. *Science*, **332**, 238-240.

26   Cha, K.B., Karolyi, I.J., Hunt, A., Wenglikowski, A.M., Wilkinson, J.E., Dolan, D.F., Dootz, G., Finnegan, A.A., Seasholtz, A.F., Hankenson, K.D. *et al.* (2004) Skeletal dysplasia and male infertility locus on mouse chromosome 9. *Genomics*, **83**, 951-960.

27   Costoya, J.A., Hobbs, R.M., Barna, M., Cattoretti, G., Manova, K., Sukhwani, M., Orwig, K.E., Wolgemuth, D.J. and Pandolfi, P.P. (2004) Essential role of Plzf in maintenance of spermatogonial stem cells. *Nature genetics*, **36**, 653-659.

28   Oatley, J.M. and Brinster, R.L. (2008) Regulation of spermatogonial stem cell self-renewal in mammals. *Annual review of cell and developmental biology*, **24**, 263-286.

29   Hertel, K.J. (2008) Combinatorial control of exon recognition. *The Journal of biological chemistry*, **283**, 1211-1215.

30   Venoux, M., Tait, X., Hames, R.S., Straatman, K.R., Woodland, H.R. and Fry, A.M. (2012) Poc1A and Poc1B act together in human cells to ensure centriole integrity. *J Cell Sci*.

31   Pearson, C.G., Osborn, D.P., Giddings, T.H., Jr., Beales, P.L. and Winey, M. (2009) Basal body stability and ciliogenesis requires the conserved component Poc1. *J Cell Biol*, **187**, 905-920.

32   Stiff, T., Alagoz, M., Alcantara, D., Outwin, E., Brunner, H.G., Bongers, E.M., O'Driscoll, M. and Jeggo, P.A. (2013) Deficiency in origin licensing proteins impairs cilia formation: implications for the aetiology of Meier-Gorlin syndrome. *PLoS Genet*, **9**, e1003360.

33   Geister, K.A., Brinkmeier, M.L., Hsieh, M., Faust, S.M., Karolyi, I.J., Perosky, J.E., Kozloff, K.M., Conti, M. and Camper, S.A. (2013) A novel loss-of-function mutation in Npr2 clarifies primary role in female reproduction and reveals a potential therapy for acromesomelic dysplasia, Maroteaux type. *Human molecular genetics*, **22**, 345-357.

34   Wu, X., Oatley, J.M., Oatley, M.J., Kaucher, A.V., Avarbock, M.R. and Brinster, R.L. (2010) The POU domain transcription factor POU3F1 is an important intrinsic regulator of GDNF-induced survival and self-renewal of mouse spermatogonial stem cells. *Biology of reproduction*, **82**, 1103-1111.

APPENDIX 3.1

Gene Name	Gene Name and Function	Coverage	Type of Variant	Variant Location (Chr9, Mm9)	Conclusions
Appendix 3.1. Variants Unique to *chagun* Uncovered Via Whole Exome Sequencing					
Ephb1	Eph receptor B1 Ephrin signaling	64X	Insertion (N/A)	101844999	Gene sequenced by Sanger Method—No variants noted
Cpne4	Copine IV	6X	Insertion (+TT)	104588727	In Poly-T Tract
Atp2c1	ATPase, Ca+2 sequestering Secretory pathway	57X	SNP (A→G)	105337374	Not in splice site or branch point
		59X	Deletion (-1)	105337375	Not in splice site or branch point
Pik3r4	Phosphatidylinositol-3-kinase, regulatory subunit, polypeptide 4, p150 PI3K signaling	42X	Deletion (-A)	105547333	In Poly-T tract
Col6a6	Collagen, type VI, alpha 6	7X	SNP (C→T)	105625146	In a CA-repeat
		8X	Insertion (+G)	105641565	Not in a splice site or branch point
Col6a4	Collagen, type VI, alpha 4	9X	Deletion (-G)	105969540	In Poly-G Tract
		8X	SNP (C→T)	105969546	In Poly-G Tract
Alas1	Aminolevulinic acid synthase 1 Embryonic lethality	48X	SNP (T→G)	106136553	In Poly-T Tract
Acy1	Aminoacylase 1 Catalyzes N-acetyl amino acids to amino acid and acetic acid	170X	SNP (A→G)	106337184	Not in splice site or branch point Not well conserved
Parp3	Poly (ADP-ribose) polymerase family, member 3 DNA repair	2X	SNP (A→G)	106377303	Not conserved, in poly-G tract
		2X	SNP (A→G)	106377304	Not Conserved, in poly-G tract

Note: All variants listed above occur in introns.

APPENDIX 3.2

Appendix 3.2. Novel Insertions Uncovered By Targeted Enrichment of the *chagun* Critical Interval				
Starting Location (Chr 9)	**Ending Location (Chr 9)**	**Transposable Element Description**	**Number of Reads**	**Description**
103901307	103901445	IAPLTR1a_I_MM	4	Overlaps a known RSINE element
105278767	105278878	RLTR25_MM	6	Located in the middle of intron 1 of *Nek11*
105462434	105463009	L10	17	Located between two MTA repeats
105538508	105538828	B2_Mm1a	6	Intergenic
105717587	7016	L1Md_Gf_5end	5	Located within *Col6a6*

CHAPTER 4

Future Directions in Skeletal Dysplasia and Infertility Genetic Research

Introduction

In this dissertation I present the identification of the genetic basis of two skeletal

dysplasia and infertility syndromes. These studies reveal the pathophysiology of disease, and set

the stage for the development of therapeutic interventions. These two examples typify two

current prominent themes in skeletal dysplasia research. First: novel genetic causes of disease

are being discovered at a phenomenal rate, largely due to high-throughput mapping and

sequencing technologies. Second: mouse models are invaluable for understanding the molecular

etiologies behind skeletal dysplasia phenotypes. Chapter 1, which focuses mainly on the first

theme, clearly demonstrates the shift in strategy toward utilizing next-generation technologies,

and how these technologies have been used in the last two years to the investigator's advantage

(Table 1.2). They will also likely be used in future work to address the remaining forms of

skeletal disorders that currently have no known genetic cause, as well as many novel skeletal

disorders that are only now being recognized (Table 1.4).

Chapters 2 and 3, on the other hand, focus on the second theme. While both mouse

models presented in this dissertation harbor mutations in genes previously shown to cause human

skeletal disorders, both models are highly valuable in that they allow us to pursue a deeper

characterization of the phenotype, which will ultimately add to our basic understanding of

skeletal growth and development, and could lead to potential therapies for skeletal dysplasia patients (Chapter 2).

There is still much to be done with regard to future exploration concerning both of these themes. There are multiple additional experiments that could be conducted with regard to understanding the mechanisms behind both the $Npr2^{pwe/pwe}$ and the $Poc1a^{cha/cha}$ mutant phenotypes. There is also the potential of developing therapies ($Poc1a^{cha/cha}$) or refining therapeutic intervention ($Npr2^{pwe/pwe}$) in both of these mouse models. While there are still unanswered genetic questions regarding the causes of many skeletal disorders, there are even more questions regarding potential modifying loci that contribute to the phenotypic variability reported in some forms of skeletal dysplasia. There are a number of approaches one could take to address these questions, including sensitized mutagenesis screens in mouse or zebrafish. All of these future directions will be discussed in the sections that follow.

$Npr2^{pwe/pwe}$: Molecular Outputs of CNP/NPR2 Signaling

Much that has been gained from the understanding of C-type Natriuretic Peptide (CNP)/Natriuretic Peptide Receptor 2 (NPR2) signaling has come from work conducted in cell lines (1) or on whole fetal tibiae treated with CNP and pharmacological inhibitors in culture (2). These studies have shown that two of the main signaling cascades regulated by CNP are the MEK/ERK (1) and p38 Mitogen-Activated Protein Kinase (2) (MAPK) pathways. Of course, with the development of many mutant alleles in these pathways, there exists the potential to cross these lines to determine the relative contributions of these pathways to bone growth. For example, gene expression profiling on animals with gain or loss of function of these genes in combination ($Npr2^{pwe/pwe}$, $Mkk3^{-/-}$ or $Mkk6^{-/-}$ double mutant animals, which would be unable to activate p38 MAPK components) could define the gene expression profile regulated by p38

MAPK in comparison to control animals. The same could be done utilizing gain and loss of function of *Fgfr3*, or loss of function of *Mkk1* in tandem with loss-of-function in *Npr2* to uncover the genes regulated by these signaling pathways. Taking a genetic approach and analyzing fetal tibiae immediately as opposed to after 6-8 days of culture (2) could reduce potential artifacts generated as a result of the *in vitro* environment. Additionally, the genes regulated by these various pathways could provide clues of further cross-talk between these pathways and other signaling pathways. This could provide information on additional therapeutic avenues for AMDM, similar to the way CNP became a major therapeutic candidate for achondroplasia (3). Obviously, models for AMDM, such as the *Npr2*[pwe/pwe] mouse, will be valuable assets for the testing of these potential therapies.

Npr2[pwe/pwe]: Improving the Therapy For the Growth Defect

It is difficult to deliver therapy directly to the growth plate through the circulation because the growth plate is an avascular tissue (4). Systemic delivery of drugs to treat mouse models of skeletal dysplasia has had mixed success (5-10). The most successful strategy was continuous supplementation with CNP in mice (6), or genetic manipulation to overexpress CNP in models of achondroplasia (11, 12). In terms of developing an easily administered therapy for human patients, which would most likely be children at the time of therapeutic intervention, neither of the more successful methods is a feasible or desirable mode of therapy. This is due to the fact that continuous supplementation intravenously during one's childhood could affect one's quality of life, and we are unable at this time to provide gene therapy. If, however, targeting to the growth plate could somehow be improved, this would undoubtedly increase the success rate of these pharmacological therapies, and minimize off-target effects on other tissues.

In order for a treatment to be deemed successful, it should not only increase growth velocity and allow the individual to reach their target height in a proportional manner, it should also cause minimal effects on the integrity of the skeletal elements themselves. In the case of continuous supplementation of CNP or a drug, it is possible that the increase in the growth rate could come at the expense of healthy long bones. In the case of MEK1/2 inhibition (5, 13), continuous supplementation could potentially accelerate the rate of long bone growth, but also cause a failure in osteoblast differentiation, a process that requires activation of ERK1/2 (14). Further, acceleration of growth plate chondocyte proliferation or hypertrophic differentiation could lead to a scenario wherein the osteoblasts cannot meet the demand for the addition of bone matrix. Likewise, the cells of the growth plate may be depleted more quickly than they should due to increased proliferation and/or differentiation. Both of these outcomes could impair the patient's ability to reach their target height, and/or affect the quality of mineralized tissue that forms. Dosage, administration method, duration of treatment, and improved targeting to the growth plate are imperative areas of future work to consider as we move forward toward developing therapies for skeletal dysplasia patients.

Npr2[pwe/pwe]: CNP/NPR2 Function in the Ovarian Follicle in Mouse and Human

Recent work on CNP and NPR2 in the regulation of meiotic arrest have shown that *Npr2* mRNA expression in isolated cumulus cells is increased by estradiol treatment *in vitro* (15). Estradiol also increased cGMP levels in cumulus cells and oocytes, presumably by increasing the expression of NPR2 (15). Hseuh and colleagues showed that treatment with hCG (LH analog) leads to a decrease in *Nppc* (CNP) mRNA expression in granulosa cells of ovarian follicles (16), while Jaffe's group showed that LH reduces NPR2 activity, as evidenced by a reduction in cGMP levels in ovarian follicles (17). All of these data support a clear role of endocrine regulation of

the CNP/NPR2 signaling pathway to maintain meiotic arrest. Additional data generated after an ovulatory dose of hCG in human patients demonstrated a decrease in CNP level in human follicular fluid (16). These data are the first to provide support that this pathway could be mediating oocyte meiotic arrest in human.

The data generated provide strong evidence implicating CNP/NPR2 in maintaining meiotic arrest in human oocytes. This raises an obvious question: are female AMDM patients fertile? First, the rarity of AMDM (18) makes it difficult to obtain information about fertility. I predict that women with this disorder would be infertile due to failed meiotic arrest, but they may be able to carry pregnancies with donor eggs. The study of female AMDM patients over time could be conducted to determine if in fact these patients are infertile. Of course, this would also provide support that the CNP/NPR2 signaling pathway is likely regulating oocyte meiotic arrest in human.

Poc1a^{cha/cha}: Proof that the correct gene has been identified.

In Chapter 3, many lines of evidence are presented that support the hypothesis that the *chagun* mutant phenotype is caused by a hypomorphic allele of *Poc1a* (Figure 3.1, Figure 3.2). We are confident that this is the causative mutation. No other obviously deleterious variants were uncovered through whole exome sequencing (Appendix 3.1). We also discovered five novel insertions in the critical interval that are not present in 16 reference strain genomes (Appendix 3.2). We will use a combination of bioinformatic analysis and PCR amplification to determine that these are true insertions, and confirm the presence or absence of these elements in the parental strains (FVB/NJ, DBA/2J, C57BL/6J). If any are found to be unique to the *chagun* strain, we will determine whether or not the insertion alters gene splicing (intragenic insertions) or gene expression (intergenic insertions). Importantly, the insertion of the processed

pseudogene (*Cenpw*) into exon 8 of *Poc1a* is the only variant we have found that will likely disrupt the function of an encoded protein.

There are two experiments that could provide additional genetic evidence that *Poc1a* is the gene causing the *chagun* mutant phenotype. First, we are conducting a Bacterial Artificial Chromosome (BAC) transgenic rescue experiment using a BAC (RP24-384G5, 196,267 bp) that contains *Poc1a* and approximately 75 kb and 50 Kb of flanking sequencing on the on the proximal and distal ends of *Poc1a*, respectively. The BAC is likely to contain all of the elements required for *Poc1a* expression. Crossing the transgenic mice harboring the BAC to our *chagun* strain will allow us to determine whether providing mutants with one functional copy of *Poc1a* corrects the phenotype. The BAC contains 3 additional genes: *Twf2*, *Alas1*, and *Dusp7*. All three of these genes are not likely to be causing the mutant phenotype. The knock-out allele of *Twf2*, which encodes twinfilin, actin binding protein, homolog 2, does not exhibit a phenotype (19). *Alas1* (aminolevulinic acid synthase 1) knock-out animals die early in embryonic development (20), and only minor variants were uncovered by whole exome sequencing (Appendix 3.1). Furthermore, no insertions were uncovered in this gene through targeted enrichment and sequencing of the entire critical interval. Dual specificity phophatase 7 (*Dusp7*) does not have a knock out allele as of yet, but no variants were uncovered through either of the two methods we employed. Thus, our choice of BAC appears to confer all the proper information to allow for *Poc1a* expression, while limiting the number of additional genes, all three of which are unlikely to cause an issue or be causing the mutant phenotype.

An alternative approach is to conduct an allelism test. This would involve crossing our *Poc1a*$^{cha/cha}$ strain with a *Poc1a*$^{-/-}$ strain to determine whether compound heterozygotes exhibit the homozygous *Poc1a*$^{cha/cha}$ phenotype. However, given that the *Poc1a*$^{cha/cha}$ allele is

hypomorphic, and the mutations in human patients are also thought to be hypomorphic alleles, it is likely that a true knock-out allele of *Poc1a* will be lethal. Therefore, it may be impossible to generate mice from the *Poc1a* knock-out ES cell clones we are in the process of obtaining (Knock-Out Mouse Project, KOMP). If so, it would be helpful to determine the embryonic stage in which the animals die, as we could utilize yet another alternative approach—an inducible cre recombinase to bypass the global knock-out's potential early embryonic lethality. Conversely, if mice are born, we will have to rigorously compare the *Poc1a* knock-out phenotype to the *Poc1a*cha/cha phenotype to see what differences exist. Crossing the knock-out allele onto the *Poc1a*cha/cha background would generate compound heterozygotes which could exhibit an intermediate phenotype: worse than the *Poc1a*cha/cha homozygous phenotype, but less severe than the knock-out phenotype. Both the BAC transgenic rescue and the allelism test will provide us with additional supporting evidence that the hypomorphic allele of *Poc1a* in *chagun* animals is indeed responsible for the mutant phenotype.

*Poc1a*cha/cha: Molecular characterization of the hypomorphic mutation

Poc1a is expressed in many tissues, based on cDNA Source Data (Mouse Genome Informatics), although no systematic assessment of gene expression has been done. Given the broad expression of *Poc1a* it is intriguing that hypomorphic mutations in POC1A cause skeletal dysplasia and male infertility, but leave other tissues intact. *POC1A*, and its close relative, *POC1B*, have both been shown in human cell lines to be required for proper mitotic spindle orientation and polarity (21). These experiments were conducted using siRNA to knock-down expression of both *POC1A* and *POC1B*, but did not lead to complete depletion of both proteins. The defects in the mitotic spindle observed in the knock-down experiment were the same defects present in human patient skin fibroblasts. Therefore, while the data from the knock-down

experiment suggest functional redundancy between these related genes, the data from human patient cells indicate that even a partial loss-of-function in one gene can affect proper mitotic spindle orientation and polarity.

This begs the question of whether or not there are tissues, such as the bone and testis, that are particularly vulnerable to *Poc1a* partial loss-of-function. One way to address this question is to conduct RT-PCR on an array of tissues to determine where each of them is expressed and assess the relative abundance. With respect to *Poc1a*^{cha/cha} animals, both members may be expressed in bone and testis, but the mutation leads to the loss of a critical function conferred by the deleted 23 amino acids in *Poc1a* in both of these tissues. This could include the loss of a binding site of a critical cofactor, leading to its failed recruitment to the centrosome. It is also possible that *Poc1a*, but not *Poc1b*, is expressed in these tissues. Both outcomes could explain the tissue specificity of the *Poc1a*^{cha/cha} phenotype encompassing bone and testis. As discussed in Chapter 3, however, there may be subtle defects in tissues with a high demand for cellular turnover (skin, hair, fingernails, intestinal epithelium, etc.) due to the predicted functions of both of these genes. Therefore, depending on the outcome of the RT-PCR survey, there may be additional aspects of the *Poc1a*^{cha/cha} phenotype that have been overlooked, and could reveal more similarities between this mouse model and human patients (22, 23).

The amino acids deleted in POC1A in *Poc1a*^{cha/cha} animals are located at the C-terminal end of the WD40 repeat domain (Figure 3.1D). While this mutation does not disrupt the open reading frame, it is possible that the folding of POC1A is disrupted C-terminal to the loss of exon 8. This could lead to suboptimal targeting of POC1A to the centrosome (24). If, however, POC1A does localize to the centrosome, the mutation could lead to the impaired recruitment of cofactors to the centrosome. Based on the phenotypes of human patients' skin fibroblasts (23),

and knock-down experiments in HeLa cells (21), the mutation could be affecting recruitment of factors required for proper centrosome maturation, mitotic spindle orientation and polarity, primary cilium formation and maintenance, as well as asymmetric cell division.

To determine if the mutant form of POC1A localizes to the centrosome, one approach would be to conduct immunohistochemistry on POC1A and γ-tubulin (centrosome marker) in mutant and wild-type mouse embryonic fibroblasts (MEFs). If mutant POC1A is found to localize to the centrosome, then the same primary antibody could then be used for coimmunoprecipitation experiments, followed by mass spectrometry, to determine what factors associate with wild-type POC1A, and those which fail to associate with mutant POC1A. Of course, these techniques are dependent on the availability of primary antibodies capable of recognizing the mutant protein.

If this proves challenging, an alternative way to test both localization to the centrosome and recruitment of appropriate cofactors is to use the biotin-tagging system (25). This would involve generating a construct with a biotin-acceptor tag sequence at the C-terminus of the mutant form of POC1A, and co-transfecting this construct into cells with a vector expressing BirA, the enzyme that catalyzes the addition of biotin to the biotin-tag sequence. Cells would then express biotin-tagged POC1A, which could be incubated with a streptavidin or avidin-conjugated fluorophore to visualize POC1A in the transfected cells. This technique in combination with immunohistochemistry for γ-tubulin will allow us to ascertain whether or not the mutant form of POC1A associates with the centrosome.

If necessary, the biotin-tagged POC1A could then also be used in coimmunoprecipitation experiments followed by mass spectrometry, to uncover the proteins that typically associate with POC1A, and those that are missing from this complex in the mutant. This approach has the

added advantage that biotinylation can also be done *in vivo* (26), by crossing mice expressing a biotin-tag with BirA expressing mice. Two lines of transgenic mice would be made, one with mutant POC1A with a biotin-tag, and one with wild-type POC1A with a biotin tag, both of which would be mated to BirA expressing mice (26), to allow for biotin labeling *in vivo*. As there may be tissue-dependent cofactors associating with POC1A, this approach may provide more detailed information regarding the molecular defects in the seminiferous tubules and growth plate of *Poc1a*$^{cha/cha}$ animals, and add to our basic understanding of POC1A function in both of these tissues.

Another crucial question to answer regarding the mutant form of POC1A is whether or not a critical point in the cell cycle is affected by the mutation. The potential exists that partial loss-of-function of POC1A leads to perturbations in all areas of the cell cycle (Figure 1.3). Studies utilizing skin fibroblasts from Meier-Gorlin Syndrome patients indicate that these cells do progress through the cell cycle (27, 28), but the gene involved can affect the rate of progression through the various phases. This means that multiple genes implicated in the development of a different form of primordial dwarfism can affect the rate of progression through the cell cycle, without causing the cells to stop cycling. Flow cytometry of *Poc1a*$^{cha/cha}$ MEFs could clarify if there is a deficiency or augmentation in one or more phases of the cell cycle. This could add much to our understanding of the phenotypes present in both the testis and the long bones. For example, if many cells remain in G2 phase, then it is possible that centrosome duplication and/or maturation is one of the primary issues in *Poc1a*$^{cha/cha}$ cells, which could affect progression to M phase, and lead to defects in mitotic spindle orientation and polarity (21). This could certainly explain the disorganization of the *Poc1a*$^{cha/cha}$ growth plate, as cell polarity and oriented cell division are critical to maintain growth plate architecture (29).

Along the same lines, it will be important to address the possible dysfunction of the mitotic spindle and the primary cilium. MEFs are an ideal choice for conducting these types of experiments. Inducing the formation of the primary cilium via serum-starvation followed by immunohistochemistry for acetylated tubulin (primary cilium marker), will allow us to quantify the frequency of cilia formation, as well as measure the lengths of the cilia that form. Conversely, culturing MEFs in the presence of serum would stimulate cell division, meaning we could capture some of the cells as they are dividing. Immunohistochemistry for tubulin and γ-tubulin would allow us to visualize the mitotic spindle and spindle poles, respectively. This experiment would provide us with a means with which to evaluate the mitotic spindle, and quantify of the number of centrosomes per cell. The state of having more than one centrosome per cell is known as centrosome amplification. This phenomenon has been reported in the human patient fibroblasts (23) and cells in which *POC1A* and *POC1B* were knocked-down by siRNA (21). It is critical to determine if the *Poc1a*^{cha/cha} fibroblasts exhibit these same cellular phenotypes. If so, it would certainly add support to our conclusion that the *Poc1a*^{cha/cha} mouse is a model of a novel form of primordial dwarfism in humans, and could provide more clues as to the nature of the cellular defects present in the growth plates and seminiferous tubules.

Primordial dwarfisms are hypothesized to be caused by a state of hypocellularity (30). This state is thought to occur by cell cycle arrest or slower progression through the cell cycle, leading to a sluggish rate of cellular proliferation, or an increased rate of cell death. In the *Poc1a*^{cha/cha} animal, understanding this balance between cell proliferation and cell death during development and in the affected tissues is of high priority. The use of EdU (5-ethynyl-2'deoxyuridine), an analog of BrdU (5-bromo-2'-deoxyuridine), to assess proliferation is an easy and more sensitive method of detection than BrdU incorporation, which requires the use of a

primary antibody. Injecting the whole animal with EdU will provide a clear view of how the

mutation is impacting the number of proliferating cells in the affected tissues. Likewise,

injecting timed pregnant mothers with EdU will allow us to assess proliferation in whole

embryos throughout development. We will also ascertain the level of cell death present in

affected tissues and throughout embryonic development. TUNEL (terminal deoxynucleotidyl

transferase dUTP nick end labeling) staining marks cells undergoing a state of DNA

fragmentation that occurs as result of committing to apoptosis. The use of this technique on

sections through the long bones, testis, and whole embryos will allow us to determine the overall

effect of the mutation on the rate of cell death.

Both of these experimental approaches must be conducted at the proper time to allow us

to see the onset of the cellular phenotype. In the testis, this may be at birth, which is the state

where the seminiferous tubules more closely resemble controls (Figure 3.5). This may also be

the best time to assess both cellular proliferation and apoptosis in the growth plate, but first we

must determine the time when the growth plate of $Poc1a^{cha/cha}$ animals resembles that of the

control. Finally, in the whole embryo, it will be important to try to determine rates of

proliferation and cell death at a variety of embryonic stages. A likely starting point would be

E9.5 (embryonic day 9.5), and every other day thereafter. This could also provide us with earlier

time points for proliferation and apoptosis in the two tissues of interest.

$Poc1a^{cha/cha}$: Understanding the molecular etiology of the growth defect

The previous section on understanding how the $Poc1a^{cha/cha}$ allele causes its cellular

phenotypes could provide much guidance in the next steps we take regarding the growth defect.

First, we must determine the onset of the growth defect in these animals and address the question

of whether or not the cells are proliferating more slowly or are undergoing more frequent cell

death. Both of these outcomes could be affected by defects in processes mediated by the centrosome. If mitotic spindle orientation and polarity are disrupted, it will be imperative to determine if the same is true in the proliferative zone. Immunohistochemistry for tubulin and γ-tubulin on many sections through $Poc1a^{\text{cha/cha}}$ growth plates could provide us the ability to visualize the mitotic spindle and spindle poles in the growth plate. It is likely that the process of oriented cell division is disrupted, which is contributing to the disorganization in this tissue.

Also likely is the reduction in frequency, length, and polarity of the primary cilium in the growth plate, an organelle known to be required for proper growth plate organization (31). WNT and Indian hedgehog (IHH) signaling components are known to localize to the primary cilium (32). Defective signaling through both of these pathways could lead to perturbations in chondrocyte rotation (WNT) (29), and proliferation and differentiation (IHH) (33). If the cilium is disrupted, Real-Time quantitative PCR on WNT and IHH target genes could provide support that these pathways are not functioning properly in the $Poc1a^{\text{cha/cha}}$ growth plate.

$Poc1a^{\text{cha/cha}}$: What is the cause of male infertility?

The first question that needs to be considered with respect to male infertility in $Poc1a^{\text{cha/cha}}$ mice is: what cell type(s) express $Poc1a$ in the testis? Immunohistochemistry on wild-type seminiferous tubules revealed that POC1A is mainly expressed in cells near the lumen of the tubule (Figure 3.3). POC1A expression is detected sporadically in cells near the basement membrane of the tubule (data not shown). This is the location of the lesser-differentiated cells (spermatogonia, etc.). It is not clear at this point whether POC1A is expressed in the somatic and/or germ cell compartments. One way to address this issue is to test for colocalization using primary antibodies against various cell populations in the testis. This will help delineate if POC1A is expressed in spermatogenic stem cells, spermatogonia, meiotic germ cells,

spermatozoa, and Sertoli cells. Given that the $Poc1a^{cha/cha}$ Sertoli cells are incapable of

supporting the resumption of the spermatogenic program with wild-type donor germ cells

(Figure 3.7), it is likely that POC1A is expressed in this cell type. What it is doing in the Sertoli

cells, however, remains to be clarified.

The next logical question that needs to be answered is how partial loss-of-function of

Poc1a causes the loss of germ cells in the testis. It is highly likely that *Poc1a* is expressed in

both cell populations. Therefore, the reciprocal testis cell transplantation assay using $Poc1a^{cha/cha}$

Rosa-LacZ labeled spermatogenic stem cells will likely show that this cell population is also

defective at establishing labeled spermatogenic colonies in wild-type testes. This experiment

must be conducted to rule out a defect in $Poc1a^{cha/cha}$ spermatogenic stem cells. The possibility

also exists of culturing spermatogenic stem cells from wild-type animals and knocking down

Poc1a expression in an attempt to understand the cellular and molecular details of *Poc1a*

function in this cell type.

If both cell populations are defective, this could complicate the analysis of the testis.

This may require the use of conditional alleles of *Poc1a* in both cell populations to remove

Poc1a function in Sertoli cells and various populations of germ cells specifically. A floxed allele

of *Poc1a* would have to be generated for these experiments to be conducted. Crossing this

animal to a cell-type specific Cre Recombinase allele would remove *Poc1a* function in that cell

type, causing a conditional loss-of-function allele. To really recapitulate the phenotype, we may

want to consider floxing exon 8 of *Poc1a*, as recombination would lead to the loss of this exon in

the mRNA transcript, and loss of 23 amino acids in the translated protein.

Diffuse POC1A expression via immunohistochemistry has been noted in some

seminiferous tubules from wild-type animals, around the areas of the tubule where Sertoli cells

surround the germ cells. This pattern of expression could indicate that POC1A is involved in regulating Sertoli cell cytoskeletal dynamics, which is required for the Sertoli cell to optimally maintain its connections to the germ cells and promote their progression through the phases of spermatogenesis (34). Currently, there is no known role for the primary cilium in the mouse or human testis, but it is possible that the Sertoli cell primary cilium is required for optimal signaling events that regulate spermatogenesis. It is also likely that the $Poc1a^{cha/cha}$ Sertoli cells generate a supportive niche for spermatogenic stem cells, but that the niche fails in supporting the spermatogenic stem cell's progression to later stages of differentiation. Rates of proliferation, apoptosis, and quantification of the various cell types in $Poc1a^{cha/cha}$ animals at the proper timepoints will help to answer some of these remaining questions. Visualization of the primary cilium and the Sertoli cell cytoskeleton in $Poc1a^{cha/cha}$ animals will provide molecular details that could rule out the dysfunction of either the cytoskeleton or the primary cilium in the development of the $Poc1a^{cha/cha}$ male infertility phenotype.

As stated previously, patients with mutations in *POC1A* have either not been extensively evaluated for male fertility, or no phenotype was reported at the time of examination (22, 23). Clearly, in the area of the growth defect, the $Poc1a^{cha/cha}$ mouse serves as a model for this form of primordial dwarfism. Interestingly, it may have also provided clues as to an additional aspect of the human phenotype (male infertility) that should be evaluated in future male patients with mutations in *POC1A*.

Modifying Loci: The New Frontiers in Skeletal Dysplasia Genetics

Both mouse models of skeletal dysplasia presented in this dissertation illustrate the probable contribution of modifying loci in the development of the mutant phenotype. The $Npr2^{pwe/pwe}$ mouse exhibits a worsening of the phenotype on the C57BL/6J genetic background,

and the lower level of lethality on the mixed background differs from what other groups have reported in their characterization of other *Npr2* loss-of-function alleles on different genetic backgrounds (35-37). The *Poc1a*cha/cha allele is compatible with life on the FVB/NJ, CAST/EiJ, and DBA/2J genetic backgrounds. On DBA/2J, *Poc1a*cha/cha mice exhibit a fully penetrant neurologic phenotype, hind leg clasping, but this feature is completely lacking on other backgrounds. Introduction of the C57BL/6J genetic background increases the severity of the growth phenotype, and the animals look sickly. Backcrossing the *Poc1a*cha/cha allele onto the C57BL/6J background for six generations results in early embryonic lethality. These scenarios in mice are not unlike the scenarios that arise in human patients—frequently patients with the same mutation can have vastly different outcomes, which is likely due to effects of additional variants elsewhere in the genome.

Hypomorphic alleles like the *Poc1a*cha/cha allele are ideal choices for conducting what are known as sensitized mutant screens. In these cases, there is already a mutant phenotype or susceptibility to a mutant phenotype present on the strain to be mutagenized, and the goal is to introduce mutations that change the phenotype in some way. Perhaps the phenotype improves, perhaps its severity increases, or, in the case of the *Poc1a*cha/cha allele, leads to a complete loss of mutant animals being born. There are a number of forms of skeletal dysplasia that can cause early lethality (38), and their ability to do so can be variable. The novel form of primordial dwarfism caused by mutations in *POC1A* is an excellent example of this phenomenon. Many of the patients evaluated with the premature termination codon died early in life or lived with some major complications (23), while those with the point mutation seemed to fare better (22). This could be due to the differences in the mutations themselves, or a variable incidence of translational read-through in some patients with the premature termination codon (23). It is also

possible that there are modifying loci in humans that exacerbate the phenotype, and a mouse

model such as the $Poc1a^{\text{cha/cha}}$ animal is an invaluable tool to use to delve into the connections

between $Poc1a$ and other genomic loci that can potentially influence the mutant phenotype.

Modifiers of mutant phenotypes obviously reflect the situation often presented in human

patients, and for that reason, they are an active area of genetic inquiry. As the genetic causes of

skeletal disorders continue to increase in number, it is likely that some of these interactions will

be addressed and their molecular underpinnings discovered through screens in mouse and

zebrafish. Pairing future work on modifiers with the development of therapies that exhibit

improved targeting to the growth plate, could truly open the field to a new era of personalized

medicine for patients with skeletal disorders and genetic modifying loci.

References

1   Krejci, P., Masri, B., Fontaine, V., Mekikian, P.B., Weis, M., Prats, H. and Wilcox, W.R. (2005) Interaction of fibroblast growth factor and C-natriuretic peptide signaling in regulation of chondrocyte proliferation and extracellular matrix homeostasis. *Journal of cell science*, **118**, 5089-5100.
2   Agoston, H., Khan, S., James, C.G., Gillespie, J.R., Serra, R., Stanton, L.A. and Beier, F. (2007) C-type natriuretic peptide regulates endochondral bone growth through p38 MAP kinase-dependent and -independent pathways. *BMC developmental biology*, **7**, 18.
3   Yasoda, A. and Nakao, K. (2010) Translational research of C-type natriuretic peptide (CNP) into skeletal dysplasias. *Endocr J*, **57**, 659-666.
4   Schipani, E., Ryan, H.E., Didrickson, S., Kobayashi, T., Knight, M. and Johnson, R.S. (2001) Hypoxia in cartilage: HIF-1alpha is essential for chondrocyte growth arrest and survival. *Genes & development*, **15**, 2865-2876.
5   Shukla, V., Coumoul, X., Wang, R.H., Kim, H.S. and Deng, C.X. (2007) RNA interference and inhibition of MEK-ERK signaling prevent abnormal skeletal phenotypes in a mouse model of craniosynostosis. *Nature genetics*, **39**, 1145-1150.
6   Yasoda, A., Kitamura, H., Fujii, T., Kondo, E., Murao, N., Miura, M., Kanamoto, N., Komatsu, Y., Arai, H. and Nakao, K. (2009) Systemic administration of C-type natriuretic peptide as a novel therapeutic strategy for skeletal dysplasias. *Endocrinology*, **150**, 3138-3144.
7   Jonquoy, A., Mugniery, E., Benoist-Lasselin, C., Kaci, N., Le Corre, L., Barbault, F., Girard, A.L., Le Merrer, Y., Busca, P., Schibler, L. *et al.* (2012) A novel tyrosine kinase inhibitor restores chondrocyte differentiation and promotes bone growth in a gain-of-function Fgfr3 mouse model. *Human molecular genetics*, **21**, 841-851.

8   Xie, Y., Su, N., Jin, M., Qi, H., Yang, J., Li, C., Du, X., Luo, F., Chen, B., Shen, Y. *et al.* (2012) Intermittent PTH (1-34) injection rescues the retarded skeletal development and postnatal lethality of mice mimicking human achondroplasia and thanatophoric dysplasia. *Human molecular genetics*, **21**, 3941-3955.

9   Lorget, F., Kaci, N., Peng, J., Benoist-Lasselin, C., Mugniery, E., Oppeneer, T., Wendt, D.J., Bell, S.M., Bullens, S., Bunting, S. *et al.* (2012) Evaluation of the therapeutic potential of a CNP analog in a Fgfr3 mouse model recapitulating achondroplasia. *American journal of human genetics*, **91**, 1108-1114.

10   Jin, M., Yu, Y., Qi, H., Xie, Y., Su, N., Wang, X., Tan, Q., Luo, F., Zhu, Y., Wang, Q. *et al.* (2012) A novel FGFR3-binding peptide inhibits FGFR3 signaling and reverses the lethal phenotype of mice mimicking human thanatophoric dysplasia. *Human molecular genetics*, **21**, 5443-5455.

11   Yasoda, A., Komatsu, Y., Chusho, H., Miyazawa, T., Ozasa, A., Miura, M., Kurihara, T., Rogi, T., Tanaka, S., Suda, M. *et al.* (2004) Overexpression of CNP in chondrocytes rescues achondroplasia through a MAPK-dependent pathway. *Nat Med*, **10**, 80-86.

12   Fujii, T., Komatsu, Y., Yasoda, A., Kondo, E., Yoshioka, T., Nambu, T., Kanamoto, N., Miura, M., Tamura, N., Arai, H. *et al.* (2010) Circulating C-type natriuretic peptide (CNP) rescues chondrodysplastic CNP knockout mice from their impaired skeletal growth and early death. *Endocrinology*, **151**, 4381-4388.

13   Geister, K.A., Brinkmeier, M.L., Hsieh, M., Faust, S.M., Karolyi, I.J., Perosky, J.E., Kozloff, K.M., Conti, M. and Camper, S.A. (2013) A novel loss-of-function mutation in Npr2 clarifies primary role in female reproduction and reveals a potential therapy for acromesomelic dysplasia, Maroteaux type. *Human molecular genetics*, **22**, 345-357.

14   Franceschi, R.T., Ge, C., Xiao, G., Roca, H. and Jiang, D. (2007) Transcriptional regulation of osteoblasts. *Annals of the New York Academy of Sciences*, **1116**, 196-207.

15   Zhang, M., Su, Y.Q., Sugiura, K., Wigglesworth, K., Xia, G. and Eppig, J.J. (2011) Estradiol promotes and maintains cumulus cell expression of natriuretic peptide receptor 2 (NPR2) and meiotic arrest in mouse oocytes in vitro. *Endocrinology*, **152**, 4377-4385.

16   Kawamura, K., Cheng, Y., Kawamura, N., Takae, S., Okada, A., Kawagoe, Y., Mulders, S., Terada, Y. and Hsueh, A.J. (2011) Pre-ovulatory LH/hCG surge decreases C-type natriuretic peptide secretion by ovarian granulosa cells to promote meiotic resumption of pre-ovulatory oocytes. *Human reproduction*, **26**, 3094-3101.

17   Robinson, J.W., Zhang, M., Shuhaibar, L.C., Norris, R.P., Geerts, A., Wunder, F., Eppig, J.J., Potter, L.R. and Jaffe, L.A. (2012) Luteinizing hormone reduces the activity of the NPR2 guanylyl cyclase in mouse ovarian follicles, contributing to the cyclic GMP decrease that promotes resumption of meiosis in oocytes. *Developmental biology*, **366**, 308-316.

18   Bartels, C.F., Bukulmez, H., Padayatti, P., Rhee, D.K., van Ravenswaaij-Arts, C., Pauli, R.M., Mundlos, S., Chitayat, D., Shih, L.Y., Al-Gazali, L.I. *et al.* (2004) Mutations in the transmembrane natriuretic peptide receptor NPR-B impair skeletal growth and cause acromesomelic dysplasia, type Maroteaux. *American journal of human genetics*, **75**, 27-34.

19   Nevalainen, E.M., Braun, A., Vartiainen, M.K., Serlachius, M., Andersson, L.C., Moser, M. and Lappalainen, P. (2011) Twinfilin-2a is dispensable for mouse development. *PloS one*, **6**, e22894.

20 Okano, S., Zhou, L., Kusaka, T., Shibata, K., Shimizu, K., Gao, X., Kikuchi, Y., Togashi, Y., Hosoya, T., Takahashi, S. *et al.* (2010) Indispensable function for embryogenesis, expression and regulation of the nonspecific form of the 5-aminolevulinate synthase gene in mouse. *Genes to cells : devoted to molecular & cellular mechanisms*, **15**, 77-89.

21 Venoux, M., Tait, X., Hames, R.S., Straatman, K.R., Woodland, H.R. and Fry, A.M. (2013) Poc1A and Poc1B act together in human cells to ensure centriole integrity. *Journal of cell science*, **126**, 163-175.

22 Sarig, O., Nahum, S., Rapaport, D., Ishida-Yamamoto, A., Fuchs-Telem, D., Qiaoli, L., Cohen-Katsenelson, K., Spiegel, R., Nousbeck, J., Israeli, S. *et al.* (2012) Short stature, onychodysplasia, facial dysmorphism, and hypotrichosis syndrome is caused by a POC1A mutation. *American journal of human genetics*, **91**, 337-342.

23 Shaheen, R., Faqeih, E., Shamseldin, H.E., Noche, R.R., Sunker, A., Alshammari, M.J., Al-Sheddi, T., Adly, N., Al-Dosari, M.S., Megason, S.G. *et al.* (2012) POC1A truncation mutation causes a ciliopathy in humans characterized by primordial dwarfism. *American journal of human genetics*, **91**, 330-336.

24 Pearson, C.G., Osborn, D.P., Giddings, T.H., Jr., Beales, P.L. and Winey, M. (2009) Basal body stability and ciliogenesis requires the conserved component Poc1. *The Journal of cell biology*, **187**, 905-920.

25 Kim, J., Cantor, A.B., Orkin, S.H. and Wang, J. (2009) Use of in vivo biotinylation to study protein-protein and protein-DNA interactions in mouse embryonic stem cells. *Nature protocols*, **4**, 506-517.

26 Driegen, S., Ferreira, R., van Zon, A., Strouboulis, J., Jaegle, M., Grosveld, F., Philipsen, S. and Meijer, D. (2005) A generic tool for biotinylation of tagged proteins in transgenic mice. *Transgenic research*, **14**, 477-482.

27 Bicknell, L.S., Walker, S., Klingseisen, A., Stiff, T., Leitch, A., Kerzendorfer, C., Martin, C.A., Yeyati, P., Al Sanna, N., Bober, M. *et al.* (2011) Mutations in ORC1, encoding the largest subunit of the origin recognition complex, cause microcephalic primordial dwarfism resembling Meier-Gorlin syndrome. *Nature genetics*, **43**, 350-355.

28 Stiff, T., Alagoz, M., Alcantara, D., Outwin, E., Brunner, H.G., Bongers, E.M., O'Driscoll, M. and Jeggo, P.A. (2013) Deficiency in origin licensing proteins impairs cilia formation: implications for the aetiology of Meier-Gorlin syndrome. *PLoS genetics*, **9**, e1003360.

29 Li, Y. and Dudley, A.T. (2009) Noncanonical frizzled signaling regulates cell polarity of growth plate chondrocytes. *Development*, **136**, 1083-1092.

30 Klingseisen, A. and Jackson, A.P. (2011) Mechanisms and pathways of growth failure in primordial dwarfism. *Genes & development*, **25**, 2011-2024.

31 Song, B., Haycraft, C.J., Seo, H.S., Yoder, B.K. and Serra, R. (2007) Development of the post-natal growth plate requires intraflagellar transport proteins. *Developmental biology*, **305**, 202-216.

32 Wallingford, J.B. and Mitchell, B. (2011) Strange as it may seem: the many links between Wnt signaling, planar cell polarity, and cilia. *Genes & development*, **25**, 201-213.

33 Kronenberg, H.M. (2003) Developmental regulation of the growth plate. *Nature*, **423**, 332-336.

34 Vogl, A.W., Vaid, K.S. and Guttman, J.A. (2008) The Sertoli cell cytoskeleton. *Advances in experimental medicine and biology*, **636**, 186-211.

35   Sogawa, C., Abe, A., Tsuji, T., Koizumi, M., Saga, T. and Kunieda, T. (2010) Gastrointestinal tract disorder in natriuretic peptide receptor B gene mutant mice. *Am J Pathol*, **177**, 822-828.

36   Sogawa, C., Tsuji, T., Shinkai, Y., Katayama, K. and Kunieda, T. (2007) Short-limbed dwarfism: slw is a new allele of Npr2 causing chondrodysplasia. *J Hered*, **98**, 575-580.

37   Tamura, N., Doolittle, L.K., Hammer, R.E., Shelton, J.M., Richardson, J.A. and Garbers, D.L. (2004) Critical roles of the guanylyl cyclase B receptor in endochondral ossification and development of female reproductive organs. *Proc Natl Acad Sci U S A*, **101**, 17300-17305.

38   Krakow, D. and Rimoin, D.L. (2010) The skeletal dysplasias. *Genetics in medicine : official journal of the American College of Medical Genetics*, **12**, 327-341.